



**Michigan
Technological
University**

Michigan Technological University
Digital Commons @ Michigan Tech

Dissertations, Master's Theses and Master's Reports

2023

BIOACCUMULATION OF POLYCHLORINATED BIPHENYL COMPOUNDS AND MERCURY IN A MINING IMPACTED AQUATIC ECOSYSTEM

Michelle Bollini
Michigan Technological University, msbollin@mtu.edu

Copyright 2023 Michelle Bollini

Recommended Citation

Bollini, Michelle, "BIOACCUMULATION OF POLYCHLORINATED BIPHENYL COMPOUNDS AND MERCURY IN A MINING IMPACTED AQUATIC ECOSYSTEM", Open Access Master's Thesis, Michigan Technological University, 2023.

<https://doi.org/10.37099/mtu.dc.etdr/1594>

Follow this and additional works at: <https://digitalcommons.mtu.edu/etdr>



Part of the [Aquaculture and Fisheries Commons](#), [Environmental Engineering Commons](#), [Environmental Health Commons](#), and the [Toxicology Commons](#)

BIOACCUMULATION OF POLYCHLORINATED BIPHENYL COMPOUNDS
AND MERCURY IN A MINING IMPACTED AQUATIC ECOSYSTEM

By

Michelle Bollini

A THESIS

Submitted in partial fulfillment of the requirements for the degree of

MASTER OF SCIENCE

In Environmental Engineering

MICHIGAN TECHNOLOGICAL UNIVERSITY

2023

© 2023 Michelle Bollini

This thesis has been approved in partial fulfillment of the requirements for the Degree of MASTER OF SCIENCE in Environmental Engineering.

Department of Civil, Environmental, and Geospatial Engineering

Thesis Co-Advisor: *Dr. Noel R. Urban*

Thesis Co-Advisor: *Dr. Judith A. Perlinger*

Committee Member: *Dr. Gordon Paterson*

Committee Member: *Dr. Cory P. McDonald*

Department Chair: *Dr. Audra Morse*

Table of Contents

List of Figures	v
List of Tables	ix
Acknowledgements.....	xi
Abstract.....	xii
1 Introduction.....	1
1.1 Historical contamination from copper mining industry	1
1.1.1 History of PCB pollution	2
1.1.2 History of Mercury pollution.....	4
1.2 Human and environmental health concerns	8
1.2.1 PCB toxicity.....	8
1.2.2 Mercury toxicity.....	9
1.3 Fish consumption advisories	10
1.4 Remediation- past and future	13
1.4.1 Past remediation.....	14
1.4.2 Future remediation.....	14
1.5 Bioaccumulation modeling.....	15
1.6 Objectives and research questions.....	16
2 Methods.....	18
2.1 Site description	18
2.2 Data availability	20
2.2.1 Atmospheric Concentration Data.....	21
2.2.2 Dissolved PCB and MeHg Concentration Data.....	22
2.2.3 Soil Sampling Data	23
2.2.4 Sediment Survey Data.....	23
2.2.5 Fish Tissue Concentration Measurements	25
2.3 Bioaccumulation Modeling	27
2.3.1 PCB modeling.....	27
2.3.2 MeHg adapted bioaccumulation model	35
2.3.3 Model validation, and sensitivity and uncertainty analyses.....	39
2.3.3.1 Model Validation	39
2.3.3.2 Sensitivity Analysis	42
2.3.3.3 Uncertainty Analysis.....	42
2.3.4 Model Experiments.....	45
2.3.4.1 PCB modeling questions.....	45
2.3.4.2 MeHg modeling questions	46
3 Results.....	48
3.1 PCB Modeling Results	48

3.1.1	Non-steady state PCB bioaccumulation model results	48
3.1.2	Model verification, validation, and sensitivity and uncertainty analyses results	49
3.1.2.1	Walleye Model Verification and Validation Results	49
3.1.2.2	Sensitivity Analysis Results.....	50
3.1.2.3	Uncertainty Analysis Results.....	53
3.1.3	Results of PCB Modeling Experiments	55
3.1.3.1	PCB Question 1 Modeling Results	55
3.1.3.2	PCB Question 2 Modeling Results	56
3.1.3.3	PCB Question 3 Modeling Results	56
3.2	MeHg Modeling Results	57
3.2.1	Non-steady state MeHg bioaccumulation model results	58
3.2.2	Model validation, and sensitivity and uncertainty analyses results ..	58
3.2.2.1	Walleye Model Validation Results	58
3.2.2.2	Sensitivity Analysis Results.....	60
3.2.2.3	Uncertainty Analysis Results.....	61
3.2.3	Modeling Experiment Results.....	62
4	Discussion	64
4.1	Validity of modeling approach.....	64
4.1.1	PCBs	64
4.1.2	MeHg	67
4.2	Predicted effects of remediation.....	70
4.2.1	Remedial impacts on PCB contaminated sediment in Torch Lake...70	
4.2.2	Revised aqueous concentrations of MeHg in Torch Lake.....	73
4.3	The influence of fish lipid content on the PCB bioaccumulated burdens	74
4.4	Potential impacts of fish immigration to and emigration from Torch Lake...74	
4.5	Future work	75
5	Reference List	79
A	Title of Appendix.....	91
A.1	Matlab model code	91
A.1.1	PCB bioaccumulation model	91
A.1.2	MeHg bioaccumulation model.....	97
A.2	Fish measurement data	101
A.2.1	PCB fish measurement data.....	101
A.2.2	Hg fish measurement data.....	103
A.3	Sensitivity analysis results.....	106
A.3.1	PCB sensitivity analysis.....	106
A.3.2	MeHg sensitivity analysis	114
A.4	Mercury temperature profile	115
B	Copyright documentation.....	116

List of Figures

Figure 1. Torch Lake PCB mass balance model from Urban et al. (2018).....	4
Figure 2. Schematic of mercury mass balance model developed by Hendricks; figure from the publication by Perlinger et al. (2018).	6
Figure 3. Trap Rock River watershed National Wetland Inventory (U.S. FWS).....	7
Figure 4. Polychlorinated biphenyl compound (PCB, 209 possible congeners) structure .	8
Figure 5. Torch Lake 2016 National Land Cover Data (NLCD) from the National Map Viewer with 30m spatial resolution (U.S. Geological Survey, 2016).	19
Figure 6. PCB congener vapor concentration (pg/m ³) measured from the Great Lakes Integrated Atmospheric Deposition Network (IADN) averaged for the Eagle Harbor Station 1991-2021. Congeners within red boxes (PCB 33, 52, 99, 101, 149, 153, and 180) were modeled in this study.....	22
Figure 7. EGLE Abandoned Mining Wastes (AMW) project total PCB concentrations in Torch Lake sediment separated into Region 1(HPA) and Region 2 (LLRA) areas with elevated PCB concentrations.	24
Figure 8. Average walleye mercury concentrations (µg/g ww or ppm) in Torch Lake as a function of walleye length (cm) measured by MI EGLE and GLIFWC (Urban, unpub.).	25
Figure 9. Temporal trend in Torch Lake walleye fish lipid content periods 2000-2018 (MI EGLE) and 2018-2022 (MTU TLPAC). Error bars represent 95% confidence intervals (Urban and Perlinger, 2022).	26
Figure 10. Temporal trend of lipid-normalized PCB concentrations in walleye from Torch Lake. Error bars represent 95% confidence intervals (Urban and Perlinger, 2022)......	27
Figure 11. PCB bioaccumulation model schematic for an individual fish (Arnot and Gobas, 2004). The bioaccumulation results from the difference between uptake and elimination rates. Uptake occurs via partitioning into the gills during respiration (k_1) and by ingestion of prey containing PCBs (k_D). Elimination includes respiration (partitioning out of the organism through the gills) (k_2), fecal excretion (k_E), and metabolic transformation (k_M).	28
Figure 12. Box- and -whisker plots of measured PCB walleye concentration in Torch Lake obtained from Michigan EGLE (2000,2007,2013, and 2018) and Michigan Technological University (MTU) as part of the Torch Lake Public Action Council (TLPAC) project (2018, 2019, 2020, and 2022).	40
Figure 13. Box- and -whisker plots of measured MeHg concentrations in walleye concentration in Torch Lake obtained from Michigan EGLE (2000, 2007, 2013, and 2018) and Great Lakes Indian Fish and Wildlife Commission (GLIFWC) for years 2018-2021 for model validation. The model predicted value is indicated by the red circle.	41

<i>Figure 14. Torch Lake walleye predicted PCB concentration (ng/g) for seven congeners selected from the non-steady state bioaccumulation modeled over 10 year- period (3650 days).</i>	49
<i>Figure 15. Change in walleye PCB 33 concentration caused by decreasing the model rate constants for trophic levels 1 (green),2(gray),3 (red), and 4 (blue) by 10%.</i>	51
<i>Figure 16. Change in walleye PCB 33 concentration caused by increasing the model rate constants for trophic levels 1 (green),2(gray),3 (red), and 4 (blue) by 10%.</i>	52
<i>Figure 17. Change in walleye PCB 180 concentration caused by decreasing the model rate constants for trophic levels 1 (green),2(gray),3 (red), and 4 (blue) by 10%.</i>	52
<i>Figure 18. Change in walleye PCB 180 concentration caused by increasing the model rate constants for trophic levels 1 (green),2(gray),3 (red), and 4 (blue) by 10%.</i>	53
<i>Figure 19. Walleye PCB 180 Monte Carlo simulation output concentration histogram. Normal distribution curve (redline).</i>	54
<i>Figure 20. Comparison of the impact of remediation of contaminated lake sediments, which are divided into Hubbell Processing Area (region 1) and Lake Linden Recreation Area (region 2) in the PCB mass balance model as potential on-going sources.</i>	55
<i>Figure 21. Impact of fish lipid concentration on walleye PCB 180 concentration (ng/g ww).</i>	57
<i>Figure 22. The non-steady state MATLAB predicted MeHg concentration in walleye over 10-year period.</i>	58
<i>Figure 23. Change in walleye MeHg concentration caused by decreasing the model rate constants for trophic levels 2 (gray), 3 (red), and 4 (blue) by 10%.</i>	60
<i>Figure 24. Change in walleye MeHg concentration caused by increasing the model rate constants for trophic levels 2 (gray),3 (red), and 4 (blue) by 10%.</i>	61
<i>Figure 25. Walleye MeHg Monte Carlo simulation output concentration histogram. Normal distribution curve (redline).</i>	62
<i>Figure 26. Comparison of Walleye PCB measured and predicted concentrations. The averaged measured concentrations in Torch Lake by MDHHS Fish Monitoring program and Torch Lake Public Action Council (TLPAC), and the predicted concentrations from MATLAB and AQUAWEB bioaccumulation models. (*model-predicted)</i>	66
<i>Figure 27. Change in walleye PCB 52 concentration caused by decreasing the model rate constants for trophic levels 1 (green), 2(gray), 3 (red), and 4 (blue) by 10%.</i>	106
<i>Figure 28. Change in walleye PCB 52 concentration caused by increasing the model rate constants for trophic levels 1 (green), 2(gray), 3 (red), and 4 (blue) by 10%.</i>	107
<i>Figure 29. Change in walleye PCB 99 concentration caused by decreasing the model rate constants for trophic levels 1 (green), 2(gray), 3 (red), and 4 (blue) by 10%.</i>	107

<i>Figure 30. Change in walleye PCB 99 concentration caused by increasing the model rate constants for trophic levels 1 (green), 2(gray), 3 (red), and 4 (blue) by 10%.</i>	108
<i>Figure 31. Change in walleye PCB 101 concentration caused by decreasing the model rate constants for trophic levels 1 (green), 2(gray), 3 (red), and 4 (blue) by 10%.</i>	108
<i>Figure 32. Change in walleye PCB 101 concentration caused by increasing the model rate constants for trophic levels 1 (green), 2(gray), 3 (red), and 4 (blue) by 10%.</i>	109
<i>Figure 33. Change in walleye PCB 149 concentration caused by decreasing the model rate constants for trophic levels 1 (green), 2(gray), 3 (red), and 4 (blue) by 10%.</i>	109
<i>Figure 34. Change in walleye PCB 149 concentration caused by increasing the model rate constants for trophic levels 1 (green), 2(gray), 3 (red), and 4 (blue) by 10%.</i>	110
<i>Figure 35. Change in walleye PCB 153 concentration caused by decreasing the model rate constants for trophic levels 1 (green), 2(gray), 3 (red), and 4 (blue) by 10%.</i>	110
<i>Figure 36. Change in walleye PCB 153 concentration caused by increasing the model rate constants for trophic levels 1 (green), 2(gray), 3 (red), and 4 (blue) by 10%.</i>	111
<i>Figure 37. Change in walleye PCB 33 concentration caused by decreasing the model partition coefficients for trophic levels 1 (green), 2 (gray), 3 (red), and 4 (blue) by 10%.</i>	111
<i>Figure 38. Change in walleye PCB 33 concentration caused by increasing the model partition coefficients for trophic levels 1 (green), 2 (gray), 3 (red), and 4 (blue) by 10%.</i>	112
<i>Figure 39. Change in walleye PCB 180 concentration caused by decreasing the model partition coefficients for trophic levels 1 (green), 2 (gray), 3 (red), and 4 (blue) by 10%.</i>	112
<i>Figure 40. Change in walleye PCB 180 concentration caused by increasing the model partition coefficients for trophic levels 1 (green), 2 (gray), 3 (red), and 4 (blue) by 10%.</i>	113
<i>Figure 41. Change in walleye PCB 33 concentration caused by increasing the model temperature, Kow, and body weight by factor of 2 (gray) and decreasing by factor of 2 (red).</i>	113
<i>Figure 42. Change in walleye PCB 180 concentration caused by increasing the model temperature, Kow, and body weight by factor of 2 (gray) and decreasing by factor of 2 (red).</i>	114

Figure 43. Change in walleye MeHg concentration caused by increasing the model temperature, Kow, and body weight by factor of 2 (gray) and decreasing by factor of 2 (red).114

Figure 44. Annual divalent, methyl, and elemental mercury concentrations predicted from Torch Lake mass balance model (Hendricks, 2018)115

List of Tables

<i>Table 1. Summary of fish consumption advisories and guidelines for Torch Lake 1993-2014 (Urban et al., 2018).</i>	10
<i>Table 2. Bioenergetic equations of the Torch Lake PCB bioaccumulation model (after Arnot & Gobas (2004))</i>	30
<i>Table 3. Biological input parameters used in Torch Lake PCB bioaccumulation model</i> .	32
<i>Table 4. Chemical input parameters used in Torch Lake PCB bioaccumulation model</i> ..	33
<i>Table 5. Environmental input parameters used in the Torch Lake PCB bioaccumulation model.</i>	34
<i>Table 6. Phytoplankton equations used in the Torch Lake MeHg bioaccumulation model (Schartup et al., 2018).</i>	37
<i>Table 7. Biological input parameters used in Torch Lake MeHg bioaccumulation model.</i>	37
<i>Table 8. Chemical input parameters used in Torch Lake MeHg bioaccumulation model.</i>	38
<i>Table 9. Bioenergetic equations Torch Lake MeHg bioaccumulation model.</i>	38
<i>Table 10. Mercury Bioaccumulation Factors (BAF) in fish (Knightes, 2008; Hendricks, 2018)</i>	42
<i>Table 11. Literature review values of dietary assimilation efficiency for PCB congeners in fish based on species type.</i>	43
<i>Table 12. Literature review values of dietary assimilation efficiency for MeHg in fish based on species type.</i>	44
<i>Table 13. Literature review values of total elimination rate constant for MeHg in fish based on species type.</i>	44
<i>Table 14. PCB bioaccumulation model verification and validation of steady-state concentration results.</i>	50
<i>Table 15. Torch Lake Walleye PCB Monte Carlo simulation mean concentration, standard deviation, upper and lower 95% confidence interval for seven congeners selected at the end of 10-year period modeled.</i>	54
<i>Table 16. Torch Lake time to reach measured bioaccumulation burden in walleye with initial concentration zero and diet concentration at steady state predicted concentration.</i>	56
<i>Table 17. Torch Lake walleye mercury modeled and observed concentrations from MI EGLE (1988, 2000, 2007, 2013, 2018) and GLIWC (2018, 2019).</i>	59
<i>Table 18. Predicted MeHg Bioaccumulation Factor (BAF) for trophic levels 3 and 4.</i> ...	59
<i>Table 19. Zooplankton MeHg concentrations reported by Back and Watras (1995).</i>	59

<i>Table 20. Torch Lake Walleye MeHg Monte Carlo simulation mean concentration, standard deviation, upper and lower 95% confidence interval selected at the end of 10-year period modeled.</i>	62
<i>Table 21. Predicted reductions in walleye concentration corresponding to different lake sediment remediation scenarios.</i>	71
<i>Table 22. MDEQ Fish Contaminant Monitoring Program walleye PCB congener concentrations (2000-2018).</i>	101
<i>Table 23. Torch Lake Public Council (TLPAC) measured PCB congeners (2018-2022).</i>	102
<i>Table 24. MDEQ Fish Contaminant Monitoring Program Walleye Hg concentration (1988-2018) and biological characteristics.</i>	103
<i>Table 25. GLIFWC Hg Monitoring Program walleye concentrations and biological characteristics (2018-2020).</i>	105

Acknowledgements

The study region is located within Ojibwa (Chippewa) homelands and ceded-territory established by the Treaty of 1842, the shared lands and waters of Native American nations in *Gakiwe'onaning* (Keweenaw Bay), *Gete-gitgaaning* (Lac Vieux Desert), *Mashkii-ziibing* (Bad River), *Odaawaa-zaaga'iganing* (Lac Courte Oreilles), *Waaswaaganing* (Lac Du Flambeau), *Miskwaabikong* (Red Cliff), *Wezaawaagami-ziibiing* (St. Croix), *Zaka'aaganing* (Sokaogon Mole Lake), *Nagaajiwanaag* (Fond du Lac), *Misi-zaaga'iganiing* (Mille Lacs), and *Gaa-mitaawangaagamaag-ininiwag* (Sandy Lake). I honor and give thanks to the beings that share this land with me, past, present, and future.

I'd like to thank my advisories Dr. Urban and Dr. Perlinger, for all your support through my years at Michigan Tech. You have taught me a lot about the world around us and the importance of the work in environmental engineering. I'm very grateful for the opportunity to work in your lab and see the different sides of the project. I'd also like to thank my committee members Dr. Paterson and Dr. McDonald for your assistance and comments on my project. Thank you to the CEGE department for the opportunity and support for being a teacher's assistant. Thank you to the cross country and track teams for their support throughout my years at MTU.

I'd also like to express my gratitude to everyone in the Toxics Analysis research group. Azmat Naseem, Enid Partika, Libia Hazra, Cailin Bishop, Sydney Peterson, Molly Greene and Wathsala Kapuralage, I am grateful to have worked with you and I appreciate all the assistance.

Thank you to the Tribal Landscape Systems research group. I am grateful to be part of a partnership between the university and Indigenous community to help support human and environment relationships. I'd like to thank the Keweenaw Bay Indian Community Natural Resource Department and staff for their contributions to this project. Thank you to the Bureau of Indian Affairs and Great Lakes Indian Fish and Wildlife Commission for their funding of this project.

Thank you to my family: Mom, Dad, Angela, Stephanie, and Gina for all your love and support always. I would not be able to do this without you. Thank you, Trent, for all your support and encouragement every day. I'd like to thank the friends I've made along the way and make Michigan Tech a special place in my heart.

Abstract

The Keweenaw area continues to be influenced by the century of copper mining that ended nearly 50 years ago. This project is focused on Torch Lake, an aquatic ecosystem that has been heavily impacted by mining waste disposal. The watershed has been impaired by mine discharge and tailings, smelter and smokestack plumes, and poor waste disposal practices. The lake is listed as a Great Lakes Area of Concern with beneficial use impairments of restrictions on fish consumption and a degraded benthic community. Polychlorinated biphenyl compounds (PCBs) and methylmercury (MeHg) are persistent, bioaccumulative, and toxic substances (PBTs). These contaminants pose threats to human and environmental health primarily via fish consumption. The use impairment of restricted fish consumption is a result of elevated concentrations of PCBs and MeHg in Torch Lake. In this research, kinetic bioaccumulation models were developed using MATLAB to estimate steady state concentrations in each trophic level of the Torch Lake food chain. The model links the contaminated environment to the bioaccumulation in a single organism. The model is most sensitive to the dietary uptake rate constants, and Monte Carlo simulations indicate that the uncertainty (95% confidence interval) is approximately 0.13 ng/g ww for PCBs and 0.02 µg/g ww for MeHg. Model-predicted concentrations agree with the steady-state model, AQUAWEB, and with concentrations measured in walleye (*Sander vitreus*). The kinetic model coupled with a mass balance model is used to predict the extent of recovery of the ecosystem following remediation actions, such as removal of local contaminant sources to the lake. Removal of contaminated sediments is predicted to reduce the PCB congener concentrations by a factor of 2-14, and elimination of in-lake methylation was predicted to reduce fish Hg concentrations by a factor of 2. Thus, the model suggests that the planned remediation under the Legacy Act will significantly reduce PCB concentrations in fish. The model indicates that adult fish entering Torch Lake from the Keweenaw Waterway could reach the observed PCB contaminant concentrations in fish within 62 days to over 10 years, but other studies have indicated that immigration of fish to Torch Lake is uncommon.

1 Introduction

1.1 Historical contamination from copper mining industry

Torch Lake is on the Keweenaw Peninsula of the Upper Peninsula of Michigan, known as the “Copper Country”. This region had 140 extractive copper mines and 40 mills to process the rock between 1849 and 1970. The native, or elemental, copper was highly sought by Calumet and Hecla (C&H) and Quincy Mining companies. There were no mines located at Torch Lake, but it provided an unlimited supply of water for milling and a convenient location for dumping large volumes of tailings and other industrial wastes (Urban et al. 2018). Torch Lake was exempted from the prohibition of dumping in navigable water of the Rivers and Harbors Act in 1899 and again in the 1940s because of the need for copper to make munitions; therefore, no restrictions were in place against dumping wastes from ore processing into the waterbody. Roughly 50% of the lake volume was filled with mine tailings, locally called stamp sands. Stamp sands are sand- to gravel-sized mine waste that can contain high concentrations of metals such as copper and mercury. Reclamation plants and secondary copper processing facilities were built to respond to the demand for copper; these resulted in much more finely-ground tailings and other chemicals in the waste stream. The mining period lasted for over 100 years, and, as technology advanced, the copper processing techniques and waste streams changed.

After the cessation of mining activities, public concerns about pollution arose. During this time the US was becoming more aware of environmental health. The Environmental Protection Agency (EPA) was created, and the Clean Water Act passed. The concerns grew with the raw residential and industrial sewage being dumped into the lake, leachate spills from the flotation plant in Lake Linden, contamination of sediments by copper, and the presence of tumors and deformities on fish. Torch Lake attracted national attention and was listed on the National Priorities List and as a Great Lake Area of Concern (AOC). The stamp sands from mine tailings, slag from smelters, and poor rock have left visible marks from the industry on the Torch Lake landscape (Urban et al., 2018). It has been estimated that 200 million tons of tailings were deposited into Torch Lake. The original volume of Torch Lake was estimated to be reduced by 50% (cf., MDNR, 1987; MDEQ, 2007; Donohue and Associates, 1990b; Donohue and Associates, 1990a). In addition, legacy copper, other trace metals, and organic pollutants persist in the lake and watershed from copper processing. This thesis project is focused on the contaminants that are of interest due to the fish consumption advisories: mercury (Hg), and polychlorinated biphenyl (PCB) compounds.

These two pollutants have different biogeochemical cycles in the environment, as well as different origins in the mining impacted aquatic ecosystem. These ubiquitous pollutants are present in the air, water, sediments, soil, and groundwater. The persistence and toxicity pose threats to human and environmental health. An Integrated Assessment on Torch Lake was performed in 2012-2014 that used the historical records from Michigan Tech archives and local interviews to identify and locate potential areas of contamination from the mining industry (Urban et al., 2018). The Integrated Assessment highlights four

problems that have impeded the remediation of Torch Lake under the governmental programs, Superfund, and the AOC: a lack funding, too narrow of a focus for a complex contamination problem, polarization of local and official viewpoints, and failure to apply new knowledge and remediation tools. The recovery of Torch Lake may take decades, if not generations.

1.1.1 History of PCB pollution

In the early years of the mining period the stamp mills were powered by a boiler house and steam engines (Urban et al., 2018). Wood from the nearby forests was supplied for the boilers, but the resource was quickly depleted. As a result, the industry transitioned to imported coal in the 1880s. Two coal handling docks were built on the western shore of Torch Lake. The advancement of modern mills and reclamation processes led to the need for a centralized power source. C&H built a centralized powerhouse in Lake Linden to provide power to multiple facilities at Torch Lake. Some of the facilities were powered by their own turbines or steam byproduct, but the power plant in Lake Linden produced power for 76% of Torch Lake operations (Urban et al. 2018). The electrification of the 1930s brought polychlorinated biphenyl compounds (PCBs) that were used in transformer oil into the industry. PCBs were used by the power facilities and substations along the western shoreline. It is possible that after the oil was changed it was dumped straight into Torch Lake, recycled in some way, or even spread out on dirt parking lots to help control dust (Zawisza, 2016).

Furthermore, reclamation of copper-containing materials and wire recycling were important during World War II. Early in the 1930's, scrap material arrived at C&H and the processing was relatively simple (Urban et al., 2018). By the end of World War II, the technology advanced and established a separate department for the production of secondary copper products. However, some copper wire required the burning of insulation, which contained PCBs, before processing. The burning was documented in the 1940s and continued for twenty years, as verified by oral interviews (Urban et al., 2018). The PCB residue from the burning was likely volatilized or deposited into the nearby soil. The Torch Lake facilities closed in 1970, with the exception of Peninsula Copper Industries (PCI). However, the stop in production did not prevent the waste disposal of residual chemicals. The historical investigation conducted by Emma Zawisza Master's thesis as part of the Torch Lake Integrated Assessment gives an overview of PCB contamination that originated from the electrification of the copper mining industry (Zawisza, 2016).

The US Environmental Protection Agency (EPA) hired consultants, Donohue & Assoc., in 1988-1992 to perform an initial Remediation Investigation and Feasibility Study (RI/FS). This study detected high levels of PCBs on the western shoreline in the sediments, water, and submerged tailings in Torch Lake (Urban et al., 2018). The Superfund site has been delisted in parts from 2002-2014, but PCB pollution was never identified as a problem nor remediated under the Superfund Program. It was not until the Michigan Department of Environmental Quality (MDEQ), which is now part of the Michigan Environment, Great Lakes, and Energy (MI EGLE) department updated the

Remedial Action Plan (RAP) in 2007 that PCB contamination in Torch Lake was formally acknowledged as an ongoing problem to be solved. The beneficial use impairments (BUIs) included (1) tumors or deformities in fish, (2) restrictions on fish consumption, and (3) degraded benthic community. The BUI for tumors or deformities in fish was removed in 2007. The BUI due to restrictions on fish consumption have been in place for elevated PCB concentrations since 1998.

Mass balance models have been used since the 1980's as important tools for identifying contaminant sources, particularly when empirical measurements may not be feasible due to technical or economic reasons (Urban et al., 2018; Arnot & Gobas 2004). In 2013 Michigan Tech presented a preliminary PCB mass balance model in Torch Lake to the EPA and MDEQ. The model results indicated that an ongoing input of PCBs to the lake was likely (Urban et al., 2018). These results sparked additional investigation of PCB sources in the watershed and in 2011-2012 the Superfund division of the MDEQ discovered locations of PCB contamination on the western shoreline of Torch Lake.

Ankita Mandelia's thesis project was part of the Torch Lake Integrated Assessment. The thesis summarized the status of contamination and remediation activities and estimated the magnitude of potential ongoing sources of PCBs to Torch Lake. The project included a mass balance model to evaluate potential unknown sources. The model was validated by comparing SPMD-estimated dissolved concentrations to the mass balance model predictions. The PCB mass balance model included three phases of PCB congeners: dissolved, DOC-bound, and particle bound. The phases influence the fate and transport of PCBs. The dissolved phase of PCBs is the bioavailable form that bioaccumulates. The inputs to the water column of Torch Lake include: atmospheric deposition, absorption, groundwater input, sediment diffusion of dissolved and DOC-bound phases, and resuspension. The outputs from the water column include: volatilization, outflow, sediment diffusion of dissolved and DOC-bound phases and settling. The inputs to and outputs from the sediments included: sediment diffusion of the dissolved and DOC-bound phases, settling, resuspension and burial out of the active sediment layer (Mandelia, 2016). A schematic of the mass balance model is shown below in Figure 1.

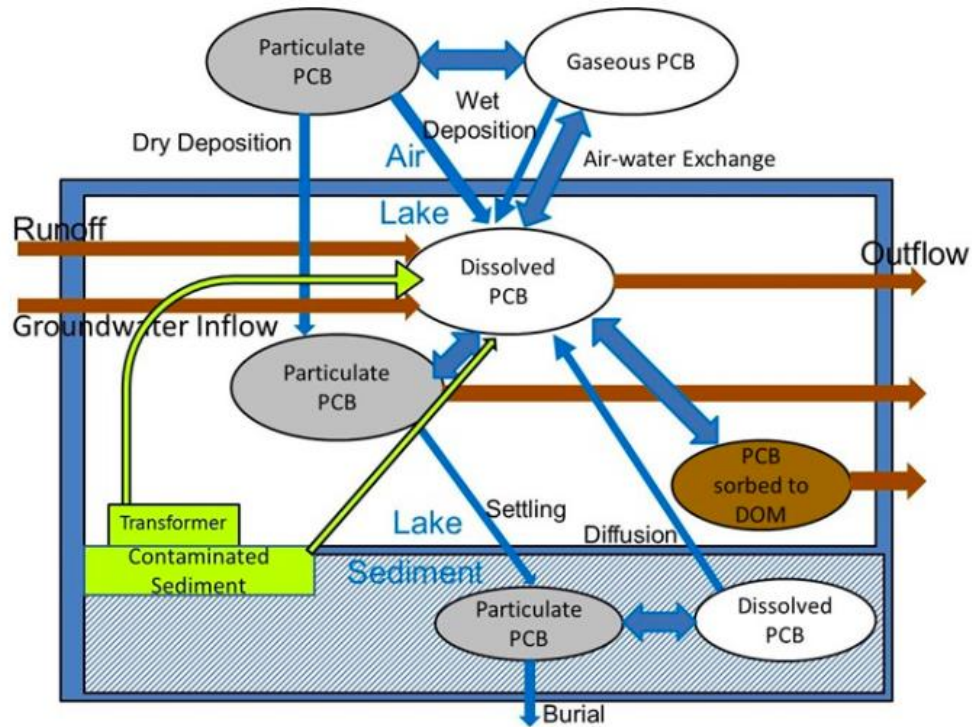


Figure 1. Torch Lake PCB mass balance model from Urban et al. (2018).

The mass balance model was constructed in Microsoft® Excel with inputs of lake specific properties such as dissolved organic carbon fraction, sediment region areas, porosity of sediments, mean depth, and burial and resuspension velocities. The PCB concentrations for lake sediment, upland groundwater, and air are in separate tabs. The model predicted the magnitude of ongoing locally-derived sources. The model was coupled with a kinetic bioaccumulation model as discussed below.

1.1.2 History of Mercury pollution

The coal-fired power plants for steam and electricity also contributed to the legacy mercury (Hg) in the environment. In addition, metal smelting releases large quantities of Hg from the ore into the atmosphere (Urban et al., 2018). Kerfoot (2002) estimated that 24 metric tons of Hg were released from copper smelting in the Keweenaw Peninsula. The copper smelters and power plant produced considerable quantities of fly and bottom ash- referred to as coal ash, from burning and pulverizing coal. The bottom ash collected in the base of boilers and smelter furnaces was likely deposited in the lake, although it contained heavy metals and polycyclic aromatic hydrocarbons (PAHs) (Urban et al. 2018). The fly ash was emitted through the smoke stacks and likely spread in plumes over nearby areas. However, later in its history C&H used fly ash as an additive in the fertilizer produced by reclaiming the metals.

Mercury in mine residues is an additional source of pollution that impacts the ecosystem. The mine residues include poor rock (9-281 ng Hg/g), stamp sands (3-265 ng/g), mine

tailings (17-95 ng/g), soils (60-200 ng/g), and lake sediments (50-600 ng/g) (Kerfoot et al., 2002; Urban et al., 2018). Drainage from abandoned mines releases a significant amount mercury into tributaries that flow into Torch Lake. Known sources include tributaries such as Hammell Creek, Slaughterhouse Creek, and Fulton Creek with elevated mercury concentrations (Hendricks, 2018). The State of Michigan measured mercury concentrations in stream waters from mines. In summer 2002 Slaughterhouse Creek, which receives drainage from multiple mines, had a settling flux of 0.57 g/d (Degraeve and McCauley, 2003). The Hg concentration and drainage from the Kingston mine (Copper City) was measured to be 310 ng/L and 0.36 g/d, respectively (Degraeve and McCauley, 2003). Osceola mine #4 had concentrations of 130 ng/L and outflow of 0.8 g/d (Degraeve and McCauley, 2003; MDEQ, 2002). In comparison, the average rate of atmospheric deposition of Hg to Torch Lake is 0.27 g/d (Urban et al., 2018). The major inflow into Torch Lake is the Traprock River and measurements suggest that a portion of Hg is derived from mine drainage or exposed tailings. The concentration below Scales Creek spiked above the 99th percentile of Upper Peninsula rivers unaffected by mining (Degraeve and McCauley, 2003).

Ashley Hendricks Master's thesis (2018) presented a non-steady state mercury mass balance based on the EPA's Spreadsheet-based Ecological Risk Assessment for the Fate of Mercury (SERAFM). In the current study, the transport and fate of mercury is modeled with three species: elemental mercury (Hg⁰), methylmercury (MeHg), and divalent (Hg II). The model integrates seasonality by including daily changes in hydrology, thermal stratification, temperature, light attenuation, solar radiation, dissolved organic carbon (DOC) concentrations, and phytoplankton concentrations. The mercury mass balance model was coupled with seasonality and a water quality model to estimate annual changes in lake and fish mercury concentrations for all mercury species. A schematic of the mercury mass balance model is shown below in Figure 2:

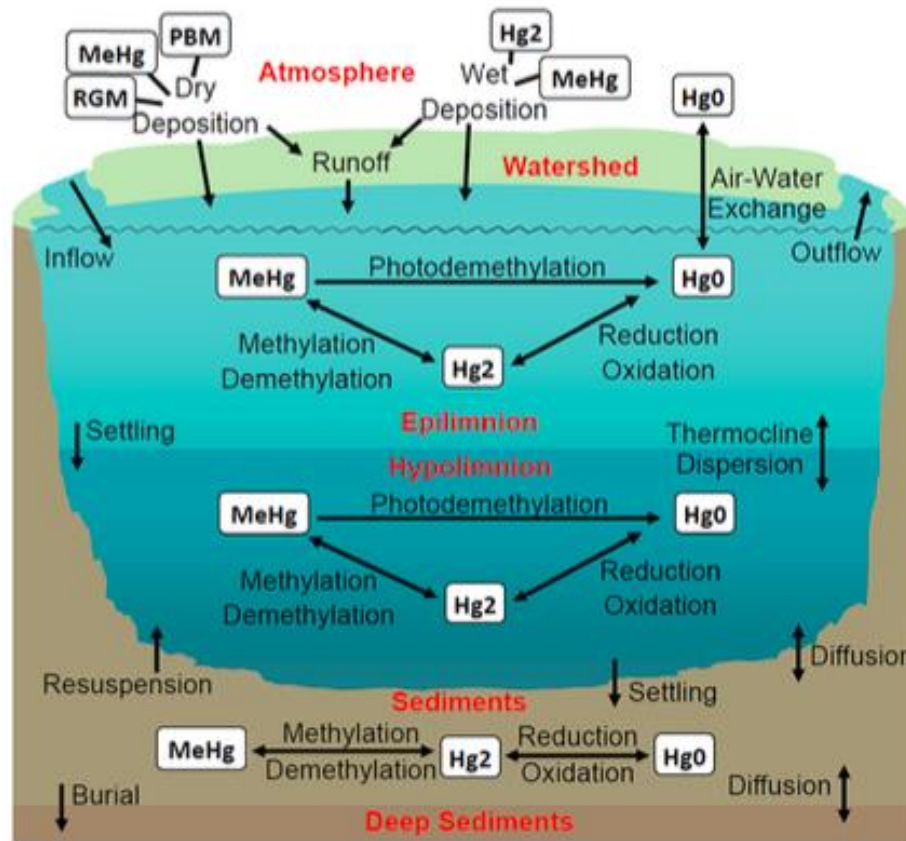


Figure 2. Schematic of mercury mass balance model developed by Hendricks; figure from the publication by Perlinger et al. (2018).

The mass balance model inputs include atmospheric deposition, discharge from tributaries, erosion, diffusion from lake sediments, and groundwater. The main removal mechanisms included outflow, volatilization, and burial into lake sediments. The atmospheric residence time is dependent on the mercury species. Elemental mercury has a long residence time of 2.7-12 months in the atmosphere which means that emissions are spread regionally to globally (Driscoll et al., 2007; Horowitz et al., 2017). Elemental Hg is oxidized in the atmosphere to Hg (II). The atmospheric residence time of Hg (II) is much shorter (0.5- 2 days); emissions of Hg (II) contribute to local and regional sources (Driscoll et al., 2007; Perlinger et al., 2018). The Hendricks model, however, does not incorporate the potential inputs of mercury from mining. It has not been analyzed how much of the Hg from mine discharges is transported to the lake vs. retained within the streams and catchment (Urban et al., 2018).

The model results indicated the hypolimnion has higher mercury concentrations than the epilimnion during stratification periods because of release from sediments and release from the epilimnion into the atmosphere (Hendricks, 2018). The complex biogeochemical cycle influences the production, destruction, and abundance of MeHg. MeHg is the toxic bioavailable form of mercury that bioaccumulates in ecosystems. The bioaccumulation of

MeHg is not only a function of regional or local deposition, but lake and watershed characteristics. Other factors affecting the bioaccumulation of MeHg include abundance of wetlands and forests, DOC, the oxygen concentration in bottom waters, lake trophic status and pH (Chen et al., 2005; Evers et al., 2007; Driscoll et al., 2007; Driscoll et al., 2010; Dittman, 2010; Kidd et al., 2013; Kidd et al., 2014). The watershed of Torch Lake promotes mobility and methylation of Hg rather than sequestration due to the abundance of wetlands that are sites of methylation and export DOC to lakes (Dennis et al., 2005; Evers et al., 2007; Depew et al., 2013). It is also suggested that these factors may cause the ecosystem to respond more slowly to changes in atmospheric deposition due to their organic-rich soils (Perlinger et al., 2018). The US Fish and Wildlife Service (U.S. FWS) National Wetland Inventory (NWI) for Torch Lake (figure 3) depicts the abundance of wetlands and forests in this area. Torch Lake has an abundance of wetlands in the catchment (13% of catchment area); this results in high DOC concentrations in the lake (8-12 mg/L) and influences the MeHg concentration.

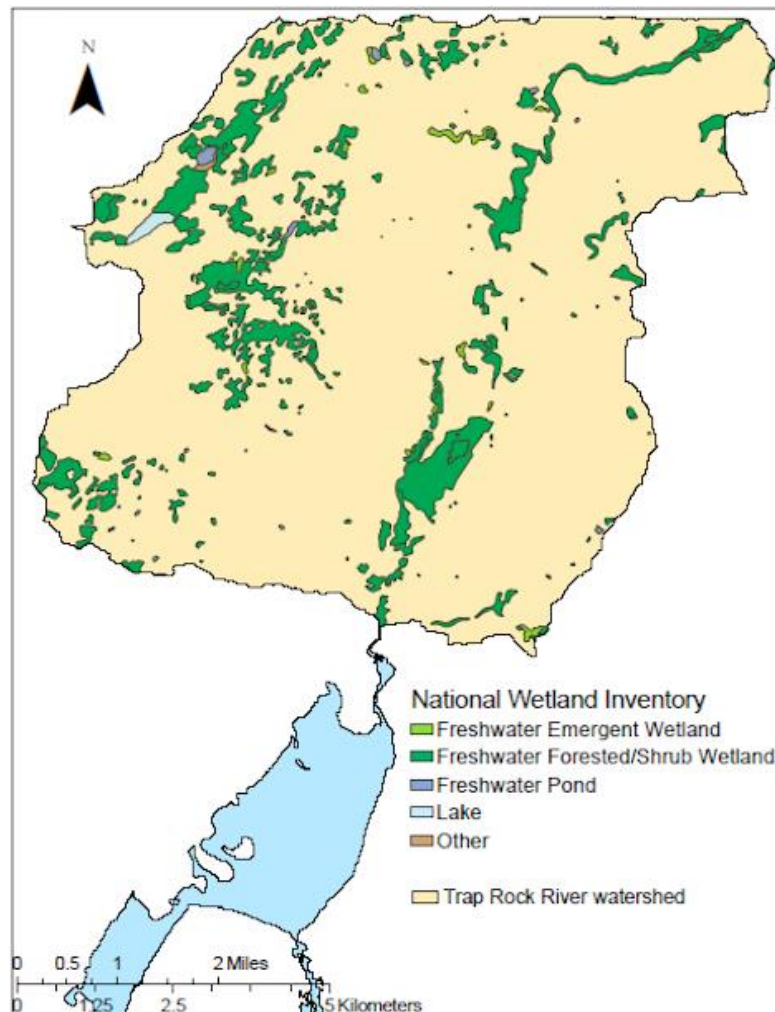


Figure 3. Trap Rock River watershed National Wetland Inventory (U.S. FWS)

It was observed that spring melt caused an increase in mercury leading to increasing mercury concentrations throughout the summer (Hendricks, 2018). The analysis of tributaries into Torch Lake determined Slaughterhouse Creek, Scales Creek, and Hammell Creek deliver much more total Hg than would be predicted based on their watershed areas. However, little of that mining-derived Hg was methylated prior to flowing into Torch Lake (Greene and Urban, 2023). Most of the MeHg flowing into Torch Lake is derived from wetlands along the Traprock River. Thus, of the total inventory of MeHg in the hypolimnion of Torch Lake approximately 50% could be derived from river inputs of MeHg into the lake. The other 50% was concluded to be derived from methylation within Torch Lake. As a result, this project examined the changes in fish concentrations due to the elimination of in-lake methylation.

1.2 Human and environmental health concerns

The fish consumption advisories are due to PCBs and mercury in Torch Lake. The persistent, bioaccumulative and toxic (PBT) substances pose threats to human and environmental health. The section below describes some of the physicochemical properties of PCBs and MeHg that cause toxicity.

1.2.1 PCB toxicity

Polychlorinated biphenyl (PCB) compounds are synthetic chemicals. PCBs are very stable molecules that are not easily broken down; they were used in a variety of industrial applications. The chemicals are composed of two phenyl rings with 1-10 chlorine atoms attached to these rings on the carbon atoms (2-6 and 2'-6') (Thomas, 2008). There are 209 congeners based on the number and position of the chlorine atoms, as shown in Figure 4.

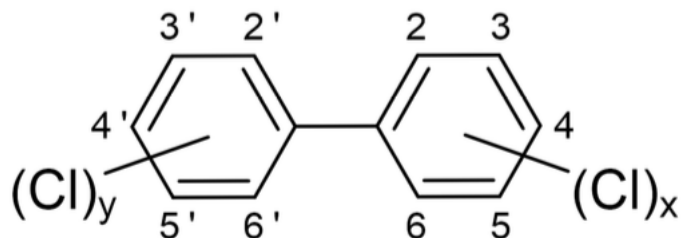


Figure 4. Polychlorinated biphenyl compound (PCB, 209 possible congeners) structure

The chemicals were primarily produced in the U.S. by the Monsanto Industrial Chemical Co., which produced mixtures of 50-100 PCB congeners called Aroclors. Aroclors are mixtures of congeners of differing chlorination wherein the heavier mixtures containing congeners having higher levels of chlorination tended to be used in the electrical industry and as lubricants (Thomas, 2008). The physicochemical properties of the compounds

include non-flammability, chemical stability, high boiling point, and low relative permittivity or dielectric constant.

The same properties that make PCBs useful cause them to be persistent in the environment. More chlorinated congeners tend to have lower aqueous solubility and vapor pressure in comparison to less chlorinated congeners (Thomas, 2008). PCBs are one class of chemical known as persistent organic pollutants (POPs) and are considered “legacy POPs” among the list of “dirty dozen” chemicals. POPs are characterized as being persistent in the environment, prone to long-range atmospheric transport and bioaccumulation in the food web, and toxic to living organisms (Schwarzenbach et al., 2017). PCBs are neutral compounds that favor bioaccumulation from air or water due to significant hydrophobicity, or “water fearing”. These non-polar compounds also tend to sorb to organic matter (particulate and dissolved) and their association with organic matter contributes to their persistence through shielding from chemical reactions such as photolysis. Association with dissolved organic matter also causes PCBs to be transported among environmental media including water and sediments. In addition, PCBs can undergo air-water exchange, leading to long-range atmospheric transport from sources.

PCB compounds are detrimental to human health, causing disruption to the endocrine, reproductive, and immune systems and neurobehavioral and developmental disorders in newborns and children and increased cancer risks (Schwarzenbach et al., 2017; Li et al., 2006). The EPA considers PCBs to be a probable human carcinogen. The final ban of PCBs came after Congress passed the Toxic Substances Control Act of 1976. However, legacy sources such as transformers and capacitors continue to emit PCBs (Schwarzenbach et al., 2017).

1.2.2 Mercury toxicity

Mercury is a naturally occurring element, but humans have greatly increased the amount circulating in the environment. The natural sources of mercury to the atmosphere include wildfires, volcanoes, and soil weathering (Driscoll et al., 2013). However, more than two-thirds of current emissions to the atmosphere originate from anthropogenic activities (Amos et al., 2013). Anthropogenic sources of Hg released into the atmosphere include fossil fuel combustion, artisanal mining, and metal smelting. Mercury is a local, regional, and global environmental issue as it is an Atmosphere-Surface Exchangeable Pollutant (ASEP; Perlinger et al., 2018).

Three common species of mercury include elemental (Hg⁰), divalent (Hg II), and (mono)methyl (MeHg). MeHg is the more toxic form; it is a known neurotoxicant that affects brain development, and it increases the risk of cardiovascular disease (Azim et al., 2011). MeHg bioaccumulates in organisms, and fish consumption is the major route of exposure for humans. The United Nations Minamata Convention on Mercury was adopted in 2013 to help reduce global emissions from anthropogenic sources. Mercury is the most common cause of fish consumption advisories in the U.S. In 2015, 36 state-wide mercury advisories were issued in the United States for freshwater fish from lakes, rivers or coastal waters.

1.3 Fish consumption advisories

Fish Consumption Guidelines (formerly termed Fish Consumption Advisories) have been in place for fish from Torch Lake for over 30 years. The public concern with regards to fish in Torch Lake began in 1972 with reports of tumors and deformities in walleye and sauger and persisted through the mid-1980s. After investigation into the cause for tumors by MTU and MDNR researchers, the Michigan Department of Health, and Human Services (MDHHS) imposed a fish consumption advisory in 1983. The advisory was viewed as a “precautionary measure” because the cause of tumors was unclear (MDNR, 1987b). It was suspected that the chemicals used in the flotation process, xanthates and polycyclic aromatic hydrocarbons (PAHs), from creosotes, were the causative agents. However, xanthates degrade quickly under the conditions in the lake, and therefore were unlikely to be the cause for reported tumors (Leddy, 1986). However, xanthates degrade quickly under the conditions in the lake, therefore, were unlikely to be the cause for reported tumors (Leddy, 1986). Walleye were stocked, and every five years monitored to determine if the causative agent remained. In 1990, the MDNR reported no presence of fish tumors, and no causative agents were found, and so the fish consumption advisory was then removed in 1993 (MDNR, 1990). However, in 1993 the Michigan Department of Community Health (MDCH) issued a generic statewide fish consumption advisory for mercury in inland lakes (MDCH, 1995). In 1998, a fish consumption advisory for PCBs in Torch Lake was added due to a change in reference dose. The fish consumption advisories for Torch Lake are summarized in Table (1; Urban et al., 2018).

Table 1. Summary of fish consumption advisories and guidelines for Torch Lake 1993-2014 (Urban et al., 2018).

Year	Fish	Population	Fish Consumption Advisory
1993-1997	SM Bass Walleye	All	Generic statewide inland lake advisory for Hg
1998 ¹	SM Bass	General Women/children	> 18” 1 meal/wk Hg, PCB > 14” 1 meal/wk > 18” 1 meal/mo
	N. Pike	General Women/children	> 30” 1 meal/wk Hg, PCB > 22” 1 meal/wk > 30” 1 meal/mo
	Walleye	General Women/children	> 22” 1 meal/wk Hg, PCB > 14” 1 meal/wk > 22” 1 meal/mo
2001 ²	SM Bass	General Women/children	All- 1 meal/wk Hg, PCB All- 1 meal/mo

	N. Pike	General Women/children	State-wide advisory Hg State-wide advisory Hg
	Walleye	General Women/children	All- 1 meal/wk Hg, PCB All- 1 meal/mo
2007/2008 ²	SM Bass	General Women/children	
	N. Pike	General Women/children	> 30" 1 meal/wk Hg, PCB < 30" 1 meal/wk > 30" 1 meal/mo
	Walleye	General Women/children	> 22" 1 meal/wk Hg, PCB < 22" 1 meal/wk > 22" 1 meal/mo
2011/2012 ³	SM Bass	General Women/children	> 18" 1 meal/wk Hg, PCB >14" 1 meal/wk > 18" 1 meal/mo
	N. Pike	General Women/children	> 30" 1 meal/wk Hg, PCB > 22" 1 meal/wk > 30" 1 meal/mo
	Walleye	General Women/children	> 22" NONE Hg, PCB > 14" 1 meal/wk > 22" NONE
2014 ⁴	SM Bass	All	> 0" 2 meal/mo Hg, PCB
	LM Bass	All	> 0" 2 meal/mo Hg, PCB
	N. Pike	All	> 0" 1 meal/mo PCB

	Sucker	All All	<16" 12 meal/mo Hg, PCB >16" 1 meal/mo Hg
	Walleye	All	<20" 12 meal/mo Hg, PCB >20" 1 meal/mo Hg

Source References Used in this Table: MDEQ (2007a)¹, MDEQ (2001, 2007b, 2008b)², MDCH (2011)³, and MDCH (2014a)⁴

Fish consumption is the primary pathway for human exposure to PCBs and MeHg. The MDHHS defines fish consumption advisories based on reference dose (RfD) and typical consumption rates by recreational anglers. However, Native American tribes have some of the highest documented fish consumption rates in the U.S., which causes a higher susceptibility to contaminants in fish (Perlinger et al., 2018). The Keweenaw Bay Indian Community (KBIC), an Anishinaabe tribe within the Great Lakes region, has the highest consumption rate of walleye during spring harvest (Gagnon, 2017). The desired rate for ceded territory for KBIC is 260 g/day without any consumption restrictions (Asher Consulting & Ad Hoc Analytics, 2016). The advisories for Torch Lake were meant to only be a temporary solution, but have been in place for 30 years, and there is no evidence of decreases in PCBs and Hg in fish tissue (Urban et al., 2018). More than 75% of the KBIC members report fish as a primary source of subsistence (Gagnon, 2017). The fish consumption advisories impact the harvesting rights of tribal members, as well as cultural identity and socio-cultural well-being (Gagnon, 2017). The contamination of Torch Lake is an environmental and social justice issue (Perlinger et al., 2018).

The KBIC and MDNR catch fish approximately every five years for the State's Fish Contaminant Monitoring Program (1988, 2000, 2007, 2013, 2018). The results are used by MDHHS for setting fish consumption advisories and by MI EGLE for assessing compliance. MTU researchers worked in collaboration with the KBIC and GLIFWC to analyze fish tissue for organic toxics to increase the frequency of measurements. The results suggest no decreasing trends in PCB concentrations in walleye based on normalization to lipid concentration, even after remedial work on the western shoreline (Urban & Perlinger, MTU Torch Lake Final Project Report, 2022).

The concentration of mercury in Torch Lake fish is greater than that in reference lakes, and there is evidence of mercury inputs because of the historical mining activities (Urban et al., 2018). The mercury in Torch Lake fish have not shown any systematic change through the years of the monitoring program. The potential sources of mercury from mining activities include exposed mine tailings, contaminated sediment, and runoff from upland catchment soils. However, analysis from tributaries in the Torch Lake watershed revealed that in watershed tributaries indicate that ~50% of MeHg is produced in the watershed, and the other ~50% is produced in the lake.

1.4 Remediation- past and future

The two main governmental agencies working on Torch Lake are Michigan Department of Environmental Quality (now part of Michigan Department of Environment, Great Lakes, and Energy, or MI EGLE) and the U.S. Environmental Protection Agency (EPA). In 1985 the International Joint Commission (IJC) designated Torch Lake as an Area of Concern (AOC). The IJC and EPA are responsible for all AOCs in the U.S.; the study, planning, and remediation of Michigan AOCs is the responsibility of Michigan DEQ (now EGLE). The AOC program defines problems as beneficial use impairments (BUI) to a water supply or water body. A Remedial Action Plan (RAP) defines the problem and proposes remedies to the site. The Michigan Department of Natural Resources (MDNR) investigated Torch Lake over the period 1983-1987. The 1987 RAP was prepared with three BUIs which included: presence of fish tumors in sauger and walleye, restrictions on fish consumption, and a degraded benthic community from contaminated sediment. The updated 2007 RAP removed the first BUI related to the presence of fish tumors (MDEQ, 2007a). However, due to the lack of funding and the narrow scope of the remedial investigation, Torch Lake is still listed as an AOC. The AOC did organize a citizen's group, Torch Lake Public Action Council (TLPAC), which has been working with both agencies since its formation in 1997.

The most prominent EPA program involved at Torch Lake is the national Superfund program. One year after the AOC listing, Torch Lake was added to the US EPA's National Priorities List (NPL) under the Comprehensive Environmental, Response, Compensation, and Liability Act (CERCLA). Torch Lake was subsequently declared a Superfund site. The first step in the Superfund program is the Remedial Investigation/Feasibility Study (RI/FS), which was conducted by Donohue & Assoc. Inc. from 1988 to 1992. The EPA is focused on human health hazards quantified as carcinogenic and noncarcinogenic hazards. The Record of Decision (ROD) was a plan to address the hazards on land, in surface water, or in drinking water supplies (Urban et al., 2018). Due to the complexity of the site, it was divided into three operating units (OU). The three OU include: Torch Lake stamp sands (OU I), Torch and Portage Lakes contaminated sediment (OU II), and other areas of Superfund site stamp sands (OU III). The primary focus was the human hazard from exposure to heavy metals in wind-blown stamp sands. It should be noted that the finalized boundary of the Superfund site did not include the western shoreline, upland industrial area, or eastern shoreline wetlands. Other contaminants identified during the RI/FS such as PCBs and asbestos were not included in the final ROD (Urban et al., 2018). The Superfund site was delisted in parts from 2002 to 2014, but it has also required emergency removal actions. The Emergency Response Division, which is separate from the Remediation Division, provides a quick response to contaminated sites that pose an immediate health threat. The remedial and emergency removal activities that were performed on Torch Lake are summarized below. Future solutions are then posed to assist with the delisting of the BUIs and to improve human-environment relationships.

1.4.1 Past remediation

The EPA reported the presence of submerged barrels along the shoreline near the smelter/coal dock in Hubbell and approximately 800 drums on the lake bottom and hired contractors to sample and remove the barrels (Kruger and Bartelt, 1992). In 1992, about 80 barrels were removed in addition to small amounts of contaminated soil (DMG, 1994). The remaining drums on the lake bottom were claimed to be empty and not removed (Urban et al., 2018).

After the initial RI/FS study (1998-1992) the EPA did not have sufficient funding, which caused a delay in remediation. Once funding became available, the remediation focused on capping the above-water stamp sands to reduce human exposure via inhalation of metal-rich dusts, and secondly to reduce the metal inputs into Torch Lake (US EPA, 1992). The remediation work started in 1999 with the stamp sands around Torch Lake (OU I). The stamp sands along the shoreline were capped with soil and vegetated. OU I sites were delisted in parts, Lake Linden in 2002 (partial) and 2007, Hubbell/Tamarack in 2004, and Mason in 2008 (Urban et al., 2018). The lake sediments (OU II) were delisted in 2002 without remediation. The No-Action Alternative was chosen with the anticipation that natural sedimentation would cover the contaminated sediments. Remediation of the lake bottom was deemed unfeasible, and the sediment contamination was thought to pose no human health threat (US EPA, 1994). Other sites within the Superfund OU-III (Boston Pond, Calumet Lake, and the North Entry) are still in the process of delisting.

After the delisting of Torch Lake as a Superfund site, the EPA has performed a series of Emergency Removal Projects to eliminate immediate human hazards due to heavy metals, PCBs and asbestos along the western shoreline. In 2007, discolored sediments from Lake Linden beach were removed due to elevated levels of PCBs, arsenic, lead, copper, barium, and cadmium (Urban et al., 2018). A year later, arsenic contaminated soil and 10 barrels of residual waste were removed from Mason stamp sands. In 2011-2014, after a site assessment the C& H Power Plant basement was cleared of asbestos and PCB-laden water (Urban et al., 2018). In 2014, the EPA removed asbestos at the Tamarack Stamp Mill (Ahmeek Mill) adjacent to a playground and residential area. Then, in 2016 residual process materials and soil samples with elevated PCB concentrations were removed in the Hubbell Processing Area (MDEQ, 2018). In 2019, the Lake Linden Recreational Area was dredged to remove metals (arsenic, lead) and PCB contaminated sediment; sediments were replaced with a sand and gravel cap (EPA, 2019a). In addition, the EPA removed PCB-contaminated residual processing materials from the Hubbell Processing Area (EPA, 2019b).

1.4.2 Future remediation

The Emergency Removal projects after the delisting of Torch Lake have left the residents confused about the hazards still present and the effectiveness of the remediation activities. The lake remains an Area of Concern with two BUIs: restrictions on fish consumption and degraded benthic community. Michigan Tech researchers collaborated with the KBIC and GLIFWC to analyze PCB concentrations in fish tissue from Torch Lake. The project aimed to measure fish contaminant concentrations more frequently to

use as tracers to determine if the remediation at Torch Lake has caused a decline in fish contaminant burdens. The results revealed that there was no indication of a decrease in lipid-normalized PCB concentrations in walleye. The PCB mass balance model points to a probable on-going source to Torch Lake (Mandelia, 2016). In 2019, the EPA signed a Great Lakes Legacy Act Project Agreement with Honeywell International, Inc. to perform a feasibility study for further remediation at Torch Lake. The focus is on the remediation of elevated PCB, lead, and arsenic concentrations in the lake sediments that contribute to the restrictions on fish consumption (BUI I). Remediation of the Lake Linden Recreational Area (LLRA) is expected to begin in 2024. A Feasibility Study is still ongoing for the Hubbell Processing Area.

The delisting of the contaminated sediments of Torch Lake (OU II) was done without remediation. The No-Action Alternative was chosen because recovery via natural sedimentation was anticipated (US EPA 1994). However, based on the low, actual sedimentation rate in the lake (McDonald & Urban, 2007), the natural attenuation would take approximately 800 years (Kerfoot et al., 2008). The copper- and trace metal-contaminated sediments have been shown to contribute to the degraded benthic community (BUI II). The settling of particles, erosion of the shoreline, and upward diffusion of metals from buried mine tailings significantly impact the time required for recovery from contaminated sediments (McDonald et al., 2010). An ongoing pilot study funded by the Great Lakes Restoration Initiative is reexamining the feasibility of capping and restoring the benthic habitat. The construction of the pilot study was completed in spring 2021 with monitoring taking place in fall 2021, 2022 and 2023. Strategic capping of lake sediments may be more cost-effective than capping of the entire lake. Planted macrophytes can stabilize the sediment caps, which would not only help restore the benthic community, but also expand wetland habitats that can generate DOC that can detoxify the contaminants in the lake (Urban et al., 2018). In addition, the area would be beneficial for fish spawning and habitat (Urban et al., 2018).

1.5 Bioaccumulation modeling

PCBs and MeHg are persistent, bioaccumulative, toxic (PBT) substances that pose risks to human and environmental health primarily via the consumption of contaminated fish. However, this risk was overlooked in the original risk assessment because of the lack of understanding of PCB bioaccumulation (Urban et al., 2018). The EPA ROD (1994) did not include human carcinogenic risk because it was assumed that because of the degraded benthic community there was no mechanism for entry of contaminant into the food web through bioaccumulation. It was not until the MDEQ updated 2007 Remedial Action Plan (RAP) that the risk associated with fish consumption of elevated PCB concentrations was reported. "Bioaccumulation" refers to accumulation of contaminants by all possible routes (Schwarzenbach, 2017). The routes of exposure for aquatic ecosystems include: passive uptake via respiration, and intake by contaminated food. The accumulation of PBTs is due to their fast uptake and relatively slow elimination. The concentration is magnified up trophic levels; therefore, PBT concentrations increase with an increase in trophic level. Bioconcentration typically refers to the passive uptake of pollutants from the water, especially for POPs, and has been shown to be more important in lower trophic

level organisms. The Bioaccumulation Factor (BAF) for phytoplankton can be on the order of 10^2 - 10^6 from water concentrations (Schartup et al., 2018). Bioaccumulation models show the transfer of contaminants from water and sediment to organisms; they have proven to be useful regulatory tools (Douillard et al., 2009). Bioaccumulation models have been used to develop remediation targets for contaminated ecosystems, and to assess exposure of pollution sources and the responsiveness of aquatic ecosystems to cleanup efforts (Arnot & Gobas 2004).

Mass balance models determine the fate and transport of compounds in the system considered. Numerous models have been developed to predict bioaccumulation of chemicals into aquatic organisms that fall into two distinct groups (Barber, 2008). Earlier models were equilibrium-based, and ratios of steady-state concentrations in organisms to those in selected exposure media were computed: bioaccumulation factors (BAFs), biomagnification factors (BMFs), and biota-sediment accumulation factors (BSAFs). These models assume either one route of exposure or that the relative contributions of multiple exposure pathways are constant (Barber, 2008). Other studies included detailed, process-based, non-equilibrium, differential equation models that calculated uptake as a function of aqueous and dietary exposures (Barber, 2008; Arnot & Gobas, 2004).

Bioaccumulation of PCBs and MeHg are dependent on factors other than the environmental media concentrations alone including water temperature and species characteristics (body weight, length, age, and lipid content). Kinetics-based models consider these factors in estimating the bioaccumulation burdens. Non-steady state kinetic models can be useful to account for changes in contaminant loadings, food web dynamics and climate change responses.

1.6 Objectives and research questions

The objectives of this thesis are to confirm field evidence suggesting that sources of PCBs and MeHg to Torch Lake fish are both atmospheric and mining-related and to estimate the contribution from each source to the bioaccumulated burdens in fish. In addition, this thesis project uses modeling experiments to address the specific research questions posed below. The overall question guiding this research is, “When will the fish be safe to eat?”

This project has been funded by a subcontract with the Keweenaw Bay Indian Community through a grant from the Bureau of Indian Affairs (BIA), “Methyl Mercury Source and Availability in the Torch Lake Watershed.” The goals of this project align with the NSF-funded TLS project, “Bridging knowledge systems and expertise for understanding the dynamics of a contaminated tribal landscape system,” to better understand human-environment relationships. The TLS project builds a partnership between Michigan Tech researchers and the tribal community to examine the impacts of anthropogenic toxic contamination and climate-related changes. This thesis project can assist with understanding the impacts of contamination from historical mining activities on food web biomagnification and human-environment relationships. In addition, the MI EGLE Area of Concern Great Lakes Restoration Initiative funded project, “Data Gap on Responses of Fish PCB Content to Remedial Actions,” provided useful insights and data for this thesis project. The project highlighted the use of fish as contaminant tracers in the

environment and examined remediation effectiveness.

This project focuses on both MeHg and PCBs in fish in Torch Lake and used bioaccumulation modeling to better understand the relationships between contaminant concentrations in fish, remediation of toxics inputs to Torch Lake, and some dynamics of fish behavior.

The research questions that are posed in this study are:

- (1) What are the predicted PCB and MeHg concentrations in Torch Lake fish if remediation now under consideration is performed?
- (2) How long must fish reside in Torch Lake in order to acquire the observed PCB and MeHg concentrations?
- (3) Can the walleye lipid content decline explain the decline in walleye PCB concentrations?

The second question was posed by the Tribe because earlier work has shown that fish move back and forth between Torch Lake and the Keweenaw Waterway. To answer both Questions 1 and 2, a food web model was developed that predicts contaminant concentrations in different trophic levels in response to concentrations in the lake water. For PCBs, a mass balance model was employed to predict dissolved PCB concentrations as a function of inputs to the lake. For MeHg, concentrations recently measured in the lake were used to drive the bioaccumulation modeling. The potential for remediation with regards to MeHg was assessed based on the findings of the MeHg mass balance developed in the BIA project, Methylmercury source and availability in the Torch Lake watershed. The third question was examined regarding the recent walleye PCB measurements in MTU TLPAC results (Urban and Perlinger, 2022). The walleye PCB lipid-normalized concentrations suggested that there is no evidence of a decline in fish PCB concentrations as a result of the remediation actions at Torch Lake. The influence of walleye health conditions on the bioaccumulation of PCBs was analyzed based on fish lipid content.

2 Methods

The two Torch Lake Area of Concern (AOC) beneficial use impairments (BUIs) that are still in place today include fish consumption advisories and degradation of the benthic, or bottom dwelling, community. The focus of this thesis project is the aquatic ecosystem responses to remediation activities performed in Torch Lake targeting sources of PCBs and Hg so that the fish consumption advisories are no longer needed. In this project separate mass balance models were created for PCBs and MeHg to answer research questions related to the ecosystem responses. PCBs and MeHg differ in their mechanisms of bioaccumulation; therefore, two different model structures were used (Li et al., 2015). The PCB model follows the well-known Arnot & Gobas (2004) model for organic contaminants in aquatic ecosystems. The mercury bioaccumulation model adopts the phytoplankton and zooplankton model from Schartup et al. (2018), in addition to the Trudel & Rasmussen (2001) model for MeHg in fish. The models were validated with available PCB and mercury concentration measurements in Torch Lake walleye and an existing bioaccumulation model, AQUAWEB. The sensitivity of the model parameters was estimated with the parameter perturbation method, and uncertainty analysis followed the Monte Carlo simulation method. This thesis builds upon two earlier Master's theses conducted at Michigan Technological University (MTU), one involving a mass balance on PCBs in Torch Lake water by Ankita Mandelia (2016) and one modeling PCBs in area lake fish by Emily Sokol (2018). In this thesis research, the mass balance model of Mandelia (2016) is coupled with a bioaccumulation model developed in Matlab to estimate the temporal trends in PCBs and MeHg in Torch Lake walleye. The models were run under different scenarios of remediation to determine the recovery responses of the Torch Lake aquatic ecosystem.

2.1 Site description

This project is focused on the designated Area of Concern (AOC), Torch Lake, Houghton County, within the historic copper mining district on the Keweenaw Peninsula of the Western Upper Peninsula of Michigan. The lake is oligotrophic, dimictic, and experiences ice cover in the winter months. The lake has a surface area of 9.73 km² and volume of 0.15 km³, which is close to half the original lake volume due to stamp sand deposits (U.S. EPA, 1992). The maximum depth is 40 m. The Trap Rock River is the major surface inflow that deposits nutrients and contaminants from the upland watershed. The remote lake has a total watershed area of approximately 81.4 km² that is 13% wetland area (estimated with ArcGIS and National Wetlands Inventory). At the beginning of the copper mining era, Torch Lake Canal Co. (owned by C&H) cut a canal that connects Torch Lake, Portage Lake, and the Keweenaw Waterway that opens a passage to Lake Superior. Figure 5 shows the 2016 National Land Cover Data (NLCD) from the National Map Viewer with 30m spatial resolution (U.S. Geological Survey, 2016). The developed area on the western shoreline of Torch Lake is surrounded by forested land.

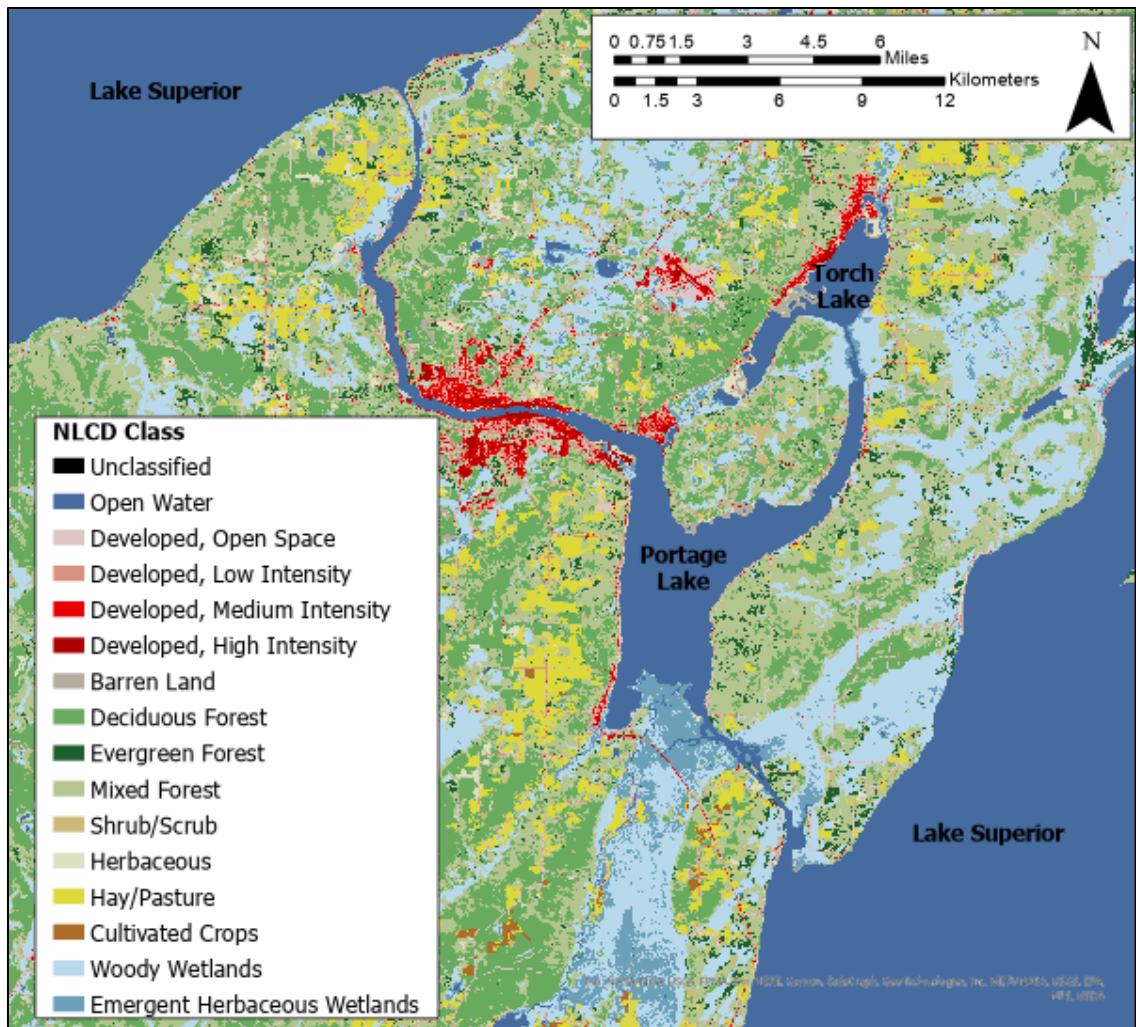


Figure 5. Torch Lake 2016 National Land Cover Data (NLCD) from the National Map Viewer with 30m spatial resolution (U.S. Geological Survey, 2016).

The remote lake was once the domain of the Ojibwe fishing peoples before the early explorers arrived in the 1700s to search for the native copper within the region. The Ojibwe settlements in the Keweenaw Bay at the southeastern base of the Keweenaw Peninsula used the area as an important resource base during the summer months (Urban et al., 2018). Although, there were no mines located directly on the lake, the western shoreline of Torch Lake was an industrial district for copper mining processes (milling, smelting, reclamation, leaching, and flotation) and deposited stamp sands and other industrial wastes in Torch Lake (Urban et al., 2018). Torch Lake was used as a disposal site with the attitude of “out-of-sight, out-of-mind” (Zawisza, 2018). The copper mining in this district was supported by the U.S. federal government because it played a critical role in the war effort. The federal government assumed control of the Keweenaw Waterway and enacted the 1899 Rivers and Harbors Act to restrict dumping of soil and rock to areas inside of the harbor lines; however, Torch Lake was specifically exempted in this legislation (Urban et al., 2018). The government’s aim was to discourage the

dumping of tailings into the Houghton/Hancock waterway. Torch Lake remained under control of the mining companies and provided an unlimited supply of water for copper processing and a site for dumping tailings. Again, from the period of the 1940s to 1965 Torch Lake was exempted from Rivers and Harbors Act regulations. Thus, the air, soil, lake sediments, groundwater, and surface water of Torch Lake and surrounding area were contaminated with physical and chemical hazardous wastes that have altered the biogeochemistry of the watershed. Once the mining activities ceased, human and environmental health concerns arose. The initial public concern over fish tumors led to studies from governmental agencies and MTU researchers. In 1985 the International Joint Commission (IJC) for the Great Lakes designated Torch Lake as an Area of Concern (AOC), and one year later the EPA listed the site on the National Priorities List under the CERCLA (Superfund) program. The remediation of Torch Lake is ongoing, even after the Superfund delisting in parts in 2002-2014. Because Torch Lake is still listed as an AOC with two BUIs present (fish consumption and degradation of benthos) that threaten human and environmental health, it is monitored and investigated. This thesis project supports the project goals of the NSF-funded TLS project, “Bridging Knowledge Systems and Expertise for Understanding the Dynamics of a Contaminated TLS.” The interdisciplinary project combines scientific and traditional indigenous knowledge to minimize contamination risk, better understand climate-related consequences, and support human-environment relationships.

2.2 Data availability

This section of the methods chapter summarizes the available datasets for PCBs and Hg that have been used for mass balance modeling (Mandelia, 2016; Hendricks, 2018; Urban et al., 2018). There have been multiple governmental agencies and nongovernmental groups who have been working on Torch Lake and sampling of the contaminants in different environmental media (e.g., air, surface water, groundwater, lake sediments, soil, and watershed tributaries).

The PCB mass balance model of Mandelia (2016) compares dissolved concentrations computed to be present based on inputs to and outputs from different sources, which are in turn based on measured concentrations in the sediment, groundwater, shoreline soil, and atmosphere, to SPMD measurements, which represent the dissolved (bioavailable) aqueous concentration (Mandelia, 2016). This project utilized Mandelia’s PCB mass balance model to predict the reduction in dissolved phase concentrations based on the most recent atmospheric PCB concentration measurements. The environmental input data used in the PCB mass balance model is summarized below, as is the fish tissue concentration measurement data that were used to validate the PCB bioaccumulation models. The follow sections describe the sources of the PCB atmospheric concentration data, dissolved PCB concentration data, soil sampling PCB data, sediment survey PCB data, and fish tissue PCB concentration data.

The mercury biogeochemical cycle is more complex relative to PCBs due to its more complex fate and transport mechanisms (Hendricks, 2018). The mercury mass balance model for Torch Lake did not account for the potential input sources from mining

activities. Therefore, instead of coupling the bioaccumulation model with the mass balance model, the MeHg dissolved concentrations in Torch Lake measured in 2021 by MDEQ were used to drive bioconcentration in the model. The modeling scenarios were based on empirical measurements from tributaries in the Torch Lake watershed (Greene and Urban, 2022). The model-predicted fish concentrations were validated against the Fish Contaminant Monitoring Program for Hg as described below.

2.2.1 Atmospheric Concentration Data

PCBs and mercury are both persistent bioaccumulative toxic substances (PBTs) that can undergo long-range atmospheric transport as an atmosphere-surface exchangeable pollutant (ASEP) and therefore, are global concerns (Perlinder et al., 2016). The mercury deposition in the region is monitored by the National Atmospheric Deposition Program's Mercury Deposition Network. PCBs are monitored by the Great Lakes Integrated Atmospheric Deposition Network (IADN) (Blanchard, 2021). The scope of this project included the impact of remediation activities on the walleye fish concentration. However, the cycle of PCBs within Torch Lake water column influences the uptake by aquatic organisms via bioconcentration of the dissolved phase, and contaminants deposited from the atmosphere into the lake must be accounted for to achieve a mass balance. Thus, the fluxes of PCBs into and out of Torch Lake were estimated using the mass balance model of Mandelia (2016) and coupled with the bioaccumulation model. Here, the atmospheric concentrations of PCBs over Torch Lake were updated in Mandelia's model from 2005 to 2021, to reflect the most recent situation.

The Environmental Protection Agency's (EPA's) Eagle Harbor IADN monitoring station on Lake Superior was used to approximate the atmospheric concentrations of PCBs over Torch Lake due to the proximity of the two lakes. Figure 6 displays the atmospheric trend in PCBs at the Eagle Harbor IADN station throughout the year 2021 (green) and averaged measurements 1991-2021 (blue). This thesis project focused on seven selected PCB congeners (33, 52, 99, 101, 149, 153, and 180) due to the limited number of congeners ($n = 12$) detected in Torch Lake and nearby control lakes (Huron Bay, Dollar Bay, and the north and south entrances of the Portage Canal) in 2005 with the deployment of semipermeable membrane devices (SPMD; MDEQ, 2006b). The red outline indicates the congeners analyzed in this study. There has been an overall decline in atmospheric concentrations at the Eagle Harbor IADN station (Figure 6). It should be noted that the PCB congener 11 is present in paint, thus contributing to its large presence in the air not related to mining activities (Guo et al., 2009). In addition, PCB 149 co-elutes with PCB 123, and PCB 153 co-elutes with PCBs 132 and 105. The air data consists mostly of lighter congeners, due to their greater tendency to volatilize in comparison to heavier congeners. Because the less-chlorinated (lighter) congeners tend to undergo global dissemination from more distant sources, the distribution of PCB congeners can indicate local sources.

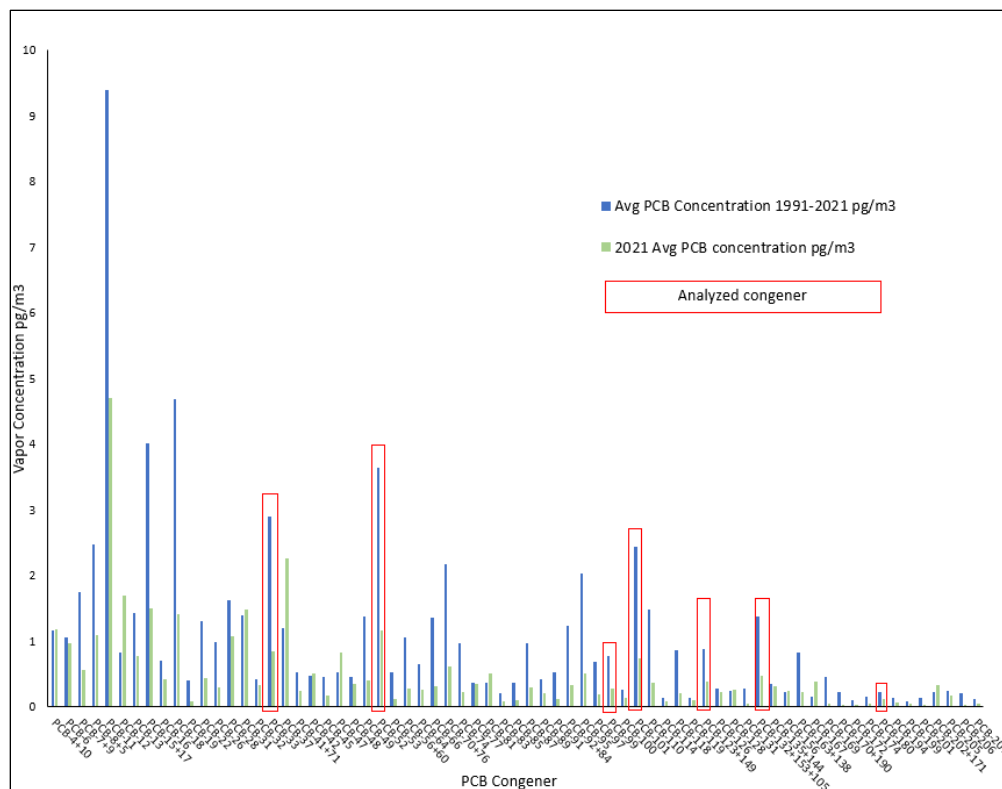


Figure 6. PCB congener vapor concentration (pg/m³) measured from the Great Lakes Integrated Atmospheric Deposition Network (IADN) averaged for the Eagle Harbor Station 1991-2021. Congeners within red boxes (PCB 33, 52, 99, 101, 149, 153, and 180) were modeled in this study.

2.2.2 Dissolved PCB and MeHg Concentration Data

In 2005 the Michigan Department of Environmental Quality (MDEQ), which is now part of the Michigan Environment, Great Lakes, and Energy (MI EGLE), deployed semipermeable membrane devices (SPMDs) for one month in the water columns of Torch Lake and four control sites: Dollar Bay, Huron Bay, and the north and south entrances of the Portage Canal. (GLEC, 2006). The passive samplers consist of an oil within a plastic sheath. Similar to their partitioning into lipids, PCBs partition into the SPMD oil from the lake water (Urban et al., 2018). Due to the diffusion mechanism, the extracts are an indirect measurement of dissolved concentrations in the lake water. The United States Geological Survey (USGS) developed a model to estimate the dissolved concentrations from SPMD extract concentrations based on first-order kinetics that was applied to Torch Lake by Mandelia (2016). These dissolved values were used as a comparison of the PCB mass balance model-predicted dissolved phase concentration. High concentrations of PCBs were detected along the western shore near the Hubbell smelter site (MDEQ, 2006; 2007). The SPMDs congener ratios indicate PCBs of local rather than airborne origin (Urban et al., 2018). The EPA simultaneously collected sediment samples at the same locations as the SPMD sampling locations for PCBs (Urban et al., 2018). In addition, the SPMD samples indicated higher concentrations in

Torch Lake as compared to control sites (MDEQ, 2007). Therefore, these results prompted further studies to identify local sources of PCBs.

The only available measurements of MeHg for Torch Lake are measurements by MI EGLE in 2021 (EGLE, unpub.). The measurements occurred in the summer months (6/30/21 - 7/22/21) when the lake was stratified. Higher MeHg concentrations were observed in the hypolimnion as compared to the epilimnion of the lake. Therefore, the average MeHg concentrations in the hypolimnion during the summer months of 2021 was used to drive the MeHg bioaccumulation model. It should be noted that in the winter, the concentrations throughout the entire water column are expected to be below the detection limit. The bioaccumulation burdens of PCBs, and to a greater extent MeHg, are dependent on the lake and watershed characteristics (Clayden et al., 2013; Clayden et al., 2014; Perlinger et al., 2018).

2.2.3 Soil Sampling Data

The most recent soils sampling for Torch Lake PCBs was performed in 2007 by Michigan Department of Natural Resources (MDNR) hired consultants, Weston Solution, Inc. (Weston Solutions, 2007) and in 2011 by MI EGLE. The groundwater input was calculated using measured Aroclor mixtures 1254 and 1260 and converted into congener concentrations using the weight fractions of congeners in the Aroclor mixtures reported in Frame et al. (1996; Mandelia, 2016). The ground water input flux was assumed to be relevant for only six weeks of the year, during snowmelt. PCB concentrations above the quantitation limit were found in soil and groundwater near historical industrial sites, which points to the source from electrical equipment (Urban et al., 2018).

2.2.4 Sediment Survey Data

The MI EGLE conducted a sediment chemistry survey in 2007 and the EPA conducted a lake wide sediment Aroclor investigation in 2008 (MDEQ, 2008; U.S. EPA, 2009). The sediment concentrations were usually reported as Aroclor 1254, and thus Mandelia's (2016) mass balance model originally converted to congener concentrations using the average weight percentages reported by Frame et al. (1996). The model also estimates the resuspension flux by subtracting the estimated burial flux measured by McDonald et al. (2010) from the measured settling flux. The EPA determined that the PCB concentrations detected in the surficial sediment in Hubbell/Tamarack area in 2007 and 2008 represented “an ongoing source of PCBs to Torch Lake [that] cannot be ruled out” (EPA, 2009). The contamination from the mining activities have caused elevated PCB concentrations in the sediment of two main regions (Mandelia, 2016), and thus Mandelia's mass balance model separated the sediment areas into two regions. Region 1 represents the Hubbell Processing Area (HPA) of the C & H Lake Linden Operations Area and Region 2 represents the Lake Linden Recreational Area (LLRA). There has been a series of Emergency Removal projects: 2007 Lake Linden beach, 2008 Mason stamp sands, 2001-2014 C& H Power plant in Lake Linden, 2014 Tamarack stamp mill (Ahmeek Mill), 2016 HPA removal of contaminated soils, and 2019 LLRA dredging of lake sediments that were designed to remove PCBs from Torch Lake sediments (Urban et al., 2018).

Beginning in 2013, the Remediation and Redevelopment Division (RRD) Upper Peninsula District office of the MI EGLE conducted the Abandoned Mining Wastes (AMW) project. The aim of this on-going project is to remediate the various sediment, soil, and water media of the different contaminants. The western shoreline was divided into three sections (Calumet & Hecla-Lake Linden (CHLL); Calumet & Hecla-Tamarack City (CHTC); Quincy-Mason (QM)) (Urban et al., 2018). The project provided a more complete representation of the extent of contamination and developed an interactive online data viewer. The sediment measurement values were reported in the Supplemental Site Investigation report from The Mannik & Smith Group, Inc (MDEQ, 2018). The highly contaminated sediment regions were divided into the Hubbell Processing Area (Region 1), and Lake Linden Recreation Area (Region 2), and added to the PCB mass balance model. Figure 7 displays the AMW project results along the western shoreline and the areas with elevated PCB concentrations.

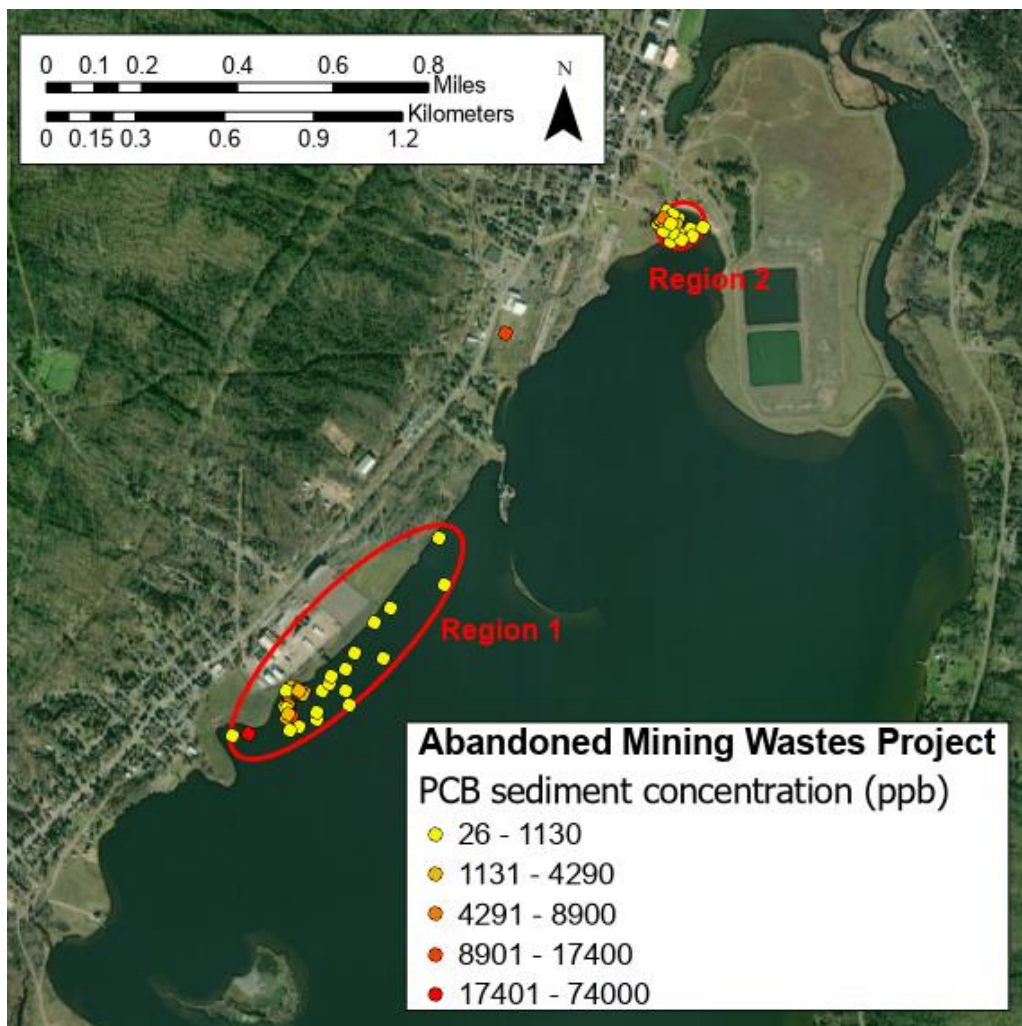


Figure 7. EGLE Abandoned Mining Wastes (AMW) project total PCB concentrations in Torch Lake sediment separated into Region 1(HPA) and Region 2 (LLRA) areas with elevated PCB concentrations.

2.2.5 Fish Tissue Concentration Measurements

Beginning in 1988, the MDNR analyzed fish tissue and, as a precautionary action listed fish consumption advisories due to the unknown cause of fish tumors on the walleye and sauger. The BUI for fish tumors was later removed, but the BUI for fish consumption remains in place today due to mercury and PCB contamination. In 1998, the Michigan Department of Community Health (MDCH) issued fish consumption advisories for Torch Lake for PCBs and Hg in walleye, northern pike, and small mouth bass. In 1993, Michigan issued a statewide advisory due to elevated mercury concentrations in predator fish (MDCH, 1995). The additional advisory related to PCBs was not based on new measurements but rather was created to account for a change in 1998 in PCB risk reference dose (Urban et al., 2018). The contaminant concentrations including PCBs and Hg in Torch Lake and control sites (Portage Lake and Huron Bay) have been measured by the State in 1988, 2000, 2007, 2013, and 2018. Prior to 2000, the State's Fish Contaminant Monitoring Program determined PCBs as Aroclor mixtures (Urban et al., 2018). This project focuses on the top predator walleye data; thus, the walleye tissue concentrations for PCBs and Hg were compiled and averaged for years 2000, 2007, 2013, and 2018.

The Natural Resources Department of the Keweenaw Bay Indian Community (KBIC) has been collecting ten walleye per year for the Hg monitoring by the Great Lakes Indian and Wildlife Commission (GLIFWC) for years 2018-2021 (Urban and Perlinger, 2022). The walleye Hg concentrations for Torch Lake analyzed by the Lake Superior Research Institute at University of Wisconsin (LSRI) in Superior were compiled and averaged. The measured walleye concentrations from EGLE and GLIFWC are shown in Figure 8 as a function of walleye length.

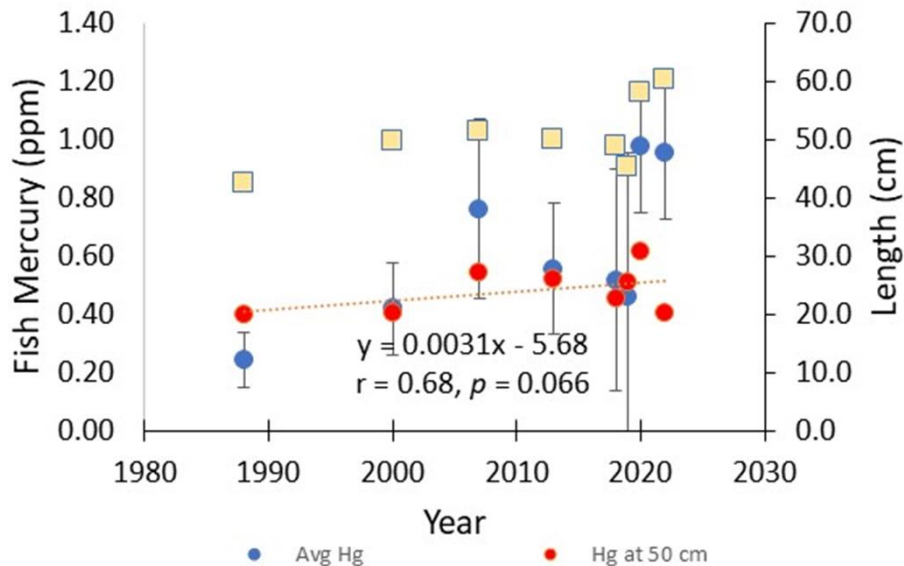


Figure 8. Average walleye mercury concentrations ($\mu\text{g/g}$ ww or ppm) in Torch Lake as a function of walleye length (cm) measured by MI EGLE and GLIFWC (Urban, unpub.).

In order to provide a higher frequency of fish contaminant monitoring than had previously been measured by the MDHHS, MTU conducted a National Science Foundation (NSF)-funded project in collaboration with the KBIC and GLIFWC. The project obtained Hg-analyzed archived homogenized fish fillets collected from Torch Lake 2018-2020, and additional samples collected in 2022. Note that the samples from 2021 were misplaced and never delivered to LSRI for analysis, and therefore were excluded from the Hg and PCB analyses. The project, “Data Gap on Responses of Fish PCB Content to Remedial Actions,” additionally measured the walleye fish lipid content to normalize the PCB concentrations and compare to the Michigan Department of Health & Human Services (MDHHS) measurements. The PCB concentrations were compiled and averaged for each year. Figure 9 displays the time trend in walleye lipid content in Torch Lake fish. The results indicate that a long-term decrease in lipid content on the order of a factor of ten is observed in Torch Lake walleye. It is common to normalize PCB concentrations to lipid content due to the tendency to accumulate in fat-rich tissues, thus eliminating differences caused by lipid content. The lipid-normalized PCB concentrations in Figure 10 show no evidence of decline in concentrations as a result of the remediation within and along the shoreline of Torch Lake (Urban and Perlinger, 2022).

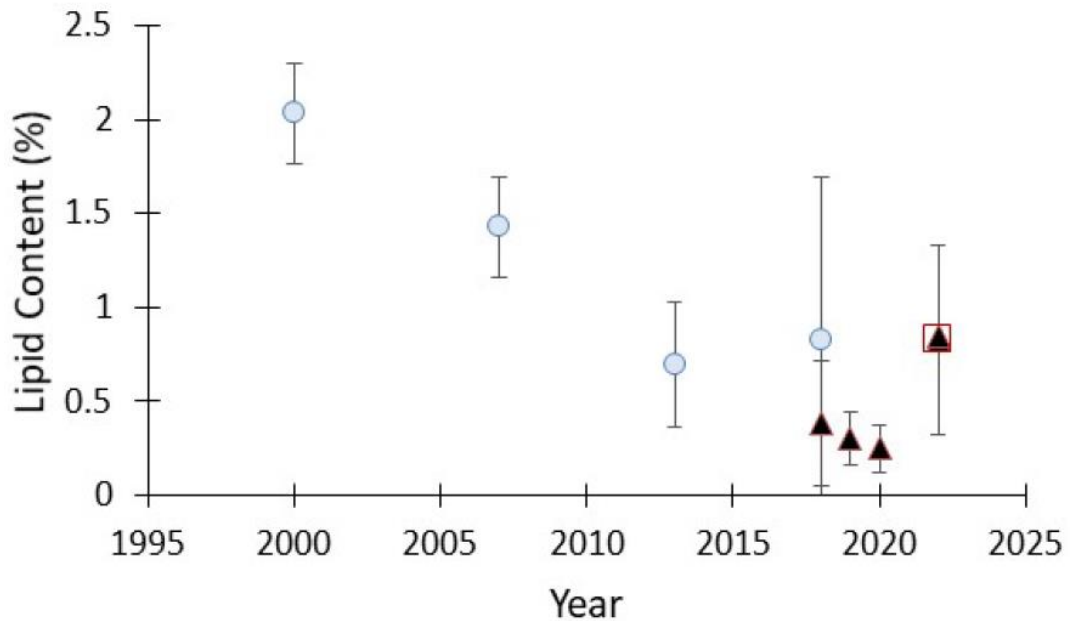


Figure 9. Temporal trend in Torch Lake walleye fish lipid content periods 2000-2018 (MI EGLE) and 2018-2022 (MTU TLPAC). Error bars represent 95% confidence intervals (Urban and Perlinger, 2022).

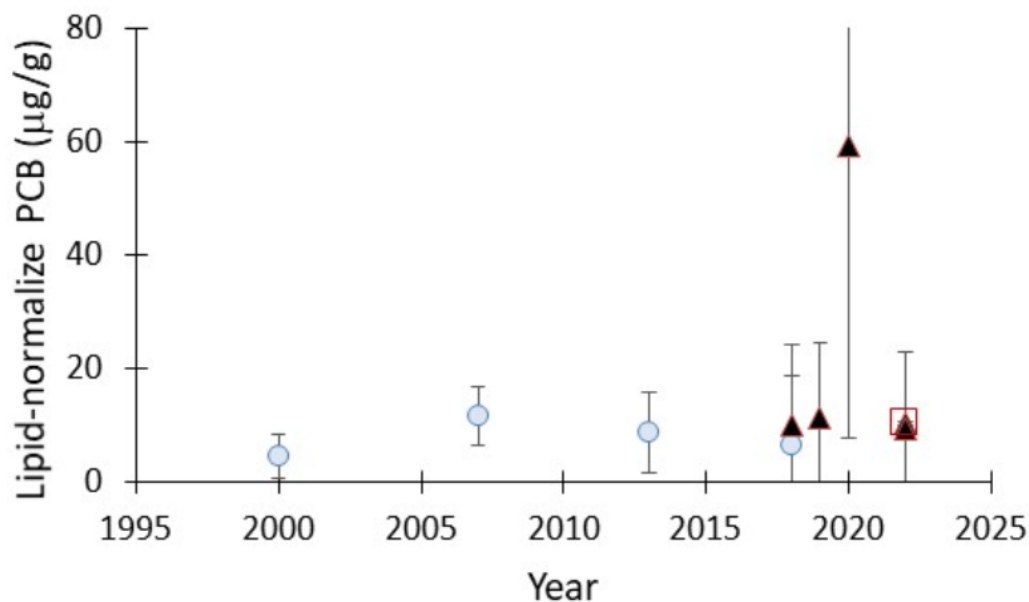


Figure 10. Temporal trend of lipid-normalized PCB concentrations in walleye from Torch Lake. Error bars represent 95% confidence intervals (Urban and Perlinger, 2022).

2.3 Bioaccumulation Modeling

Bioaccumulation models link contaminated environments to aquatic organisms. These models can be used to assess the exposure of biota affected by pollution sources and determine the responsiveness to cleanup efforts (Arnot and Gobas, 2004). This project developed bioaccumulation models to investigate the relationship between PCB and Hg concentrations in the water and sediments and resulting concentrations in the organisms of Torch Lake. The model is used as a supplementary tool to evaluate human health and ecological risks with different scenarios. Two different models were created due to the different bioaccumulation mechanisms for these contaminants. The section below discusses the Arnot & Gobas (2004) model adapted for PCB congeners in Torch Lake. Then, the bioaccumulation model for MeHg is presented as a combination of Schartup et al. (2018) for lower trophic organisms, and Trudel & Rasmussen (2001) for Torch Lake forage and predator fish species.

2.3.1 PCB modeling

A non-steady state kinetic bioaccumulation model for PCB congeners was created and based on the well-known Arnot & Gobas (2004) model for nonionic, hydrophobic organic chemicals (HOCs) in aquatic organisms. The model estimates the transfer and distribution of organic chemicals within a single organism to assess the exposure of aquatic organisms (Arnot & Gobas, 2004). The model is relatively simple with limited number of needed site-specific environmental and biological input parameters, reducing the amount of model uncertainty. The model was built for chemicals with a log K_{ow} value between 1 and approximately 9, and K_{ow} is the only required input of chemical characteristics. The uptake mechanisms include bioconcentration from the dissolved and

biomagnification from the diet. The elimination mechanisms included respiration, fecal excretion, and metabolic transformations. The kinetics processes are regulated depending on the organism body weight, lipid content, and chemical absorption efficiencies. For example, chemical absorption efficiencies are a function of biological (lipid content), abiotic (temperature), and chemical properties (log Kow) The bioaccumulation of the PCB congeners results from fast uptake rates and slow elimination rates. The model outputs time varying PCB congener-specific bioaccumulated burden in an individual organism. Bioaccumulation is defined as a food web process; however, the actual mechanism occurs at an individual scale (Li et al., 2015). A schematic of the individual organism model is shown in the figure below.

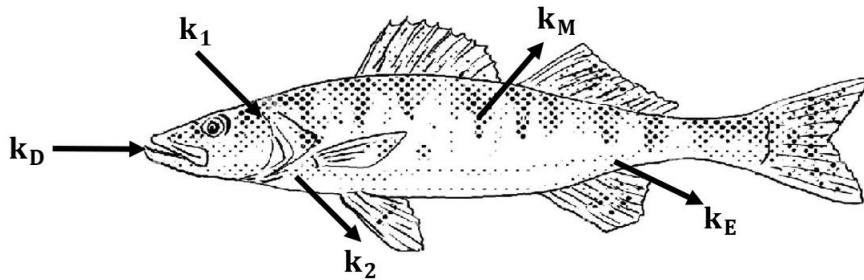


Figure 11. PCB bioaccumulation model schematic for an individual fish (Arnot and Gobas, 2004). The bioaccumulation results from the difference between uptake and elimination rates. Uptake occurs via partitioning into the gills during respiration (k_1) and by ingestion of prey containing PCBs (k_D). Elimination includes respiration (partitioning out of the organism through the gills) (k_2), fecal excretion (k_E), and metabolic transformation (k_M). (<https://www.shutterstock.com/image-illustration/cartoon-style-line-drawing-walleye-sander-2204922671>)

The mass balance equation for the model is given below for the bioaccumulation of PCBs in walleye from the Torch Lake ambient environment (Equation 1). The definitions for each of the variables included in the model are outlined in Table 2.

$$\frac{dM_B}{dt} = \left\{ W_B * \left(k_1 * [m_o * C_{WD,O} + m_p * C_{WD,S}] + k_D * \sum (P_i * C_{D,i}) \right) \right\} - (k_2 + k_E + k_M) * M_B \quad (1)$$

The key assumptions of the model are 1) homogenous distribution of the PCB compounds within the organism, 2) the organism as a single compartment, and 3) negligible chemical elimination via egg deposition or sperm ejection. The adaptation of the model to Torch Lake ignored the uptake of the contaminants from pore water in the sediments, because of the degraded benthic community in Torch Lake as a result of stamp sands sediments. The fraction of respiration of pore water (m_p) in the sediment was set equal to zero. Therefore, the model estimates the transfer of PCBs from the water column through an aquatic food chain. The food chain structure was simplified to four trophic levels (phytoplankton, zooplankton, forage fish, and predatory fish). The higher-

trophic-level organism diet was assumed to be 100% of the lower-trophic-level organism. Feeding relationships vary between species, life stage of species, time of year, and other factors (Gobas & Arnot, 2010). Therefore, it is not possible, or necessary to include all species in Torch Lake, rather to represent the trophic transfer between trophic levels 1-4. The phytoplankton at the bottom of the food web were assumed to have a diet uptake rate of zero, and an insignificant fecal elimination rate constant (Arnot & Gobas, 2004). The metabolic transformation rate constant (k_M) was assumed to be zero because PCBs are nonmetabolizable compounds. The “pseudo-elimination” of growth was ignored in this model and will be discussed later. The limitation of this model includes constant weight and food web characteristics that may influence the bioaccumulation of PCBs. In addition, the model assumes constant aqueous and dietary exposures through thermodynamic partitioning; exposures may be more complex and dynamic (Barber, 2008a).

The main drivers of the model include the partition coefficients between the chemical in the water and the biological organism (k_{BW} , or k_1/k_2) and between the gastrointestinal tract (GIT or k_D/k_E) and the biological organism (K_{GB} , unitless). The partitioning of PCBs within the organism was separated into three phases, lipid, nonlipid organic matter (NLOM, e.g., proteins and carbohydrates), and water (Arnot & Gobas, 2004). PCBs have a higher tendency to partition into the fat-rich lipid phase and the octanol-water partition coefficient (K_{ow} , unitless) is assumed to be an equal substitute for the lipid-water partition coefficient. The sorption affinity of PCBs to NLOM is lower than that to octanol, and therefore a proportionality constant is applied. The proportionality constant for expressing NLOM to that of octanol (β , unitless) was assumed to be equal to 0.035 (Gobas et al., 1999). Therefore, even though the sorption affinity to NLOM is 3.5% that of octanol, it can play an important role in low lipid content organisms (Arnot & Gobas, 2004). The proportionality constant is replaced with 0.35 in the phytoplankton-water partition coefficient (K_{BW} , unitless).

The rate at which PCBs are absorbed from the water via the respiratory surface (e.g., gills and skin) is represented by the aqueous uptake rate constant (k_I , $L \times kg^{-1} \times d^{-1}$). In trophic levels 2-4 (zooplankton, forage fish, and predatory) k_I is a function of the ventilation rate (G_v , L/d), and diffusion rate across the respiratory surface area. The gill uptake efficiency (E_w , unitless) is approximated by an empirical equation based on the PCB congener K_{ow} (Gobas et al., 1988). There are no empirical measurements of ventilation rates of aquatic organisms in Torch Lake, therefore G_v was approximated from a single linear relationship between the wet weight and oxygen consumption based on observations of different fish species (Arnot & Gobas, 2004). Uncertainty in the G_v and E_w in k_I estimation are canceled out by the estimation of the chemical partitioning elimination via the respiratory area (k_2 , d^{-1}), due to the relationship with the K_{BW} . The aqueous uptake by phytoplankton is modeled as a water-organic carbon two-phase resistance model as a function of K_{ow} and constants A and B (Arnot & Gobas, 2004). The default values for A (6.0×10^{-5}) and B (5.5) are derived from phytoplankton field data in the Great Lakes.

Studies have shown that in aquatic organisms the uptake via ingestion of prey containing PCBs is the main source of bioaccumulation for chemicals with a K_{ow} greater than $\sim 10^5$ -

10^6 (Thomann et al., 1990; Gobas et al., 1999). The rate at which PCBs are absorbed from the diet via the GIT is represented by the dietary uptake rate constant (k_D , kg food/kg organism \times d⁻¹) and a function of the dietary chemical transfer efficiency (E_D), the feeding rate (G_D , kg/d), and the wet-weight of the organism (W_B , g wet-weight). There are no empirical measurements of organism feeding rates in Torch Lake. Therefore, an empirical equation was used for trophic levels 2-4 based on a general bioenergetic relationship that was derived from studies in Lake Michigan lake trout to represent coldwater aquatic organisms. The E_D can have large variability due to food digestion between different species, however an equation based on the lipid-water two-phase relationship was selected as a function of K_{ow} . Thomann et al. (1992) showed that E_D for chemicals with $K_{ow} > 10^6$ are negatively correlated with K_{ow} similar to E_w (Barber, 2008). The elimination via egestion of fecal matter is represented by the fecal elimination rate constant (k_E , d⁻¹). The k_E is also a function of E_D as well as the fecal egestion rate (G_F , kg feces/kg organism \times d⁻¹). G_F is modeled as a function of the feeding rate and composition of the diet. The relationship between the k_D and k_E with the K_{BG} , cancels out the uncertainty in the feeding rate and dietary uptake efficiency.

Walleye (*Sander vitreus*) was selected as the top-predator in the model because of importance in recreational fishing and cultural significance to the Keweenaw Bay Indian Community (KBIC). There are certain times of the year when walleye are consumed at higher quantities than recommended by fish consumption advisories (Hendricks, 2015). The PCB concentration in fish is commonly lipid normalized, therefore the lipid content is reported in the measurements obtained from EGLE and MTU. The lipid content in walleye was assumed to be 1% in the model, because recent measurements show the decline in lipid content in Figure 9. Brown bullhead (*Ameiurus nebulosus*) was selected as the forage fish due to its abundance in Torch Lake and its contribution to the walleye diet composition (Hanchin, 2013). The default biological input parameters were used to represent phytoplankton and zooplankton. The bioaccumulation burden of seven congeners (33, 52, 99, 101, 149, 153, and 180) that were common for the PCB mass balance model were selected for coupling with the bioaccumulation model. The K_{ow} is the only physicochemical input parameter needed for the model and was estimated from the poly-parameter linear free relationships (pp-LFERs) from Schwarzenbach et al. (2017), where detailed calculations were presented by Priyadarshini (2018). Tables 2-4 display the biological, environmental, and chemical specific input parameters for the PCB bioaccumulation model.

Table 2. Bioenergetic equations of the Torch Lake PCB bioaccumulation model (after Arnot & Gobas (2004))

Equation Description	Units	Equation	Eqn. No.
Aqueous uptake clearance rate constant	L/kg \times d ⁻¹	$k_1 = E_W \times G_V / W_B$	2

Equation Description	Units	Equation	Eqn. No.
Aqueous uptake clearance rate constant (phytoplankton)	L/kg × d ⁻¹	$k_1 = (A + (B/K_{OW}))^{-1}$	3
Gill chemical uptake efficiency	-	$E_W = (1.85 + (155/K_{OW}))^{-1}$	4
Gill Ventilation rate	L/d	$G_V = 1400 \times W_B^{0.65} / C_{OX}$	5
Dissolved oxygen conc.	mg O ₂ /L	$C_{OX} = (-0.24 \times T + 14.04) \times S$	6
Aqueous elimination rate constant	1/d	$k_2 = k_1 / K_{BW}$	7
Organism-water partition coefficient	-	$K_{BW} = \gamma_{LB} \times K_{OW} + \gamma_{NB} \times \beta \times K_{OW} + \gamma_{WB}$	8
Organism-water partition coefficient (phytoplankton)	-	$K_{BW} = \gamma_{LB} \times K_{OW} + \gamma_{NB} \times 0.35 \times K_{OW} + \gamma_{WB}$	9
Dietary uptake clearance rate constant	kg food/kg organism × d ⁻¹	$k_D = E_D \times G_D / W_B$	10
Dietary chemical transfer efficiency	-	$E_D = (3.0 \times 10^{-7} \times K_{OW} + 2.0)^{-1}$	11
Feeding rate	kg food/d	$G_D = 0.022 \times W_B^{0.85} \times \exp(0.06 \times T)$	12

Equation Description	Units	Equation	Eqn. No.
Fecal elimination rate constant	1/d	$k_E = G_F \times E_D \times K_{GB}/W_B$	13
Fecal egestion rate	kg feces/kg organism × d	$G_F = \{(1 - \varepsilon_L) \times \gamma_{LD} + (1 - \varepsilon_N) \times \gamma_{ND} + (1 - \varepsilon_W) \times \gamma_{WD}\} \times G_D$	14
Organism GIT-overall body partition coefficient	-	$K_{GB} = \gamma_{LG} \times K_{OW} + \gamma_{NG} \times \beta \times K_{OW} + \gamma_{WG}/K_{BW}$	15
Fraction lipid in organism gut	kg lipid/kg digesta	$\gamma_{LG} = \frac{(1 - \varepsilon_L) \times \gamma_{LD}}{[(1 - \varepsilon_L) \times \gamma_{LD} + (1 - \varepsilon_N) \times \gamma_{ND} + (1 - \varepsilon_W) \times \gamma_{WD}]}$	16
Fraction NLOM in organism gut	kg NLOM/kg digesta	$\gamma_{LG} = \frac{(1 - \varepsilon_N) \times \gamma_{ND}}{[(1 - \varepsilon_L) \times \gamma_{LD} + (1 - \varepsilon_N) \times \gamma_{ND} + (1 - \varepsilon_W) \times \gamma_{WD}]}$	17
Fraction water in organism gut	kg water/kg digesta	$\gamma_{WG} = \frac{(1 - \varepsilon_W) \times \gamma_{WD}}{[(1 - \varepsilon_L) \times \gamma_{LD} + (1 - \varepsilon_N) \times \gamma_{ND} + (1 - \varepsilon_W) \times \gamma_{WD}]}$	18
Organism growth rate	1/d	$k_G = 0.0005 \times W_B^{-0.2}$	19

Table 3. Biological input parameters used in Torch Lake PCB bioaccumulation model

Variable Name	Units	Symbol	Trophic Level Values				Ref.
			1	2	3	4	
Wet weight of biomass	kg	W	5.7×10^{-7}	5.7×10^{-8}	0.5	1.45	1,2
Fraction of respiratory ventilation	-	m_o	1	1	1	1	

overlying water								
Fraction of respiratory ventilation pore water	-	m_p	0	0	0	0		
Assimilation efficiency-lipid	-	ε_L	0	0.75	0.92	0.92	2	
Assimilation efficiency-NLOM	-	ε_N	0	0.75	0.60	0.60	2	
Assimilation efficiency-water	-	ε_W	0	0.50	0.50	0.50	3	
Fraction of organism-lipid	-	γ_{LB}	0.005	0.007	0.056	0.010	1, 2	
Fraction of organism-NLOM	-	γ_{NB}	0.195	0.20	0.20	0.20	2	
Fraction of organism-water	-	γ_{WB}	0.80	0.793	0.744	0.790	2	
Fraction of diet-lipid	-	γ_{LD}	0	0.005	0.007	0.056		
Fraction of diet-NLOM	-	γ_{ND}	0	0.195	0.20	0.20		
Fraction of diet-water	-	γ_{WD}	0	0.80	0.793	0.744		

Source References Used in this Table: MI EGLE fish data¹, Arnot & Gobas (2004)², AQUAWEB (Arnot Research & Consulting)³

Table 4. Chemical input parameters used in Torch Lake PCB bioaccumulation model.

Variable Name	Units	Symbol	PCB Congener Values							Ref.
PCB congeners	-	-	33	52	99	101	149	153	180	

Log (Octanol-water partition coefficient)	-	$\log K_{ow}$	5.5	5.6	6.1	6.1	6.5	6.6	7.1	1
Dissolved water concentration	pg/L	$C_{WD,O}$	1.5	10.6	5.2	8.3	12.0	7.5	2.2	2
Dissolved water concentration sediment pore water	g/L	$C_{WD,S}$	8.6	8.6	8.6	8.6	8.6	8.6	8.6	2

Source References Used in this Table: Khan (2018)¹, Mandelia (2016)²

Table 5. Environmental input parameters used in the Torch Lake PCB bioaccumulation model.

Variable Name	Units	Symbol	Value	Ref.
Water temperature	°C	T	10	1
Degree of oxygen saturation in water	%	S	90	assume
Dissolved oxygen concentration in water	mg/L	C_{ox}	10.5	2

Source References Used in this Table: Mandelia (2016)¹, Arnot & Gobas (2004)²

The model was encoded in MATLAB using ordinary differential equations (ODEs) to solve the mass balance equations for each congener and individual organism. The *ODE15s* function was selected as a variable order method to solve stiff differential equations (MathWorks, 2023a). The model with a daily time step was run over a period of 10 years due to the persistence of the higher PCB congeners. The initial mass of each congener in each trophic level was assumed to be close to zero (10^{-17} g PCB). The indices were organized for rows to represent congener number, from lowest to highest chlorination level, and the columns to represent trophic levels 1-4. For example, the aqueous uptake rate constant for PCB 33 in trophic level four would be $k_l(1,4)$. The MATLAB code is available in the Appendix (A.1).

2.3.2 MeHg adapted bioaccumulation model

The bioaccumulation of mercury was modeled in a similar format to that of PCBs. However, the uptake and elimination mechanisms differ between PCBs and Hg (Li et al., 2015). For example, PCBs undergo passive partitioning between the different phases (e.g., water, lipid, and non-lipid organic matter; NLOM) in organisms. In contrast, Hg exhibits a strong association with sulfur-rich proteins and is poorly associated with tissue lipids (Li et al., 2015). The dominant species of Hg in aquatic organisms is MeHg; thus, the inorganic form was ignored (Trudel & Rasmussen, 2006; Li et al., 2015). The bioaccumulation model for MeHg in fish was adapted from that of Trudel & Rasmussen (2001). The model is relatively simple and can predict the mercury concentration in freshwater fish species based on exposure through contaminated prey.

The kinetic mass balance model for MeHg bioaccumulated burden used for fish is shown in the equation below:

$$\frac{dM_{fish}}{dt} = (E_D \times C_D \times I \times W_B) - k_{tot} \times M_{fish} \quad (20)$$

The uptake of dissolved MeHg from the water accounts for less than 0.1% of the mercury accumulated in fish, therefore bioconcentration is assumed to be negligible (Trudel & Rasmussen, 2001). The uptake mechanism in the diet is modeled as a function of the assimilation efficiency (E_D , unitless), concentration of Hg in diet (C_D , mg/g), food ingestion rate (I , g food/g organism/d), and weight of the organism (W_B , g). The Trudel & Rasmussen (2001) study compared the predictions of this model and its bioenergetic equations with a feeding rate based on measured uptake of radiolabeled cesium (^{137}Cs). There are no measurements of feeding rates or activity costs for Torch Lake walleye; therefore, the general bioenergetic relationship that was used in the PCB model above was implemented. The feeding rate for trophic level 3 was based on the bioenergetics model for brown bullhead (Hartman, 2017). The model calculations are shown in the forage fish and predator fish section of Table 9.

The elimination of MeHg is much faster as compared to PCBs; however, the physiological mechanism of Hg elimination is largely unknown for fish (Li et al., 2015). Hypothesized mechanisms include demethylation biotransformation reactions, protein turnover during routine metabolism, or hormonally controlled elimination (Madenjian et al., 2014b). Because Hg elimination is less understood and the bioenergetics have not been analyzed for Torch Lake walleye, an overall elimination rate constant (k_{tot}) is implemented based on an updated empirical equation of Trudel & Rasmussen (1997). A study by Yoa & Drouillard (2019) compared three different empirical elimination models based on Trudel & Rasmussen (1997) and data published after 1997. The Trudel & Rasmussen (1997) original model is represented by Model 1 and has been commonly used in bioenergetic-toxicokinetic models. Model 2 included a thermal category (TC) to incorporate the relationship between fish metabolic rate and temperature. The TC 1, 2, or 3 represented cold, cool, and warm water fish, respectively. Model 2 performed best even against Model 3, which included species specific routine metabolic rate (RMR) as estimated from the Wisconsin Fish Bioenergetic Model (Deslauriers et al., 2017).

Therefore, Model 2 was used to estimate the elimination rate constant for forage and predatory fish in the bioaccumulation model. The empirical model is a function of body weight, temperature, and thermal category (TC).

$$\ln k_{tot} = -0.52 \pm 0.05 \times \ln W_B + 1.89 \pm 0.73 \times \ln(T) + 4.29 \pm 1.15 \times TC - 1.44 \pm 0.44 \times (\ln T \times TC) - 9.19 \pm 1.78 \quad (21)$$

Walleye were assumed to be cool water fish, corresponding to a TC of 2. Brown bullhead were assumed to be warm water fish species corresponding to TC of 3. The calculated k_{tot} for a temperature of 10 °C for bullhead and walleye were 0.0058 d⁻¹ and 0.0013 d⁻¹, respectively. Walleye have an optimum temperature preference of 22°C (~75°F). Thus, k_{tot} may be underestimated at a temp of 10°C (Kitchell et al., 1997).

The MeHg model treats the fish as a single compartment with uptake only from the diet, and elimination via all pathways (including growth) are combined into one in the second term. The model assumes a homogenous distribution of MeHg, and thus the concentrations in the muscle tissue and whole body are equal. Additionally, the model assumes that the daily losses from the body tissue to the gonads are negligible in comparison to other pathways because of the association with the protein matrix rather than with lipids (Harris et al. 2003; Trudel and Rasmussen, 2006). For simplicity, the release of Hg-contaminated eggs and sperm during spawning is assumed to be negligible. Because most mercury in fish is in the MeHg form, the model assumes that the assimilation of inorganic Hg in the intestine of fish from the consumed prey is negligible. The assimilation efficiency (E_D) for Hg in piscivorous fish typically ranges between 0.6 and 0.95; with a middle value of approximately 0.8 often used (Trudel & Rasmussen, 2001). MeHg is covalently bonded to sulfur in proteins that have an assimilation efficiency of around 80%. Therefore, it is assumed that E_D is equal to 0.8.

The bioaccumulation model for fish is driven by the concentration of Hg in the prey in the fish diet, but there are no empirical observations in Torch Lake except for top-predator fish species (e.g., walleye, northern pike, and small mouth bass). Therefore, the concentration of MeHg in the diet (C_d) was predicted based on modeling from measurements of the dissolved phase concentration in the water column. There are fewer bioaccumulation models for lower trophic level organisms for MeHg in comparison to PCBs. However, this project implemented a model based on Schartup et al. (2018) for Northwest Atlantic Ocean phytoplankton and zooplankton. Phytoplankton take up MeHg via diffusion from lake water across the cell membrane. The Schartup (2018) steady-state phytoplankton model combined studies from Lee & Fisher (2016) and Luengen et al (2012) to model the aqueous uptake (U , amol μm^{-3} nM) as a function of cell size and DOC concentration. Note it is assumed that the phytoplankton achieve equilibrium with the water over 4 hours (Lee & Fisher, 2016).

$$C_{phyto} \left(\frac{ng}{g} \right) = \frac{U * C_{WD,T} * V}{W_B} * 200.59 * 10^{-12} \quad (22)$$

Therefore, the steady state predicted MeHg concentration is shown in Equation 22 as a function of aqueous uptake rate constant, MeHg concentration in the water ($C_{WD,T}$, pM),

and the volume of the cell ($V, \mu\text{m}^3$). The radius of the phytoplankton cell in Torch Lake ($r, \mu\text{m}$) was assumed to be $25 \mu\text{m}$, contributing to a surface area (SA, μ^2) to volume ratio of 0.12.

Table 6. Phytoplankton equations used in the Torch Lake MeHg bioaccumulation model (Schartup et al., 2018).

Equation Description	Units	Equation
Empirical relationship between net MeHg uptake rate and cell $S_A:V$	$\text{amol } \mu\text{m}^{-3} \text{ nM}^{-1}$	$U = t \frac{0.118S_A}{V} \exp(-0.008 \times DOC)$ where $t = 4h$
Volume of cell	μm^3	$V = \frac{4}{3}\pi r^3$
Surface area to volume ratio (spherical)	μm^{-1}	$S_A:V = 3/r$

The Schartup et al. (2018) model implemented a non-steady state bioaccumulation model for herbivorous (small) and omnivorous (large) zooplankton. Bioconcentration is significant for zooplankton, and thus the equation has a similar structure as for PCBs. The zooplankton mass balance equation is shown below (Equation 23). The variables for this equation are listed in Table 7.

$$\frac{dM_{zoo}}{dt} = (W_B \{(k_1 * C_{wDO}) + (k_D * C_D)\}) - (k_{tot} * M_{zoo}) \quad (23)$$

The uptake included both respiratory intake through the gills (k_I) and ingestion of contaminated phytoplankton (k_D). The aqueous uptake rate is a function of the gill chemical uptake efficiency (E_D , unitless), as estimated in the Arnot & Gobas (2004) model, in addition to the clearance rate (F , L/d) and weight of the organism (W_B , g). The dietary uptake rate constant is a function of the effective depth-averaged suspended particle matter (SPM) concentration (E_{SPM} , g/L) which was assumed to be 75% of the SPM. In addition, the k_D was modeled as a function of the clearance rate, dietary assimilation efficiency (E_D , unitless) and body weight. The E_D for zooplankton ranges between 50% and 70% and therefore is simulated probabilistically using a uniform distribution; this is equivalent to setting E_D to 60% (Schartup et al., 2018). The phytoplankton represents 100% of the diet for zooplankton. The fecal elimination (k_{tot} , d^{-1}) is dependent on the body burden and water temperature. Pseudo-elimination via growth dilution was included in the Schartup et al. (2018) model, but the results indicated a balance between uptake and growth. The zooplankton were growing faster but consuming more contaminated food. However, studies of freshwater systems have indicated the importance of growth dilution, which is discussed in section 4 (Pickhardt et al., 2002; Barber et al., 2015).

Table 7. Biological input parameters used in Torch Lake MeHg bioaccumulation model.

Variable Name	Units	Symbol	Trophic Level Values				Ref.
			1	2	3	4	
Weight of biomass	g	W_B	5.7×10^{-4}	5.7×10^{-5}	500	1,450	1,2
Dietary chemical transfer efficiency	-	E_D	0	0.60	0.80	0.80	3,4

Source References Used in this Table: MI EGLE fish data¹, Arnot & Gobas (2004)², Schartup et al. (2018)³, Trudel & Rasmussen (2001)⁴.

Table 8. Chemical input parameters used in Torch Lake MeHg bioaccumulation model.

Variable Name	Units	Symbol	Value	Ref.
Octanol-water partition coefficient	-	K_{ow}	$10^{1.7}$	1
Dissolved water concentration	ng/L	C_{wdO}	0.151	2
Molecular weight of Hg	g/mol	MW_{Hg}	201	
Molar dissolved water concentration	pM	C_{wdOM}	0.751	

Source References Used in this Table: Schartup et al. (2018)¹, EGLE (unpub.)²

Table 9. Bioenergetic equations Torch Lake MeHg bioaccumulation model.

Equation Description	Units	Equation	Eqn. No.	Ref
Zooplankton				
Aqueous clearance rate constant	$L/g \times d^{-1}$	$k_1 = E_W \times F/W_B$	24	2
Gill chemical uptake efficiency	-	$E_W = (1.85 + (155/K_{OW}))^{-1}$	25	1
Clearance rate	L/d	$F = 1.777 \times e^{0.234 \times T} \times (0.002 \times W_B \times 10^5)^{0.681} \times \exp(0.0199 \times T)$	26	2
Dietary uptake clearance rate constant	g SPM/g organism $\times d^{-1}$	$k_D = F \times E_{SPM} \times E_D/W_B$	27	2
Particle Scavenging efficiency	g SPM /L	$E_{SPM} = 0.75 \times SPM$	28	2

Equation Description	Units	Equation	Eqn. No.	Ref
Elimination rate constant	d ⁻¹	$k_{tot} = 0.00335 \times W_B^{-0.195} \times \exp(0.0066 \times T)$	29	2
Forage & Predatory Fishes				
Dietary uptake clearance rate constant	g food/g organism × d ⁻¹	$k_D = E_D \times G_D / W_B$	30	1
Feeding rate	kg food/d	$G_D = 0.022 \times W_B^{0.85} \times \exp(0.06 \times T)$	31	1

The MeHg model was encoded in a format in MATLAB software similar to the PCB bioaccumulation model. The mass balance equations for zooplankton and fish were solved with separate functions because of the negligible magnitude of bioconcentration as compared to biomagnification. The ODE (ode15s) solver was implemented to solve the dynamic mass balance equations over a 10-year period with a daily time step. The initial mass for each trophic level was assumed to be close to zero (1×10^{-17} ng of MeHg). The MATLAB code is available in the Appendix (A.1).

2.3.3 Model validation, and sensitivity and uncertainty analyses

2.3.3.1 Model Validation

All mathematical models are simplifications of reality; therefore, it is important to validate the models to determine the accuracy or ability to predict realistic concentrations (Trudel & Rasmussen, 2006). The PCB bioaccumulation model was validated with measured fish tissue concentrations, as well as with the established steady state model, “AQUAWEB”, by Arnot Research and Consulting (ARC). The PCB walleye values from the MI EGLE and MTU Torch Lake Public Action Council project were used to compare with the bioaccumulation model. The box-and-whisker plot of the measured concentration for the different congeners is shown in Figure 12. The box represents the uncertainty, the mid-point represents the mean value, and the whiskers represent the 95% confidence interval of concentrations in walleye.

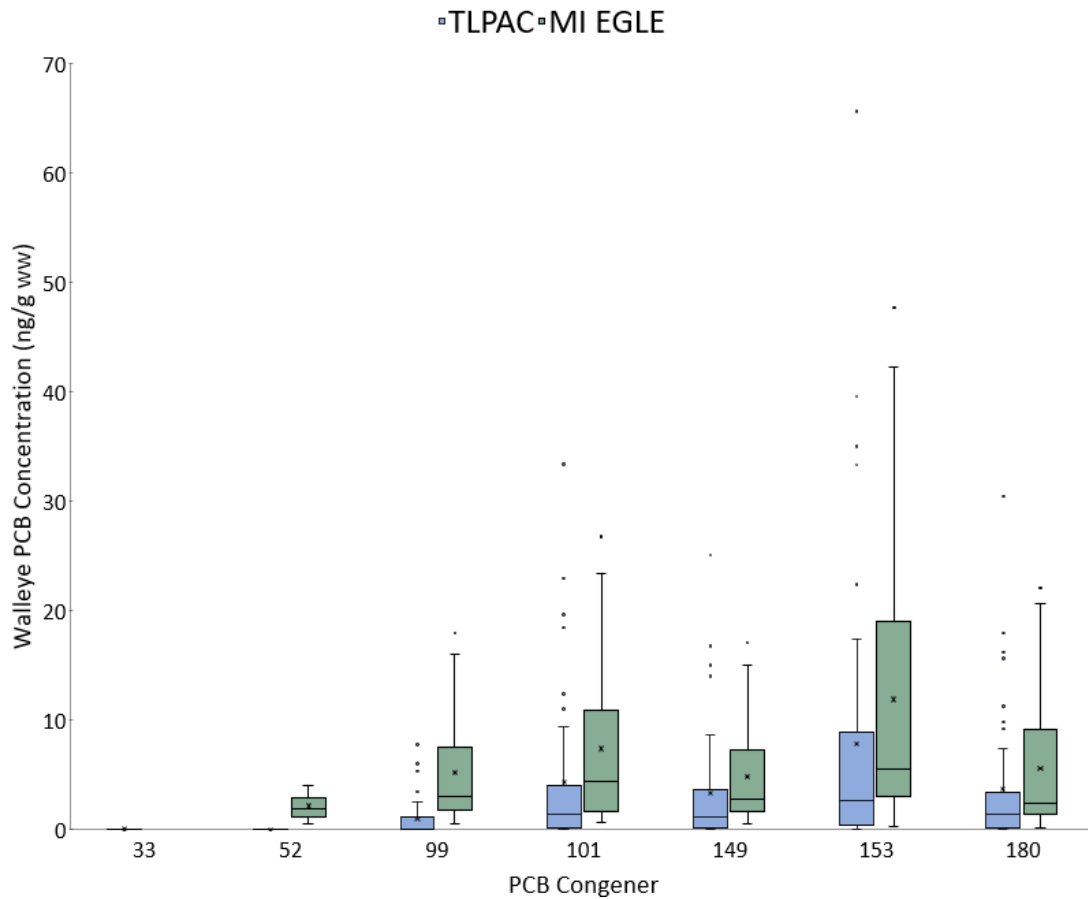


Figure 12. Box- and -whisker plots of measured PCB walleye concentration in Torch Lake obtained from Michigan EGLE (2000,2007,2013, and 2018) and Michigan Technological University (MTU) as part of the Torch Lake Public Action Council (TLPAC) project (2018, 2019, 2020, and 2022).

AQUAWEB uses the equations from Arnot & Gobas (2004) to estimate a steady-state concentration of the PCB congener in individual organisms of different trophic levels. The model is coded in Microsoft Excel workbook with user input of site-specific environmental, biological, and chemical parameters. The input values of the AQUAWEB model were identical to the Matlab model for Torch Lake parameters in Tables 7-9. Therefore, the rate constants and concentrations were verified against the established model under steady-state conditions. The MeHg bioaccumulation model was validated with the average observed walleye concentrations obtained from MI EGLE and GLIFWC. The box-and-whisker plot of walleye measured mercury concentrations is shown in the Figure 13 below:

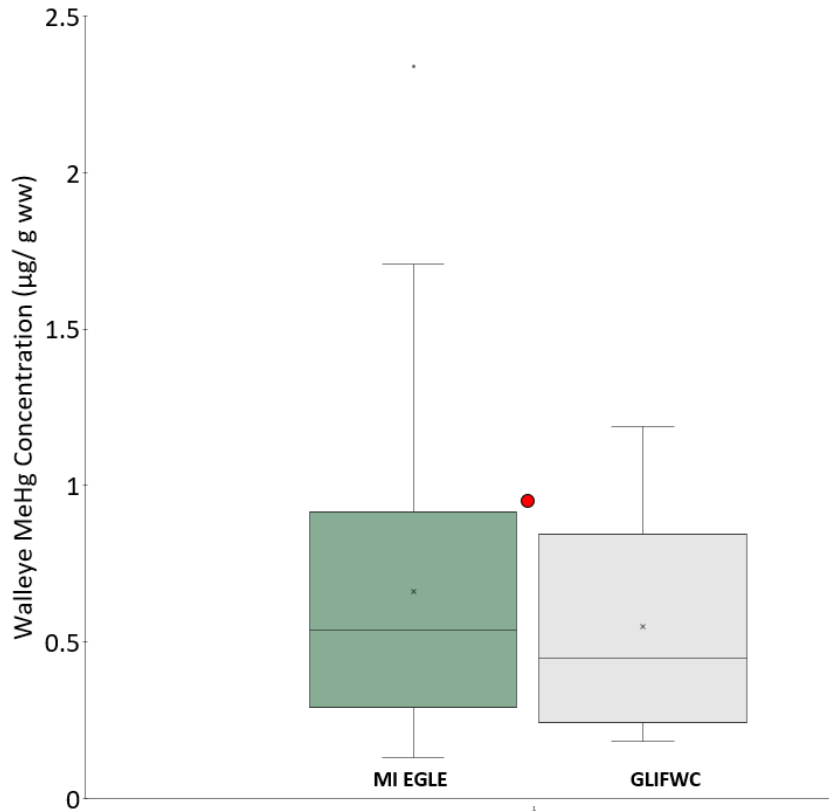


Figure 13. Box- and -whisker plots of measured MeHg concentrations in walleye concentration in Torch Lake obtained from Michigan EGLE (2000, 2007, 2013, and 2018) and Great Lakes Indian Fish and Wildlife Commission (GLIFWC) for years 2018-2021 for model validation. The model predicted value is indicated by the red circle.

There are no data are available for the other trophic levels in Torch Lake, however, a Bioaccumulation Factor (BAF) has been previously used in mercury mass balance models (Hendricks, 2018). The BAF is defined by the ratio of the contaminant concentration in fish tissue to the dissolved contaminant concentration in the lake water, Equation 32:

$$BAF = \frac{C_{fish} (\mu g/kg)}{C_{water} (\mu g/L)} \quad (32)$$

The BAF is a simple steady-state calculation to estimate the concentration in aquatic species (C_{fish}) based on the water concentration (C_{water}). The mercury BAF of trophic levels 3 and 4 were estimated from the 5th, 25th, 50th, 75th, and 95th percentiles presented in Knights (2008) used by the U.S. EPA. The predicted BAF from the MATLAB bioaccumulation non-steady state model was compared with the empirical BAF values shown in Table 10.

Table 10. Mercury Bioaccumulation Factors (BAF) in fish (Knights, 2008; Hendricks, 2018)

Percentile	Trophic level 3 $\times 10^6$	Trophic level 4 $\times 10^6$
5 th	0.46	3.3
25 th	0.95	5.0
50 th	1.6	6.8
75 th	2.6	9.2
90 th	5.4	14

The validation of the bioaccumulation models (PCB and MeHg) with observed measurements characterizes the overall model error, including model parameterization errors and natural variability with measured values (Arnot & Gobas, 2004). The model performance was assessed by calculating the percent error, shown in the equation below:

$$\text{percent error} = \frac{|C_{pred,i} - C_{obs,i}|}{C_{obs,i}} \times 100 \quad (33)$$

where, the percent error is a function of the steady-state predicted ($C_{pred,i}$) and measured concentrations ($C_{obs,i}$) for each of the seven congeners divided by the number of observations (n).

2.3.3.2 Sensitivity Analysis

The sensitivity analyses of the PCB and MeHg bioaccumulation models were performed by the parameter perturbation method. The objective of this method is to determine the sensitivity of the model to an individual parameter. The selected individual model parameters were varied by \pm a fixed amount while holding all other terms constant (Chapra et al. 2008). The parameters that were selected for the sensitivity analysis of PCB model included the uptake and elimination rate constants ($\pm 10\%$), partition coefficients (\pm factor of 2), water temperature ($\pm 5^\circ\text{C}$), and fish wet weight (\pm factor of 2). These parameters were chosen because they are thought to be values that strongly impact the predicted concentrations.

2.3.3.3 Uncertainty Analysis

The uncertainty analyses of the PCB and MeHg bioaccumulation models were performed with Monte Carlo simulations. This method uses random values to generate a series of outcomes to create a distribution of the predicted concentrations (Chapra et al., 2014).

The random values selected for each selected parameter were assumed to follow a normal distribution and estimated using the Matlab function *normrnd*, which is dependent on the mean, standard deviation, and size of the array (Mathworks, 2023b). The standard deviation was estimated, with literature review values of dietary uptake of PCBs in fish estimated from assimilation efficiency, which can be easily measured. The trophic transfer efficiency (E_D) is the efficiency with which the contaminant in the food ingested by predator is transported through the gut wall (Madenjian et al., 2014a). The transfer efficiency is an important parameter for modeling bioaccumulation, and laboratory and field studies suggest that E_D can be influenced by the feeding rate and digestibility of the dietary matrix.

The four most sensitive parameters selected for the PCB Monte Carlo simulation included: T , k_D , C_{wd} , and K_{ow} . The literature review values of assimilation efficiency of modeled PCB congeners based on species type used for the uncertainty analysis shown below:

Table 11. Literature review values of dietary assimilation efficiency for PCB congeners in fish based on species type.

Estimated dietary assimilation efficiency (E_D)							Species	Ref
PCB 33	PCB 52	PCB 99	PCB 101	PCB 149	PCB 153	PCB 180		
0.25	0.35	0.34	0.39	0.40	0.64	0.56	Marbled sole	1
0.10	0.19	0.12	0.29	0.47	0.65	0.46	Koi	2
0.25	0.24	0.10	0.30	0.36	0.37	0.30	Koi	2
		0.38	0.28	0.39	0.44	0.44	Goldfish	3
0.47	0.49	0.51	0.54	0.50	0.50	0.56	Goldfish	4
	1.001	0.551					Whitefish	5
0.775	0.775	0.775	0.775	0.775	0.775	0.775	Walleye	6
0.848	0.911	0.675	0.705	0.628	0.653	0.681	Lake trout	7

Source references used in this table: Kobayasni et al. (2011)¹, Lui et al. (2010)², Li et al. (2015)³, Bruggeman et al. (1981)⁴, Madenjian et al. (2008)⁵, Barber et al. (2008)⁶, Madenjian et al. (2014a)⁷.

The three most sensitive parameters selected for the MeHg Monte Carlo simulation were: T , E_D , and k_{TOT} . The dietary assimilation efficiency and total elimination rate constant based on literature values are shown in Tables (12-13) below:

Table 12. Literature review values of dietary assimilation efficiency for MeHg in fish based on species type.

Estimated dietary assimilation efficiency (E_D) for MeHg	Species	Ref
0.64	Lake whitefish	1
0.77	Lake trout	2
0.98	Goldfish	3
0.89	Redear sunfish	4
0.94	Tilapia	5
0.85	Tilapia	5
0.68	Rabbitfish	6
0.94	Largemouth bass	7

Source references used in this table: Madenjian and O'Connor (2008)¹, Madenjian et al. (2012)², Li et al. (2015)³, Pickhardt et al. (2006)⁴, Wang et al (2010)⁵, Peng et al. (2016)⁶, Bowling et al. (2011)⁷.

The total elimination rate constant can be easily measured in laboratory and field studies. Studies such as, The Mercury Experiment to Assess Atmospheric Loading in Canada and the United States (METAALICUS), have utilize mercury stable isotopes to analyze fate and transport in the environment and whole-ecosystem response to changes in loadings (Harris et al., 2007 ; Blanchfield et al., 2021). The total elimination rate constant can be estimated by transferring fish from a spiked environment to a different lake (VanWellegham et al., 2007 ; VanWalleghem et al., 2013).

Table 13. Literature review values of total elimination rate constant for MeHg in fish based on species type.

Estimated total elimination rate constant (k_{TOT} , 1/d) for MeHg	Species	Ref
1.42×10^{-3}	Yellow perch	1
6.32×10^{-4}	Northern pike	2

3.80×10^{-4}	Lake Trout	3
9.50×10^{-4}	Whitefish	3
7.30×10^{-4}	Whitefish	4
2.44×10^{-4}	Lake Trout	5

Source references used in this table: VanWalleghem et al, (2007)¹, VanWalleghem et al., (2013)², Blanchfield et al. (2022)³, Madenjian and O'Connor (2008)⁴, Madenjian et al. (2012)⁵

The bioaccumulation models were adapted to output only the trophic level 4 concentrations with the parameter variations to estimate the uncertainty in the walleye concentration. The model included 10,000 iterations (N = 10,000) to estimate the corresponding output concentrations. The 95% confidence interval of the PCB congener and MeHg concentrations were estimated in MATLAB with the built-in function *paramci*. To compute the mean and standard deviation of the walleye concentrations, the results were fit to a normal distribution with the MATLAB function *fitdist*.

2.3.4 Model Experiments

The different scenarios of Torch Lake with the kinetic bioaccumulation models of PCBs and MeHg to understand the dynamics of PCB bioaccumulated burdens depending on changes in PCB sources, remediation efforts, and food web characteristics. The objective was to answer the questions posed in this study:

- (1) What are the expected PCB and MeHg concentrations in Torch Lake fish if remediation now under consideration is performed?
- (2) How long must fish reside in Torch Lake in order to acquire the observed PCB and MeHg concentrations?
- (3) Can walleye lipid content decline explain the decline in walleye PCB concentrations?

This section outlines the methods used in the modeling experiments to answer the above questions. There was only one scenario involved for the mercury modeling due to the natural background concentration not associated with the mining activities.

2.3.4.1 PCB modeling questions

The PCB mass balance model for the lake used to estimate the expected rate of decrease in the PCB concentrations in Torch Lake water and fish following remediation (Urban et al., 2018; Mandelia, 2016). Although, the dissolved phase is the only bioavailable form of PCBs, this fraction is dependent on the overall fate and transport of PCBs. The first experiment was performed by eliminating the source of PCBs from the highly contaminated lake sediment areas in regions 1 and 2. The areas of the sediment regions were calculated using ArcGIS to draw circles around points of PCB concentration that

met or exceeded detection limits. The average concentration of PCBs in the lake sediments was set to zero in each region individually and together, to determine the magnitude of change in the steady-state dissolved concentrations. The sediment concentrations were calculated as the median value due to there being a few high concentrations in the contaminated sediment regions. The concentration of the PCB concentrations in the air were updated from the 2005 measurements to IADN 2021 measurements from January 10th to December 24th. The model was run to estimate the steady-state dissolved PCB concentration. This concentration in the water was used in the bioaccumulation model to estimate the concentration in the aquatic organisms. The rate of decrease in the fish PCB concentration was estimated by using the reduced dissolved concentrations in the bioaccumulation model.

The MDNR conducted a tag-and-recovery study on the Portage-Torch Lake System (PTLS), which revealed that walleye tagged in Torch Lake frequently moved into Portage Lake, and not the other way around (Hanchin, 2013). A recent telemetry study revealed that for 60% of walleye tagged and released into Portage and Torch Lake, the total time was spent in Portage Lake (Steve Shier, personal communication). The second question was examined by setting the initial PCB concentrations in trophic levels 1-3 at their predicted steady-state concentrations and trophic level 4 to zero. This scenario represents the migration of fish into Torch Lake from lower contaminant levels in the Keweenaw Waterway. The longer the exposure time of fish to PCBs causes a greater accumulation via respiration and contaminated diet.

The third question focused on estimating the changes in bioaccumulated burden in walleye depending on the lipid content. The walleye in Torch Lake have a low lipid content and has been undergoing a long-term decrease (Urban and Perlinger, 2022). The hydrophobicity of PCBs causes the compounds to accumulate in the fat-rich tissues; therefore, the lipid content of the fish has a large impact on the PCB concentration in the fish. The recent measurements of walleye have a lipid content close to 1%, potentially indicating an unhealthy fish population. The low lipid content may be a result of the degraded benthic community causing limited food sources. However, if the ecosystem recovers following remediation, it is important to predict the impacts on fish concentrations of PCBs in fish. Therefore, the fish lipid content in the bioaccumulation model was set to values between 0.1-9.5% to observe the trends in PCB congener concentrations in the walleye.

2.3.4.2 MeHg modeling questions

Estimating the remediation effectiveness with mercury is different than for PCBs due to the background concentrations from methylation in the lake and surrounding watershed (i.e., wetlands). The spatial and temporal distribution in tributaries of the Torch Lake suggested 50% of MeHg is produced from wetlands discharging water into Trap Rock River. The other ~50% was concluded to be produced from in-lake methylation (Greene and Urban, 2022). Therefore, to answer the first question in regard to mercury, the measured MeHg concentration was reduced by 50% to eliminate the source of in-lake methylation (EGLE, unpub.). Under these conditions, the model can estimate the effects

of potential remediation actions that focus on the elimination of in lake sources to decrease the concentrations of MeHg available for bioaccumulation.

The same method was performed for MeHg as for PCBs for answering the second question. The initial concentrations in trophic levels 1-3 were set to their predicted steady-state concentrations. However, the trophic level 4 MeHg initial concentration was set to zero. Therefore, the bioaccumulation of MeHg could be modeled under steady-state conditions in the other trophic levels.

3 Results

3.1 PCB Modeling Results

This section summarizes the results of the PCB bioaccumulation modeling for Torch Lake. The predicted walleye response time for each of the seven congeners over the modeled 10-year period from the non-steady state model is presented. The MATLAB model predicted results are compared with measured PCB concentrations in fish and steady state concentrations predicted with AQUAWEB (Arnot Research & Consulting) to quantify the “accuracy” of the non-steady state model. The seven PCB congeners 33, 52, 99, 101, 149, 153 and 180 were modeled because of the mass balance model validation of these congeners detected in the 2005 SPMD measurements. The sensitivity analysis and uncertainty analysis show some of the limitations of the model and identify the parameters to which the model is most sensitive; future model improvements could focus on obtaining more accurate values of these parameters. Then, the bioaccumulation model is coupled with the PCB mass balance model by Mandelia (2016) to predict the success of remedial activities.

3.1.1 Non-steady state PCB bioaccumulation model results

The predictions of the PCB bioaccumulation model for Torch Lake are displayed in Figure 15 for the walleye concentrations (ng/g wet weight) for seven PCB congeners over a 10-year period. The model was run for 10 years because this is the estimated age of walleye of the weight modeled (e.g., 1.45 kg). The time to reach steady state followed the expected pattern of heavier congeners taking longer to reach steady state as compared to the lighter weight congeners. Congener 33 reaches steady state within about 2 years, but the most chlorinated congener modeled (PCB 180) does not reach steady-state within the 10-year period. The kinetics are relatively slow for chemicals with $K_{ow} > 10^{7.5}$ in large, high-lipid content organisms (Arnot & Gobas, 2004; Paterson et al., 2007b; McLeod et al., 2016). The heavier weight PCB congeners have a greater affinity for lipids as compared to lighter congeners due to their greater hydrophobicity.

These results must be interpreted with caution. Clearly, a 10-year-old fish would not remain the same size for another ten years. The results do indicate that if a fish were to swim into Torch Lake from Portage Lake (or possibly from Lake Superior), it would take several years for it to reach concentrations in equilibrium with PCBs in Torch Lake water.

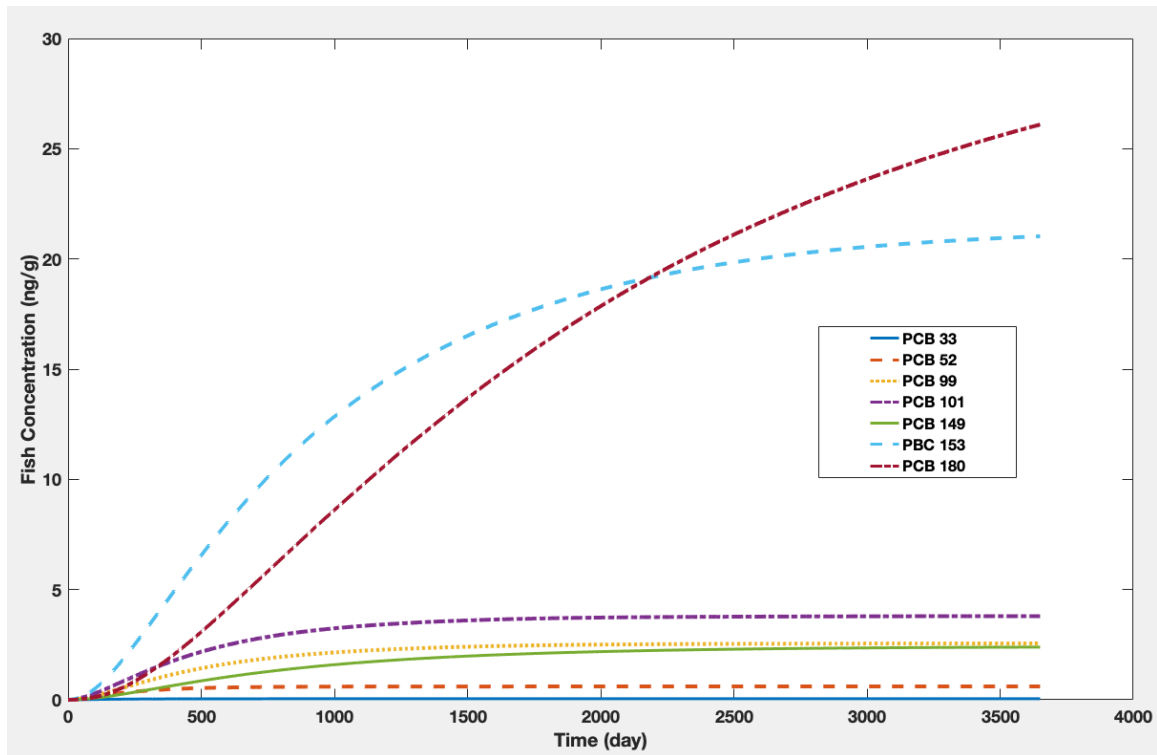


Figure 14. Torch Lake walleye predicted PCB concentration (ng/g) for seven congeners selected from the non-steady state bioaccumulation modeled over 10 year- period (3650 days).

3.1.2 Model verification, validation, and sensitivity and uncertainty analyses results

3.1.2.1 Walleye Model Verification and Validation Results

The model was verified by comparing its predicted congener concentrations in walleye (concentrations predicted after 10-year exposure to Torch Lake water and food web) with those from an established steady-state version of the Gobas model, “AQUAWEB”. This serves primarily to verify that the Matlab model is correctly coded. The Matlab model predictions were validated by comparison with fish PCB concentrations measured (2000-2018) by the State of Michigan’s monitoring program and those measured in the MTU TLPAC project for fish caught between 2018 and 2022. The use of AQUAWEB also assisted with the verification of choice of kinetic rate constants for the Arnot & Gobas (2004) bioaccumulation model. The comparison of the Matlab and AQUAWEB steady state predicted concentrations for PCB congeners in Torch Lake walleye and the average measured concentrations are shown in Table 14

Table 14. PCB bioaccumulation model verification and validation of steady-state concentration results.

	PCB 33	PCB 52	PCB 99	PCB 101	PCB 149	PCB 153	PCB 180
	Torch Lake Walleye PCB Concentration (ng/g ww)						
MATLAB predicted (10-yr period)	0.05	0.60	2.56	3.80	2.39	21.03	26.09
AQUAWEB predicted (steady state)	0.05	0.70	2.99	4.41	2.82	24.62	27.62
MI EGLE average measured	0.00	2.23	5.19	7.41	4.89	11.93	5.56
MTU TLPAC average measured	0.05	0.00	0.88	3.97	3.03	7.29	3.39
	Calculated percent error (%)						
	88.4	46.5	17.4	35.3	41.8	112.1	461.6

The results show that concentrations predicted by the steady-state (AQUAWEB) and non-steady state (MATLAB) models agreed well with measured concentrations for the lighter congeners but tended to overestimate concentrations of the heavier congeners. However, as expected, both model predictions show the trend of higher concentrations with the increase of chlorination levels. The percent error between the model-predicted and average measured walleye PCB concentrations ranged from 17.5-461.6%. The error increased with increasing chlorination level. The more recent MTU TLPAC measured concentrations were lower than the measurements by EGLE, which may be due to declining atmospheric deposition. The 2005 SPMD measurements were used as the dissolved phase for MATLAB and AQUAWEB models.

3.1.2.2 Sensitivity Analysis Results

The sensitivity of the model-predicted PCB concentrations in walleye to model parameters is displayed in Figures 15-18. In the sensitivity analysis, individual model parameters were changed by plus or minus 10%, and the graphs show the magnitude of the change in predicted PCB concentrations (only for congeners 33 and 180) in walleye. In Figures 15-18, results are shown for changes in values of k_1 , k_D , k_2 , and k_E ; sensitivities to other parameters are presented in Appendix (A.3). The k_1 and k_D values represent the

uptake via absorption from gills and ingestion of prey, respectively. The other rate constants k_2 and k_E represent the elimination via respiration from gills and excretion, respectively. The figures display the changes in walleye concentrations with the change in plus or minus 10% of the parameter value. The most sensitive parameters are identified as those showing >10% change of the walleye concentration. The PCB bioaccumulation model was determined to be most sensitive to the trophic level 4 dietary uptake rate constant (k_D), as shown in the larger concentration change for the k_D value in the series of Figures 15-17. The model was also sensitive to the water temperature, K_{ow} , and the weight of walleye as shown in the Appendix (A.3).

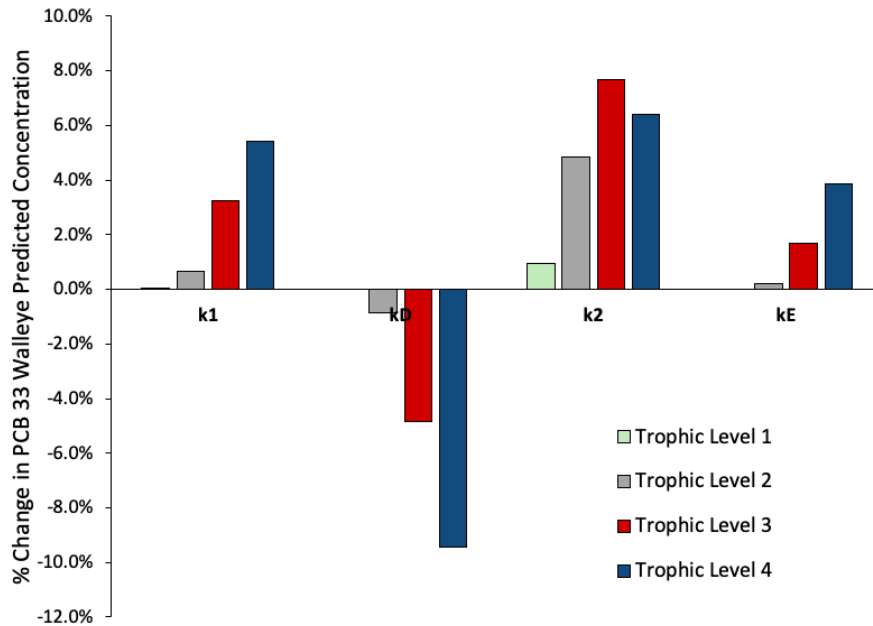


Figure 15. Change in walleye PCB 33 concentration caused by decreasing the model rate constants for trophic levels 1 (green), 2 (gray), 3 (red), and 4 (blue) by 10%.

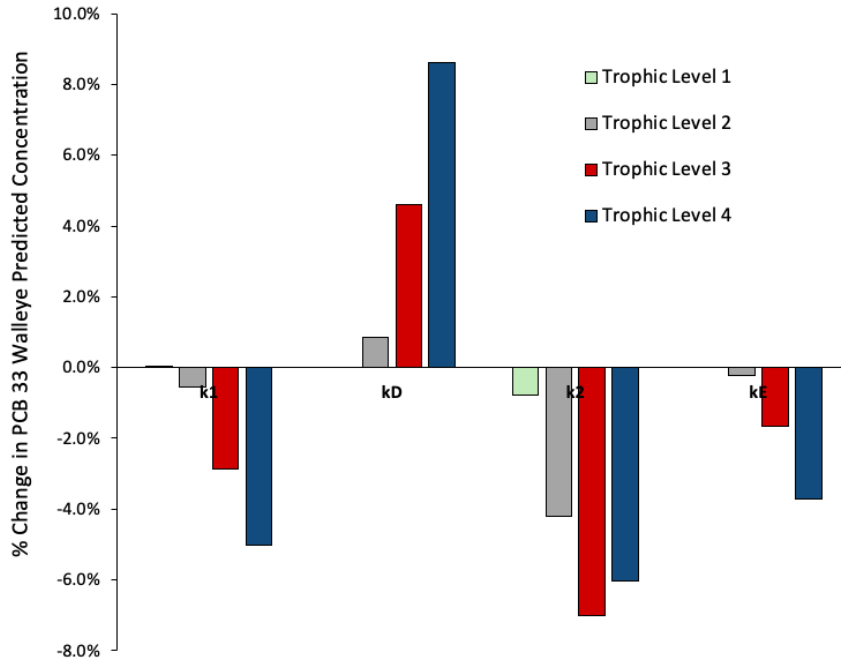


Figure 16. Change in walleye PCB 33 concentration caused by increasing the model rate constants for trophic levels 1 (green), 2 (gray), 3 (red), and 4 (blue) by 10%.

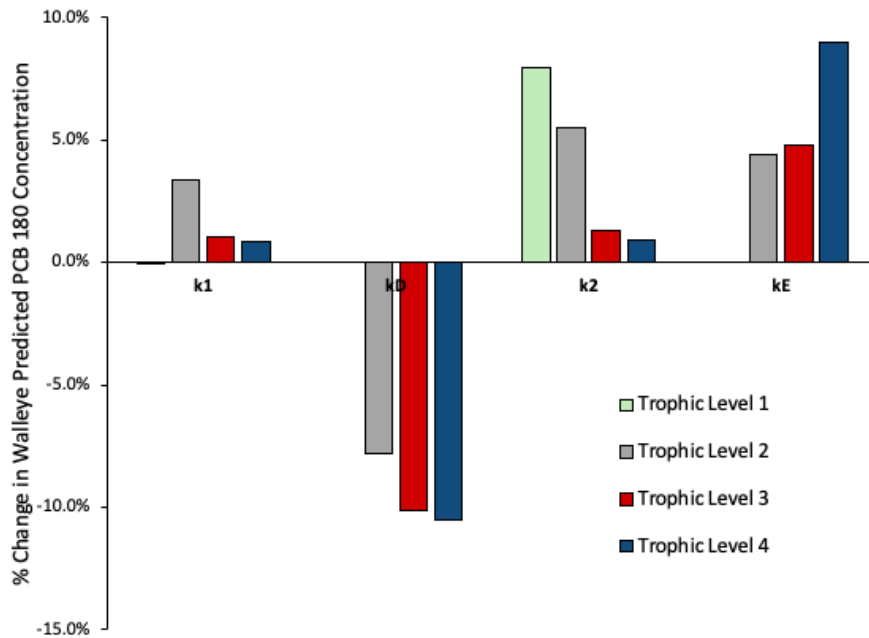


Figure 17. Change in walleye PCB 180 concentration caused by decreasing the model rate constants for trophic levels 1 (green), 2 (gray), 3 (red), and 4 (blue) by 10%.

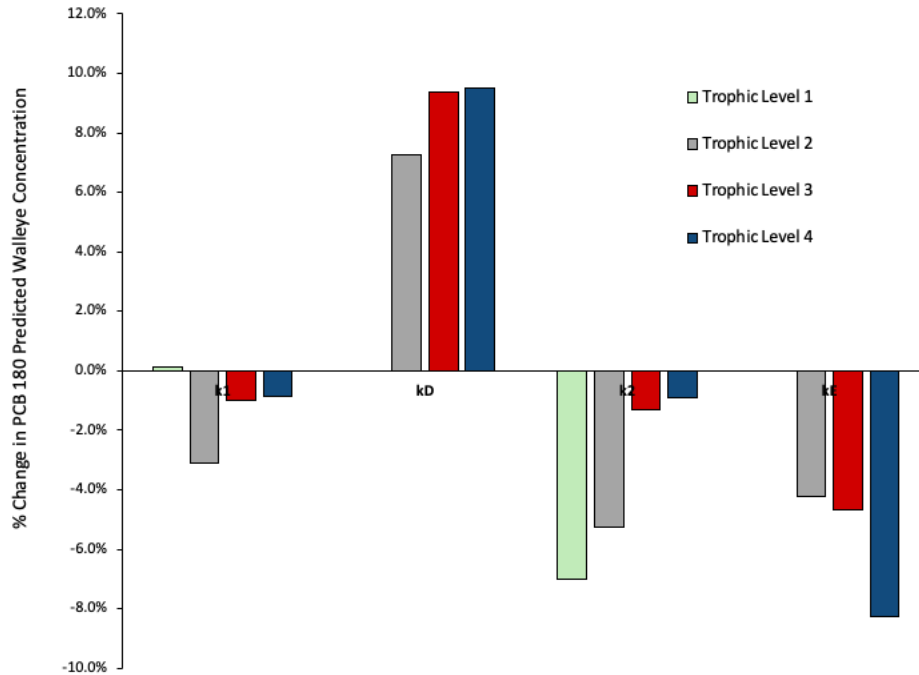


Figure 18. Change in walleye PCB 180 concentration caused by increasing the model rate constants for trophic levels 1 (green), 2 (gray), 3 (red), and 4 (blue) by 10%.

3.1.2.3 Uncertainty Analysis Results

The Monte Carlo simulation included 10,000 iterations with normally distributed, random values of the selected parameters: K_{ow} , C_{wDO} , T , and K_D . These parameters were selected because sensitivity analysis revealed that the model was most sensitive to these parameters. For each iteration, the values of the four parameters were varied independently using a random number generator that followed a normal distribution. The frequency distribution of predicted (10-year) walleye PCB concentrations is displayed in Figure 19 for congener 180. The statistical results of the Monte Carlo Simulation with the mean, standard deviation, and 95% confidence intervals for each congener are shown in Table 15.

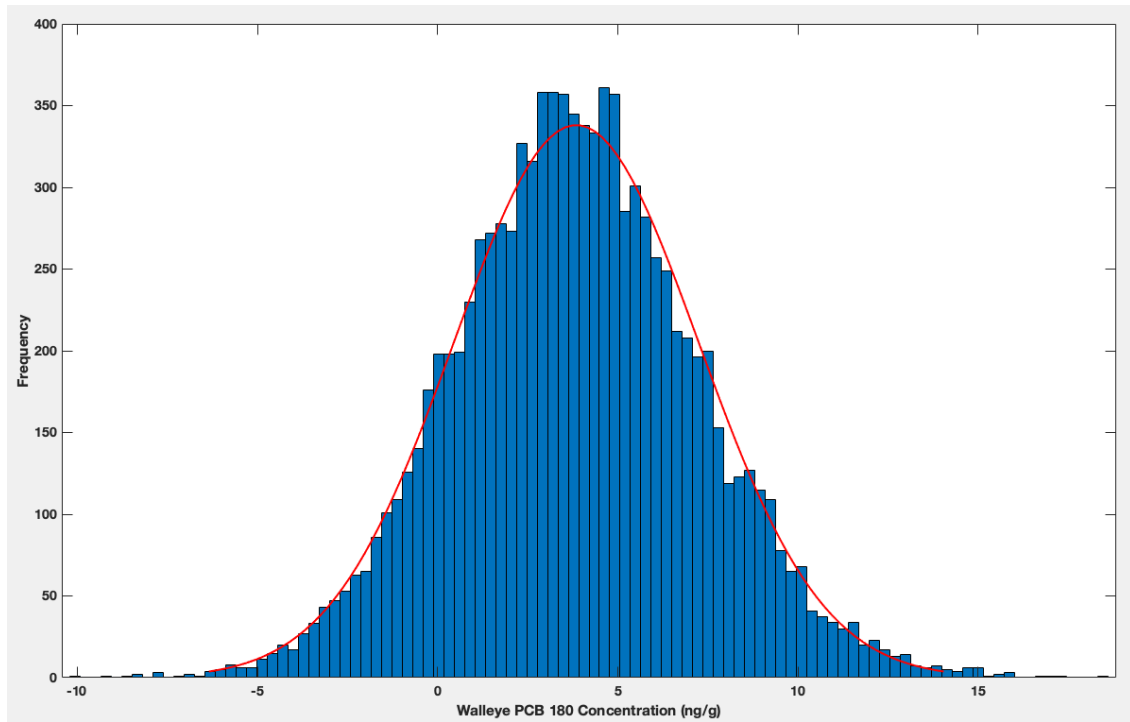


Figure 19. Walleye PCB 180 Monte Carlo simulation output concentration histogram. Normal distribution curve (redline).

Table 15. Torch Lake Walleye PCB Monte Carlo simulation mean concentration, standard deviation, upper and lower 95% confidence interval for seven congeners selected at the end of 10-year period modeled.

	PCB 33	PCB 52	PCB 99	PCB 101	PCB 149	PCB 153	PCB 180
Mean Concentration (ng/g ww)	1.47	1.83	2.88	2.86	3.42	3.60	3.85
Standard deviation (ng/g ww)	0.73	0.81	1.61	1.27	1.49	1.66	3.40
Lower 95% confidence interval	1.46	1.81	2.85	2.84	3.39	3.57	3.78
Upper 95% confidence interval	1.49	1.84	2.91	2.89	3.45	3.63	3.91

The results indicate that the 95% confidence interval and standard deviation increased with the increase in PCB chlorination level. As a percent of the mean, the confidence interval increased from 2% for congener 33 to 3.4% for congener 180. The uncertainties are, therefore, small relative to the predicted concentrations. Nonetheless, the model could be calibrated to narrow the range of predictions shown in Figure 19.

3.1.3 Results of PCB Modeling Experiments

3.1.3.1 PCB Question 1 Modeling Results

(1) *What is the expected decrease in PCB and MeHg concentrations in Torch Lake water and fish tissue following remediation?*

The bioaccumulation model was coupled with the PCB mass balance model with the the areas of sediment regions 1 and 2 set equal to 0 m². This change is equivalent to complete remediation in which all internal sources of PCBs are removed, and atmospheric deposition is the only source of PCBs to the lake water column. The results of the modeling experiment for question 1 indicate that there is a relatively minimal impact of atmospheric deposition, as compared to the highly contaminated lake sediment regions, on the predicted PCB concentrations in top predator fish in Torch Lake. The comparison of different remediation scenarios with the sediment regions 1 and 2 being remediated individually and together is shown in Figure 20.

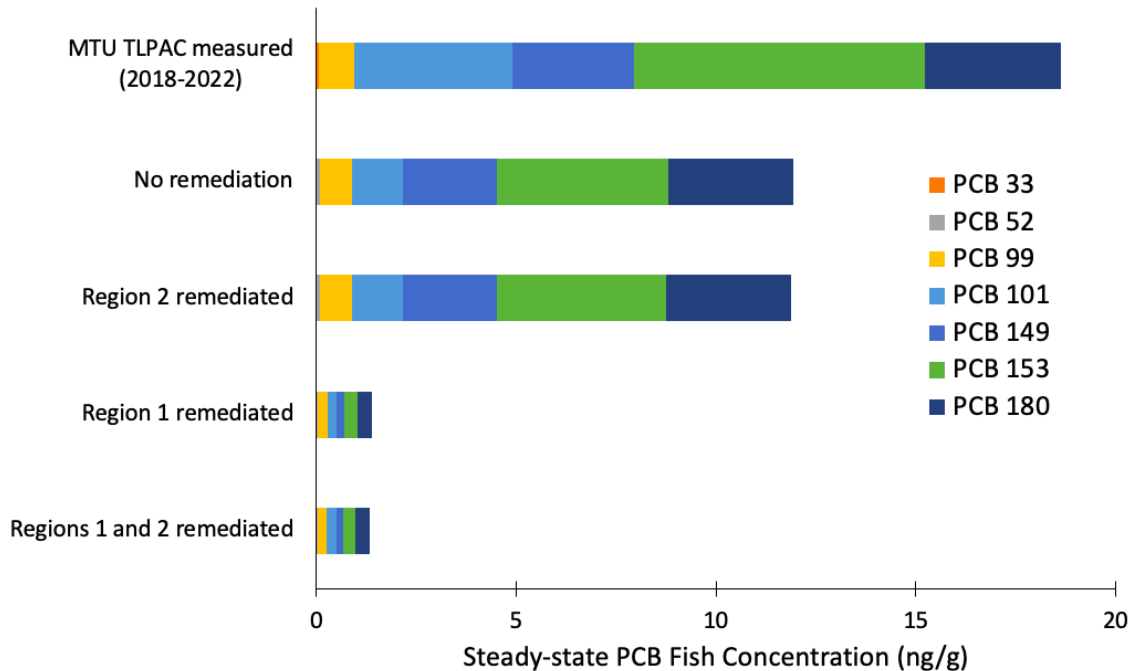


Figure 20. Comparison of the impact of remediation of contaminated lake sediments, which are divided into Hubbell Processing Area (region 1) and Lake Linden Recreation Area (region 2) in the PCB mass balance model as potential on-going sources.

The remediation of region 1 had the greatest effect that was almost equal to the effect of both sediment areas being remediated. The heavier congeners are most dominant in the lake sediments, and therefore they are predicted to show the greatest reduction in concentration in the Torch Lake walleye.

3.1.3.2 PCB Question 2 Modeling Results

(2) How long do fish reside in Torch Lake in order to acquire unhealthy PCB bioaccumulated burdens?

The longer a fish resides in Torch Lake, the longer it is exposed to PCBs in the water and in prey. Therefore, the movement of a fish impacts the bioaccumulated burden over its lifetime. The model simulation predicted the time it would take to accumulate the PCB concentrations measured in Torch Lake walleye if an individual walleye migrated from the Keweenaw Waterway into Torch Lake. The concentrations of the lower trophic level organisms were kept at steady state concentrations.

Table 16. Torch Lake time to reach measured bioaccumulation burden in walleye with initial concentration zero and diet concentration at steady state predicted concentration.

Time to reach bioaccumulated burden in Walleye fish (years)						
PCB 33	PCB 52	PCB 99	PCB 101	PCB 149	PCB 153	PCB 180
0.47	N/A	1.0	N/A	0.47	N/A	0.17

The results did not show any relationship of times to reach measured concentrations and chlorination level of PCB congeners. These results also indicate the disadvantages of having few measurements to validate the model.

3.1.3.3 PCB Question 3 Modeling Results

(3) What is the impact of lipid content of Torch Lake fish on the PCB bioaccumulated burden?

The lipid content in aquatic organisms influences the bioaccumulation of PCBs due to their hydrophobicity. Therefore, the health condition of walleye influence the risk associated with fish consumption. Lipid content of walleye is interpreted as an indicator of fish health. Changes in lipid content had the same magnitude of impact on each congener modeled. The results of PCB 180 are shown in Figure 22 as an example. For congener 180, increasing the lipid content two orders of magnitude (0.1-9.5 %) causes a 10-fold increase in wet-weight PCB concentration (~10 to ~100 ng/g). The lipid-normalized concentration divided by the fugacity capacity would give the fugacity. It is assumed that PCBs are in equilibrium with the lipid fraction in fish. The results indicate that after the assumed steady-state condition (after 10-year period), the PCB 180 congener is not at equilibrium. This is not surprising as the highly chlorinated PCB congeners have shown to never reach steady state within the fish’s lifetime.

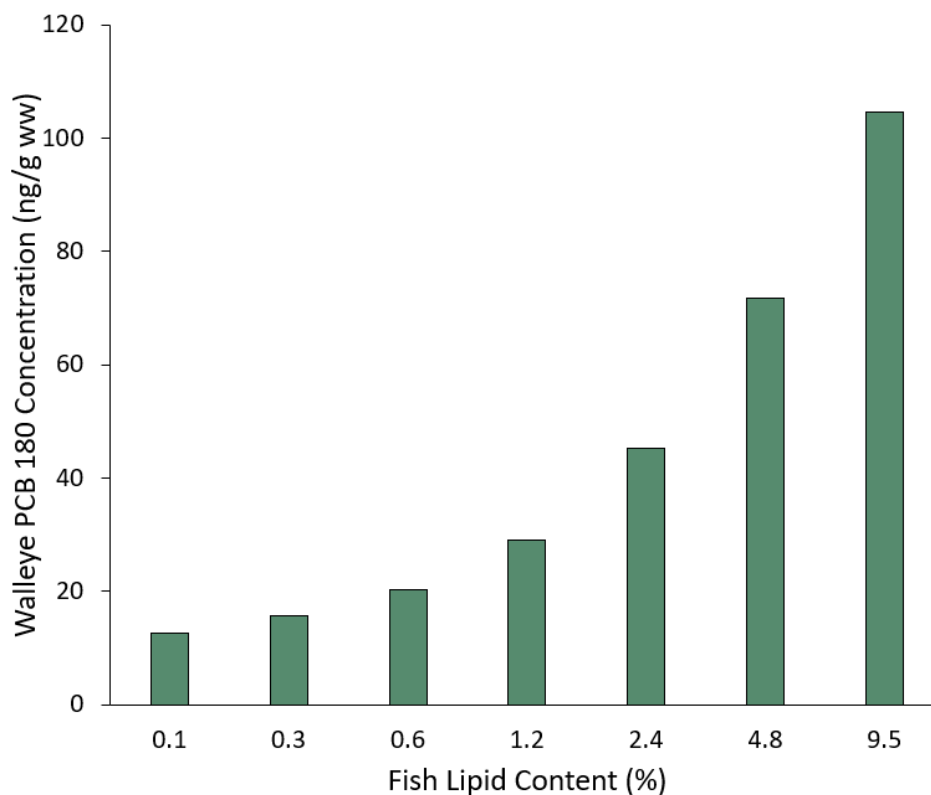


Figure 21. Impact of fish lipid concentration on walleye PCB 180 concentration (ng/g ww).

The Arnot & Gobas (2004) model assumes a constant lipid content, which is not realistic as the organism grows (McLeod, et al., 2016); generally, lipid content increases with increasing size of fish. There has been a long-term decline in lipid content in walleye in Torch Lake walleye (see Figure 9). Currently, walleye have an average lipid content of 1%; this contrasts with the 4% lipid in walleye caught in Keweenaw Bay. The lipid content can vary depending on the water quality and abundance of food. The degradation of the benthic community due to the contaminated lake sediments may be the cause of the low lipid content. Therefore, the remediation of the lake sediments may impact the bioaccumulation of PCBs because of the elimination of within-lake sources, but also help improve the benthic community; therefore, influencing the food web length.

3.2 MeHg Modeling Results

This section gives an overview of the MeHg bioaccumulation model results in Torch Lake. Figure 21 displays the whole-ecosystem recovery of Torch Lake aquatic ecosystem over the 10-yr period. The sensitivity and uncertainty analysis results show the limitations to the non-steady state model and assist with future model improvements. The experimental modeling of reducing the dissolved MeHg concentrations in the lake water examines the response of the walleye MeHg concentration to source eliminations.

3.2.1 Non-steady state MeHg bioaccumulation model results

The predictions of the MeHg bioaccumulation model for Torch Lake are displayed in Figure 21 for the walleye concentrations ($\mu\text{g/g}$ ww or ppm) over a 10-year period. The model was run for 10 years because this is the estimated age of walleye of the weight modeled (e.g., 1.45 kg). Trophic levels 1 and 2 reach steady state within one year, but it requires about two years for trophic level 3 and 10 years for trophic level 4. Trophic level 4 has a steady state concentration about 10 times higher than trophic level 3 which is about 10-fold higher than trophic level 1. Concentrations in trophic level 2 plateau at a value within a factor of two of the steady state concentration in trophic level 3.

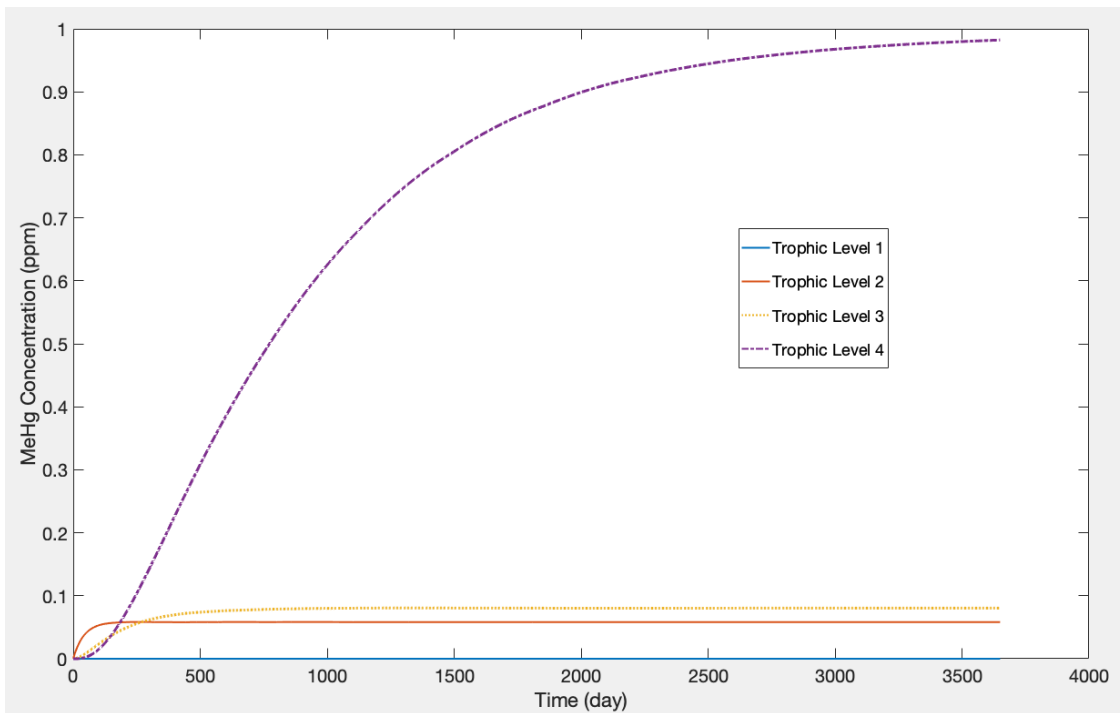


Figure 22. The non-steady state MATLAB predicted MeHg concentration in walleye over 10-year period.

3.2.2 Model validation, and sensitivity and uncertainty analyses results

3.2.2.1 Walleye Model Validation Results

The MATLAB predicted concentration of mercury in walleye were about two-fold higher than the observed concentrations from GLIFWC and MI EGLE (see Table 17). The percent error between the model-predicted concentrations and the measured walleye concentration was estimated to be 78% using Equation 24. There are limitations of the model that may have resulted in values higher than those measured. For example, the model assumes a constant organism body weight; thus, it ignores the potential impacts of

growth dilution. The implications will be discussed later together with recommendations for model improvement.

Table 17. Torch Lake walleye mercury modeled and observed concentrations from MI EGLE (1988, 2000, 2007, 2013, 2018) and GLIWC (2018, 2019).

Torch Lake Walleye Mercury Concentration (µg/g ww)		
MATLAB predicted (10-yr period)	GLIFWC average measured (2018-2019)	MI EGLE average measured (1988-2018)
0.98	0.55	0.61

The predicted BAF from the non-steady state bioaccumulation model are reported in Table 18 below:

Table 18. Predicted MeHg Bioaccumulation Factor (BAF) for trophic levels 3 and 4.

Trophic level 3	Trophic level 4	Literature values trophic level 4 log BAF ¹
0.53×10^6	6.5×10^6	$10^{6.5} - 10^{7.69}$

Source references used in this table: Raymond and Rossmann (2009)¹

The BAF for trophic level 3 was higher than the 90th percentile and trophic level 4 was higher than measured BAF values indicated in Table 10 in methods.

The zooplankton measurements from northern Wisconsin lakes presented in Back and Watras (1995) were used to compare the model-predicted concentrations. The zooplankton were collected from twelve different lakes and separated by taxa. The ranges of MeHg based on taxa are presented in Table 19. The results from this study showed a decrease in zooplankton bioconcentration of Hg as an increase in lake DOC.

Table 19. Zooplankton MeHg concentrations reported by Back and Watras (1995).

Zooplankton taxa	Measured MeHg range (ng/g dry wt)
Herbivorous	1 - 479
Omnivorous	24 - 30

The model-predicted herbivorous zooplankton concentrations were within the range with a value of 58 ng/g ww. The study by Back and Watras (1995) revealed that zooplankton from lakes <10 mg/L DOC had higher bioconcentration of both Hg and MeHg. The dissolved organic carbon concentration in the Torch Lake water was assumed to be 7.9 mg/L based on the 10-year average (Mandelia, 2016).

3.2.2.2 Sensitivity Analysis Results

The parameter perturbation method for the MeHg bioaccumulation model was performed in a similar manner to the PCB bioaccumulation model. The uptake and elimination rate constants were varied by $\pm 10\%$ shown in Figures 24 and 25. It should be noted that the rate constants were included in the analysis because the steady-state assumption for the MeHg concentration in phytoplankton. The MeHg model was most sensitive to the total elimination rate constant (k_{TOT}) in trophic levels 2 and 3, the bioconcentration uptake rate in trophic level 2 (k_1) and the ingestion rate in trophic levels 3 and 4 (I).

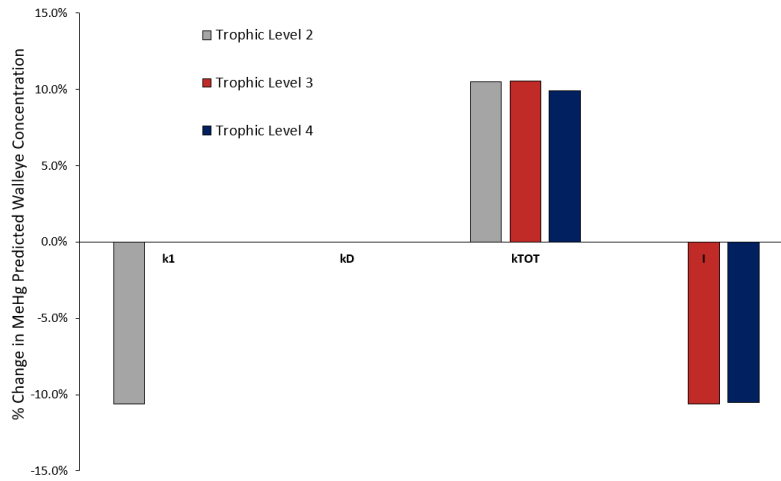


Figure 23. Change in walleye MeHg concentration caused by decreasing the model rate constants for trophic levels 2 (gray), 3 (red), and 4 (blue) by 10%.

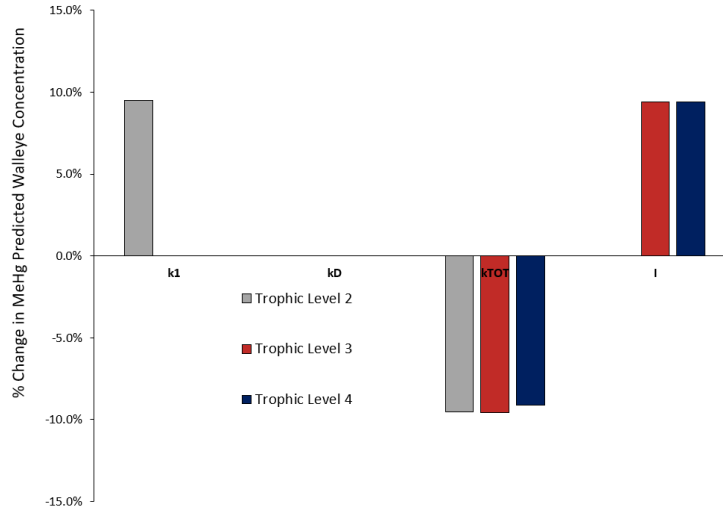


Figure 24. Change in walleye MeHg concentration caused by increasing the model rate constants for trophic levels 2 (gray), 3 (red), and 4 (blue) by 10%.

3.2.2.3 Uncertainty Analysis Results

The Monte Carlo simulation was run for 10,000 iterations of the MeHg bioaccumulation model. Values for the dietary assimilation efficiency (E_D), total elimination (k_{TOT}) rate constants and temperature (T) followed a normal distribution and were randomly and independently selected. The simulation results are shown in Figure 26. The calculated mean MeHg concentration, standard deviation, and 95% confidence interval from the Monte Carlo Simulation are displayed in Table 20.

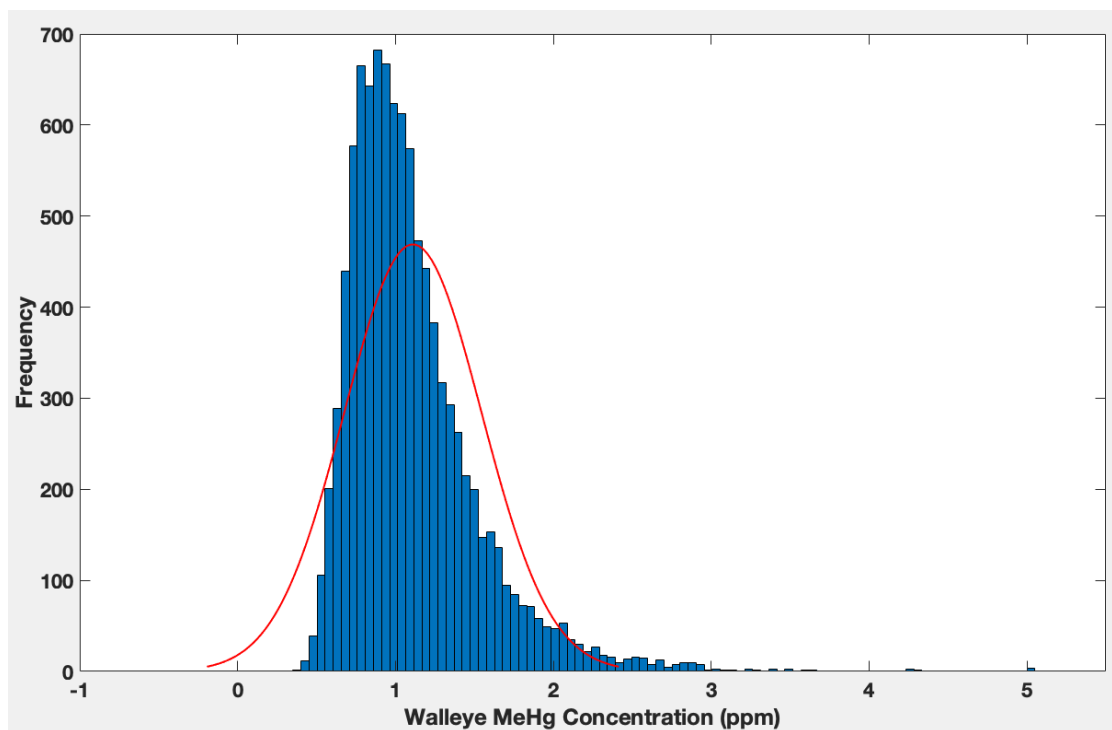


Figure 25. Walleye MeHg Monte Carlo simulation output concentration histogram. Normal distribution curve (redline).

Table 20. Torch Lake Walleye MeHg Monte Carlo simulation mean concentration, standard deviation, upper and lower 95% confidence interval selected at the end of 10-year period modeled.

Mean Concentration ($\mu\text{g/g ww}$)	Standard deviation ($\mu\text{g/g ww}$)	Lower 95% confidence interval	Upper 95% confidence interval
1.11	0.43	1.10	1.12

The results from the Monte Carlo simulation show that the model predictions did not follow a normal distribution. As a percent of the mean, the 95% confidence interval was 1.8%. The uncertainties are, therefore, small relative to the predicted concentrations ($0.98 \mu\text{g/g ww}$). Nevertheless, the range of values predicted by “reasonable values” of the parameters in the Monte Carlo simulation is large ($\sim 3 \mu\text{g/g ww}$) relative to measured concentrations ($< 1 \mu\text{g/g ww}$). If bias exists in the model predictions, it would be easy to tune the model to predict lower values.

3.2.3 Modeling Experiment Results

The lake water dissolved MeHg concentration was set to half of the value measured in 2021 to represent the reduction in MeHg if there was no ongoing source in the lake due to

in-lake methylation. The model-predicted 10-year steady state concentration in walleye was 0.49 $\mu\text{g/g ww}$; therefore, a 50% reduction in MeHg in the lake caused a reduction in the bioaccumulated burden by 50%. The simulation results highlight the dependence of the predicted walleye concentrations on dissolved MeHg concentrations. In addition, the results show the maximum potential impact of remediation actions on in-lake methylation. The results of the second model experiment to determine the time to reach the average measured bioaccumulated burden in Torch Lake walleye to be 619 days, or ~2 years.

4 Discussion

4.1 Validity of modeling approach

Mathematical models simplify the complexity of nature by making assumptions. It is important to verify and validate models with measured observations to determine the accuracy of the assumptions made. The target species for this project is walleye in Torch Lake. The reasons for focusing on walleye are not only is walleye an important species for recreational and tribal community fishing, but the species has been part of the MDEQ Fish Contaminant Monitoring program since 1998 for Torch Lake and control sites (Portage Lake and Huron Bay). The presented bioaccumulation models for PCBs and MeHg are validated against measured observations of these contaminants in Torch Lake. The steady state predicted concentrations for an averaged size walleye (e.g., 1.45 kg) is compared with the average measured concentrations in Torch Lake. In addition, to the long-term study of the Fish Contaminant Monitoring program, GLIFWC and the TL PAC have recent measurements for validation and estimation of current concentrations. The established steady state model, “AQUAWEB” (Arnot, Research, & Consulting) was used as another tool for verification of the PCB bioaccumulation model. The steady state model was used as a means of verifying the Matlab coding as well as the choice of rate constants used to predict steady state concentrations in all four trophic levels. Literature values of measured MeHg concentrations in lower trophic levels were compared with the model-predicted concentrations for validation (see Table 19). The bioaccumulation factor (BAF) was used as a comparison of the previously used tool for estimating mercury concentrations in forage and predatory fishes. The bioaccumulation models agreed well with measured concentrations as shown below; for this reason, no calibration of the model was performed. Sensitivity and uncertainty analysis are also important for validation of assumptions for natural systems.

4.1.1 PCBs

Approaches for modeling of bioaccumulation of hydrophobic organic contaminants have evolved from simple partitioning to dynamic kinetic models of uptake and elimination from organisms. The first equilibrium-based approaches estimated the steady-state concentrations in fish by the ratio of exposed environmental media. Kinetic models were developed to account for multiple pathways of exposure for organisms. The kinetic food-web bioaccumulation model of Arnot & Gobas (2004) bioaccumulation model has been widely used for environmental risk assessments. The model includes the two routes of exposure for aquatic organisms: uptake via gill ventilation (respiration or bioconcentration) and ingestion of contaminated prey (biomagnification). The adaptation of the model for Torch Lake excluded respiration of sediment pore-water because of the paucity of benthic organisms. The model included elimination of PCBs via respiration and fecal excretion. It was assumed that the metabolic transformation of PCB congeners was negligible. The non-steady state mass balance model was applied to the Torch Lake food web (phytoplankton, zooplankton, forage, and predatory fishes) as a whole-ecosystem assessment of PCB congeners. The model congeners selected (PCB 33, 52, 99, 101, 149, 153, and 180) showed a range of chlorination level and were all at detectable

concentrations in the 2005 SPMD measurements (MDEQ, 2006). The uptake and elimination rate constants were estimated as a function of temperature, organism body weight, and chemical efficiency that varied among congeners and trophic levels. The net bioaccumulation of PCBs results from fast uptake rates and slow elimination rates.

The output values from the AQUAWEB model were used as verification of the MATLAB model for Torch Lake. Identical biological, chemical, and environmental parameters were used in both models. For example, the organism body weight, temperature, PCB congener octanol-water partition coefficient and dissolved phase concentrations were the same. The calculated uptake and elimination rate constants agreed well between both models. The similar results for both models suggest that the coding in the MATLAB model adapted from Arnot & Gobas (2004) is correct. In addition, the predicted steady state PCB concentrations in the four trophic levels agreed well between the two models. The AQUAWEB model predicted slightly higher concentrations than compared to the MATLAB model for each congener. This may be due to differences in the steady state and non-steady state calculations for dissolved water concentrations. The bioavailable, dissolved phase PCB concentrations in the AQUAWEB model are calculated from measured total concentrations in the water column. The dissolved phase is estimated as a function of dissolved organic carbon (DOC) and particulate organic carbon (POC) in the water column. The MDEQ SPMD measurements in 2005 are an indirect measurement of the dissolved concentration in the water column (Mandelia, 2016). Thus, the MATLAB model used the estimated dissolved phase concentrations from the SPMD measurements to drive the bioconcentration in the model.

The model-predicted concentrations agreed well with the concentrations measured by EGLE and the MTU TLPAC project, except for heavier congeners (specifically, congeners 153 and 180). The calculated percent error for each congener ranged from 17-462%. The models over-predicted concentrations in walleye by a factor of two and four for congeners 153 and 180, respectively. However, it should be noted that the time to reach steady-state for the more chlorinated congeners was much greater than for the less-chlorinated (lighter) congeners. The slow response is similar to findings of other studies in which very slow, or no, elimination of hydrophobic PCB congeners with a $\log K_{ow} > 6.5$ has been observed resulting in the fish never reaching steady state within their lifetime (Niimi and Oliver 1983; McLeod et al., 2016). The relatively long (~10 years) response time of heavier chlorinated PCBs for the modeled walleye may not represent a comparable estimated concentration. The average weight for walleye measured from the Fish Contaminant Monitoring program was used as the modeled organism. The average weight of walleye is 1.45 kg, which represents ~10-year-old fish based on the GLIFWC measurements in Torch Lake. The oldest fish in the study was reported to be 15 years old. Therefore, the modeled predicted concentrations would not reach steady state within the lifetime of the organism.

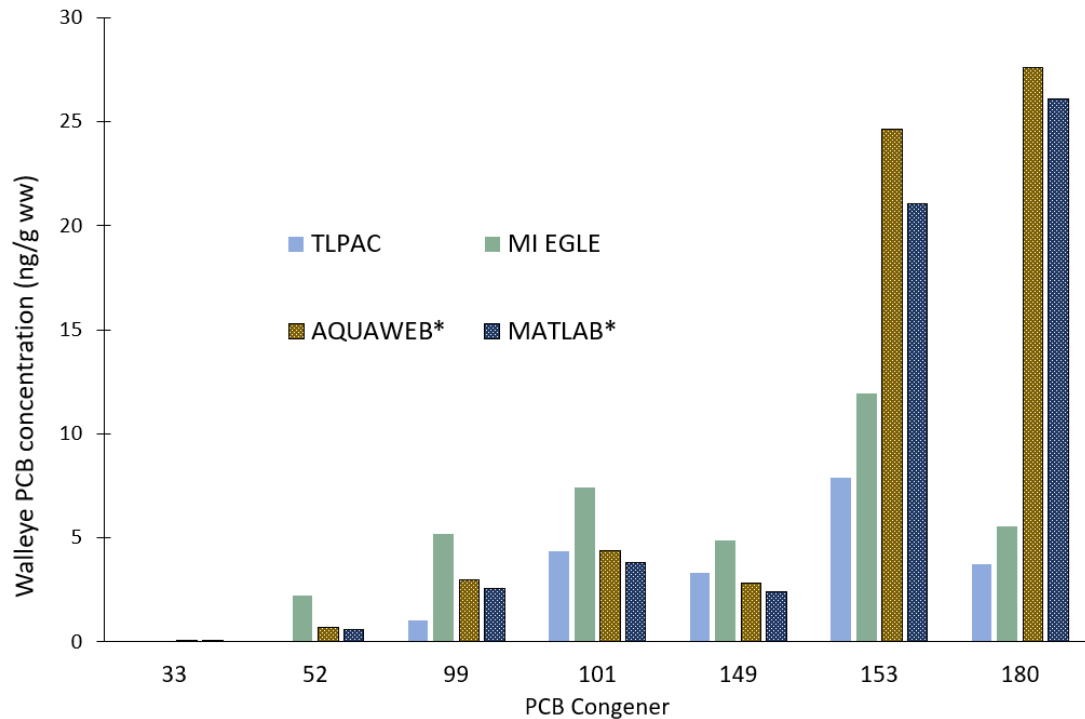


Figure 26. Comparison of Walleye PCB measured and predicted concentrations. The averaged measured concentrations in Torch Lake by MDHHS Fish Monitoring program and Torch Lake Public Action Council (TLPAC), and the predicted concentrations from MATLAB and AQUAWEB bioaccumulation models. (*model-predicted)

The model-predicted walleye concentrations were most sensitive to the trophic-level-four dietary uptake and fecal excretion rates (see section 3.1.2.2). This sensitivity is not unexpected, because the major route for PCBs for fish is via their diet and increases with an increase in log K_{ow} (Barber, 2008; McLeod et al., 2015). The uptake of PCBs via food dominates gill uptake of most fish of a log $K_{ow} > 6$, however bioconcentration should not be ignored (Barber, 2008). As presented in section 3.1.2.3, the Monte Carlo simulation produced 95% confidence intervals and standard deviations that increased with an increase in PCB chlorination level. This indicates that the uncertainty in the dietary assimilation efficiency and K_{ow} has a greater effect on fish concentrations for heavier congeners. The Monte Carlo uncertainty analysis also indicated that the confidence interval about the predicted concentrations was only ~ 0.13 ng/g; a value small in comparison to the predicted concentrations (1.47-3.85 ng/g). The model was not calibrated because of the good precision and reasonable accuracy of the model predictions.

In addition, the models may have overestimated the PCB 153 and 180 concentrations because of the model sensitivity to consumption and elimination, which are dependent on temperature. The model was run under constant temperature of 10°C for the 10-year period; however, the optimal temperature for adult walleye is approximately 18-22°C (GLIFWC, 2023). Therefore, the model may be overpredicting consumption and

elimination of PCBs under the lower-than-optimum temperature. This may be the cause of the overestimation of PCB concentrations for congeners that are more sensitive to these parameters. The rate of consumption would have a greater impact because of the modeled fish is older and slow growing; thus, elimination is very slow and close to zero. The organism feeding rate has been shown to be sensitive to temperature (McLeod et al., 2015; Hansen et al., 2022).

The bioaccumulation of organic contaminants is a whole ecosystem process, but it often is studied at the level of an individual organism (Li et al., 2015). The model developed here is for an individual organism at each trophic level; population dynamics were not included. Other bioaccumulation models such as the U.S. EPA Bioaccumulation and Aquatic System Simulator (BASS) model incorporate a population model (Barber, 2008b). The predictions for this model should only be considered valid for the lifetimes of the organisms involved (days for algae, weeks for zooplankton, up to perhaps 15 years for fish in trophic levels three and four) although we show predictions out to 10 years for all trophic levels. This model does not include short-term fluctuations (weekly to seasonal) such as those caused by seasonal temperature changes or cyclical blooms and die-off of plankton populations. The model also assumes constant conditions in the lake; it does not include trends such as induced by climate change, changing rates of atmospheric contaminant deposition, or lake remediation. Similarly, changes in diet, food availability, and food web structure influence the accumulation of contaminants in fish. Food webs are generally more complex than the four-member chain used in this project. This simplification may be justified, however; the degradation of the benthic community likely simplified the food web in Torch Lake to four trophic levels: phytoplankton, zooplankton, forage fish, and predator fish. Despite these limitations, the model is thought to provide useful simulations of contaminant concentrations in all four trophic levels under the conditions of each scenario. The Arnot & Gobas (2004) model has been widely used to understand food web bioaccumulation in global locations. The model has been adapted and calibrated to derive remediation targets in different ecosystems and species (Drouillard et al., 2009; Gobas & Arnot, 2010; Figueiredo et al., 2014; Wellman & Haynes, 2022; Lombard et al., 2023; Niu et al., 2023). The model can be adapted to be site specific with the inputs of measured species-specific biological attributes such as, ventilation and feeding rates and fractions of lipid, NLOM, and water in the organism. An alternative approach would be to calibrate the kinetic rate constants to meet agreement with empirical measurements of concentrations.

4.1.2 MeHg

Following the deposition of mercury into the aquatic ecosystem, the mercury can then undergo transformations to the bioavailable form, methylmercury (MeHg). MeHg is of interest because it is a persistent, bioaccumulative, toxic (PBT) substance. The human exposure of the neurotoxicant is primarily through the consumption of fish. The elevated concentrations of MeHg in Torch Lake fish have caused fish consumption restrictions. Mechanisms of MeHg bioaccumulation are less understood as compared to those of PCBs (Li, Drouillard et al. 2015). Furthermore, the cycling of mercury in lakes is much more complicated than that of PCBs because multiple pathways exist for the rapid

conversions between oxidized (Hg II) and reduced (Hg 0) forms as well as for the methylation and demethylation of mercury. The EPA's recommended surface water quality criterion for methylmercury is actually a concentration of 0.3 mg/kg total mercury in fish (U.S.EPA, 2001). The SERAFM model (Knights, 2008) has been widely used to determine the loading of mercury to a surface water that will maintain fish tissue mercury concentrations below the water quality criterion. This model explicitly accounts for many of the complexities of mercury cycling (oxidation-reduction, methylation-demethylation), but then uses Bioaccumulation Factors (BAFs) to estimate concentrations in aquatic life forms. This method was used recently by Hendricks (2015) and Perlinger et al. (2018) to estimate fish mercury concentrations in lakes in Michigan's Upper Peninsula. Arguably, BAFs should only be used to understand bioaccumulation in the system in which they were measured because of the many environmental influences on bioaccumulation of MeHg (Driscoll et al., 2007; Madenjian et al., 2021).

For this reason, a combination of different models was used to estimate the mercury concentration in the top-predator fish, walleye, because the measured concentrations in Torch Lake are limited to top predator fish species (walleye, northern pike, smallmouth bass). The Trudel & Rasmussen (2001) bioaccumulation model was adapted to estimate the concentration in walleye in Torch Lake. The widely used kinetic model estimates the bioaccumulation of mercury in fish. The uptake of MeHg from water accounts for less than 0.1% of bioaccumulated MeHg in higher trophic level organisms; thus bioconcentration commonly is assumed to be negligible (Trudel and Rasmussen 2001). The elimination of mercury is modeled as a total elimination rate constant. The elimination of mercury is less well understood as compared to PCBs and involves diffusive and complex biotransformation mechanisms (Wang and Wang 2015; Wang et al., 2017; Li et al., 2018). Past mercury mass balance models in fish used the empirically-estimated rate constant derived in Trudel and Rasmussen (1997) as a function of organism body weight and water temperature. However, recent studies have shown that the empirical elimination constant tends to underestimate observed concentrations in natural systems (Madenjian et al., 2021). Therefore, an updated elimination rate constant presented in (Yao and Drouillard 2019) that included a fish thermal category was used in the MATLAB model. The bioaccumulation of MeHg is dominated by the uptake via contaminated food (Hall et al., 1997). However,, there are no measurements of mercury in Torch Lake's lower three trophic levels. The Schartup et al. (2018) model for marine phytoplankton and zooplankton was applied to Torch Lake to estimate the bioaccumulated burden in the lower trophic levels that drive the biomagnification in the higher trophic level species. Rather than starting with a mass balance model and implementing the complex mercury cycling model as in SERAFM, the model used here utilizes methylmercury concentrations measured in Torch Lake in summer of 2021 (EGLE, unpub.).

The model-predicted MeHg concentrations in walleye were validated against measured concentrations in Torch Lake from the Fish Contaminant Monitoring program and the GLIFWC mercury monitoring program. The model-predicted concentrations were within a factor of two of the average measured concentrations (see Table 19 and Figure 13). Therefore, the model predicted reasonable concentrations with the use of the summer

2021 dissolved MeHg concentrations of 0.15 ng/L (EGLE, unpub.). Since there are no measured concentrations of MeHg in lower trophic level organisms, literature values were used to assess the reasonableness of model predictions. Based on intensive studies on northern Wisconsin lakes, Back and Watras (1995) reported dissolved MeHg concentrations of 0.03-1.95 ng/L; this range brackets the value used in this study. The predicted zooplankton concentrations 1 to 479 ng/g dry weight were also within the range reported by Back and Watras (1995) in the same Wisconsin lakes (See Table 19). The model developed in this study appears to predict reasonable concentrations for at least two of the trophic levels.

The sensitivity analysis results indicate that the walleye MeHg concentration is most sensitive to the dietary uptake and total elimination rate constants in trophic levels 3 and 4. The uncertainty of MeHg biotransformation reactions causes uncertainty in the total elimination rate constant. The assimilation efficiency of MeHg from the diet is also highly uncertain with differences in laboratory- and field experiments (see Table 12). The Monte Carlo simulations had a 95% confidence interval of 1.8% about the mean value. Therefore, the model uncertainty is small in comparison to the predicted concentrations for MeHg in walleye.

The BAF was previously used to estimate fish concentrations in past mercury mass balance models in Torch Lake (Knightes, 2008; Hendricks, 2015). In this study, the BAF for forage fish (brown bullhead) and predator fish (walleye) were calculated to be 0.53×10^6 and 6.5×10^6 , respectively. The values for forage fish and predatory fish lie within the 5th-25th and 25th-50th percentiles, respectively, reported by Knightes (2008) (see Table 10). The BAF for phytoplankton and zooplankton were 33 and 0.38×10^6 , respectively. The reported values by Schartup et al. (2018) for marine phytoplankton and herbivorous zooplankton ranged between $10^{2.4}$ - $10^{5.9}$ and $10^{4.6}$ - $10^{5.8}$, respectively. The MeHg concentrations were dependent on the ecosystem biogeochemical characteristics. For example, the lowest phytoplankton concentrations, were found under the highest concentrations of dissolved organic carbon (DOC). This phenomenon, known as “bloom dilution”, has also been shown in freshwater ecosystems (Pickhardt, Folt et al. 2002). However, the increase in nutrients and DOC can also enhance the production of MeHg that can be available for uptake through the food web (Driscoll et al., 2007, Dittman et al., 2010; Clayden et al., 2013; Clayden et al., 2014; Kerfoot et al., 2018).

The bioavailable form of mercury, MeHg, is greatly influenced by upland watershed and lake biogeochemical characteristics (Perlinger et al., 2018). For this reason, the bioaccumulation of MeHg is also a function of environmental conditions (Chen et al., 2005; Harris et al., 2007; Blanchfield et al., 2022). The SERAFM model (Knightes, 2008) does predict the changes of MeHg concentrations in fish due to change in the loadings in the watershed, but uses the steady-state linear relationship, BAF. The model presented in this project combines kinetic based models that are useful for whole-ecosystem assessments when limited data are available. The degradation of the benthic community likely simplifies the food web in Torch Lake to four trophic levels (phytoplankton, zooplankton, forage fish, and predator fish) as were used in the MATLAB model. The model does not include seasonality which may influence the

methylation/demethylation of mercury. The model assumes constant lake conditions such as water temperature, dissolved oxygen, and dissolved organic carbon. Despite these limitations the bioaccumulation model for mercury developed in this project can provide useful insights into changes of MeHg concentrations in fish due to changes in the water column. The knowledge of MeHg bioaccumulation is evolving; elimination mechanisms are less understood than for non-ionizable contaminants. Ecosystem studies of stable isotopes can help better understand the uptake and elimination mechanisms as well as improve the predictions of bioaccumulation models (Harris et al., 2007; Van Wallegghem et al., 2007; Van Wallegghem et al., 2013; Blanchfield et al., 2022).

4.2 Predicted effects of remediation

One of the aims of this thesis project is to understand the responses of Torch Lake fish to possible remedial activities including elimination of sources of PCBs and MeHg. Bioaccumulation models are useful tools to examine the potential effectiveness of remediation by using organisms as tracers. The MI EGLE Fish Contaminant Monitoring program shows temporal trends after changes in global and regional mercury sources resulting from regulatory actions, and it also is expected to show effects of local remediation activities. The fish consumption advisories due to elevated concentrations of PCBs and MeHg are still one of the two beneficial use impairments (BUI) in Torch Lake. The fish consumption advisories were meant to be short-term solutions to manage fish contamination; however, the advisories related to MeHg and PCBs fish contamination have been in place since 1993 and 1998, respectively. The advisories impact recreational fishing, and the surrounding community's view of the clean-up that has taken place since the end of the mining activities five decades ago. The local Indigenous tribe, KBIC, is one of the most vulnerable communities due to its high fish consumption rate. The different remediation scenarios in this project are presented below. The impacts of proposed remediation of sediment areas with elevated PCB concentrations (regions 1 and 2) on fish concentrations are described in the following section. The effects of reducing lake MeHg concentrations on fish MeHg bioaccumulation are described below. Analysis of MeHg in watershed tributaries indicated that ~50% of MeHg is produced in the watershed, and the other ~50% is produced in the lake. Thus, the measured 2021 MeHg concentrations in Torch Lake were reduced by 50% to simulate the fish concentrations without in-lake methylation.

4.2.1 Remedial impacts on PCB contaminated sediment in Torch Lake

The bioaccumulation model coupled with the PCB mass balance model of Mandelia (2016) can predict the response of PCB concentrations in aquatic organism to changes in the bioavailable, dissolved, water concentrations resulting from remedial activities. One of the modeling scenarios predicted the fish PCB concentrations if atmospheric deposition was the only source of PCBs to Torch Lake; this is equivalent to removing all other sources of PCBs to the lake. The models predicted that the more heavily chlorinated congeners would exhibit the greatest reduction through elimination of other PCB sources (i.e., contaminated lake sediments). Lighter PCB congeners dominate atmospheric

concentrations, as depicted in Figure 6. The less chlorinated (lighter) congeners have higher vapor pressures and volatilize into the atmosphere and undergo long-range transport (Perlinger et al., 2016). Because population dynamics were not considered in this model, the time frame for PCB reductions in the food web was not modeled. For other lakes, a lag in fish tissue concentrations relative to decreases in atmospheric concentrations from a few years to a decade has been estimated (Khan 2018; Urban et al., 2020).

The remediation at Torch Lake in the past has included soil capping to prevent the airborne exposure of particulates to humans. Part of the objectives of this thesis were to determine the impact of proposed remediation of Torch Lake sediments on predicted fish concentrations. The scenarios focused on the two regions of elevated PCB concentration, Hubbell Processing Area (region 1) and Lake Linden Recreation Area (region 2). PCB mass balance modeling points to these areas as on-going sources of PCBs into the Torch Lake water column (Mandelia, 2016). The model predicted Region 1 to be the greater contributor of PCBs to the water column as shown in Table 21. Based on the AMW sediment measurements, the PCB 180 concentrations were higher in region 1 (median = 2.4 µgPCB/kg solids, min = 0.14 µgPCB/kg solids, max = 112.6 µgPCB/kg solids) in comparison to region 2 (median = 0.037 µgPCB/kg solids, min = 0.001 µgPCB/kg solids, max = 2.5 µgPCB/kg solids). Therefore, the larger area (3.1×10^{-1} vs. 8.63×10^{-2} km²) and measured concentrations in region 1 may be driving the elevated PCB concentrations in Torch Lake; accordingly, the proposed remediation in HPA (region 1) should cause a reduction in fish concentrations.

Table 21. Predicted reductions in walleye concentration corresponding to different lake sediment remediation scenarios.

	Model-predicted PCB concentrations						
	PCB 33	PCB 52	PCB 99	PCB 101	PCB 149	PCB 153	PCB 180
No Remediation	0.02	0.07	0.81	1.26	2.36	4.29	3.13
Region 2 Remediated	0.01	0.07	0.80	1.26	2.35	4.25	3.12
Region 1 Remediated	0.01	0.02	0.23	0.23	0.18	0.34	0.36
Regions 1 and 2 Remediated	0.01	0.02	0.23	0.23	0.18	0.30	0.35

Remediation of the contaminated Torch Lake sediment is intended to reduce human exposure to metals, but it may also contribute to work removing the fish consumption advisories due to elevated PCB concentrations. Exposure to PCBs via fish consumption

poses threats to human and environmental health. Additionally, the fish consumption advisories cause social and environmental injustice to the local tribal community. The KBIC members are vulnerable to contaminant exposure because of their higher-than-average fish consumption rate. The spring walleye harvest is when the fishing activities are the highest (Perlinger et al., 2018). The KBIC retains treaty-protected homelands and harvesting rights across ten-million acres of the Lake Superior watershed, including the majority of the western UP (Perlinger et al., 2018). The fish advisories in this region impact the cultural identity, well-being, and health of the KBIC tied to the environmental health (Norman, 2013).

In an assessment of PCBs within lakes of this region, Sokol (2015) estimated a PCB concentration of 2.88 ng/g ww in fish would enable KBIC members to consume their desired quantities of fish. The desired consumption rate was equal to 8 ounces (230 g) of fish per day (Gagnon, 2014). However, the desired quantities have been updated since this assessment and the intake has been calculated to be equal to 260 g of fish per day. This consumption rate is based on the 95th percentile of highest consumption rates, if there were no restrictions on fish consumption. This estimate includes the spring harvest activities in this region's lakes. In comparison, the consumption rate of recreational anglers in Michigan is equal to 14 grams of fish per day (Shaw & Urban, 2022). The MDCH reference dose (RfD) is set as 0.02 µg/kg-day to protect against harmful immune system effects caused by PCBs (MDCH, 2012). The allowable contaminant concentration can be determined with the EPA Equation 34 to estimate the consumption limit (EPA, 2000):

$$\text{contamination concentration} \left(\frac{\mu\text{g contaminant}}{\text{kg fish}} \right) = \frac{\text{RfD} \left(\frac{\mu\text{g}}{\text{kg-day}} \right) \times \text{BW}(\text{kg})}{\text{fish consumption rate} (\text{kg/day})} \quad (34)$$

The safe consumption limit is protective of sensitive subgroups (children under 15 and women between the ages of 15-45). Therefore, the body weight (BW) is set to 65.4 kg. The updated fish consumption rate calculates an allowable contaminant concentration of 5.03 ng/g ww, thus increasing the prior estimate by a factor of 1.7.

$$\text{contamination concentration} \left(\frac{\mu\text{g contaminant}}{\text{kg fish}} \right) = \frac{0.02 \left(\frac{\mu\text{g}}{\text{kg-day}} \right) \times 65.4 \text{ kg}}{0.260 (\text{kg/day})} = 5.03 \frac{\mu\text{g}}{\text{kg}} \quad (35)$$

The allowable concentration estimated with the desired fish consumption rate is important to protect the treaty rights in addition to the health and well-being of the Indigenous community. The above criterion is met for the model-predicted concentrations - except for PCB congeners 153 and 180. However, the advisories should not be used as a long-term solution to protect human exposure. The remediation of Torch Lake can assist with delisting the AOC site, so that the fish consumption advisories are no longer needed (Gagnon et al., 2017). Additionally, a full cost-benefit analysis would ensure that Native Americans do not suffer health, social, and cultural consequences as a result of the advisories (Hoover et al., 2013). The consumption of fish holds traditional value greater than solely as a nutrient rich source of omega-3 fatty acids.

4.2.2 Revised aqueous concentrations of MeHg in Torch Lake

The source elimination for mercury is more complicated as compared to PCBs because of the greater dependence on watershed and lake biogeochemical characteristics (Wiener et al., 2003; Chen and Folt, 2005; Driscoll et al., 2007; Ward et al., 2010; Wiener et al., 2012). Torch Lake is within a highly sensitive landscape due to the large percentage of wetlands in its catchment; wetlands are sites of methylation (Evers et al., 2007; Kerfoot et al., 2018). Landscape characteristics have a greater impact on mercury concentrations in this region, as compared to changes in atmospheric deposition (Perlinger et al., 2018). For this reason, the reduction of MeHg in fish tissue is not just a function of regional or local atmospheric deposition, as explained by Chen et al. (2005).

The mining activities that occurred along the western shore of Torch Lake such as copper smelting and electrification produced considerable quantities of fly and bottom ash that contributed to the deposition of mercury within the watershed. It would be difficult to determine the magnitude of “new” Hg and “old” Hg cycling in the aquatic ecosystem (Dittman, 2010). The bioaccumulation model predicted the response of the aquatic ecosystem to dissolved lake water concentrations reduced by half of the 2021 EGLE measured concentrations. This reduction is based on the estimate that 50% of MeHg content in the lake hypolimnion in summer is derived from watershed inputs (primarily runoff from wetlands) and 50% is derived from methylation within the lake (Greene and Urban, 2022). It is assumed that the in-lake methylation is due to high total mercury concentrations (0.8 ng/L in epilimnion and 1.6 ng/L in the hypolimnion) in the lake that result from leaching of mercury from the mine tailings that occupy ~50% of the lake’s former volume (Great Lakes Environmental Center, 2003; Urban et al. 2018). By eliminating in-lake methylation, the predicted MeHg concentration in walleye is reduced by 50%. The results point to the dependence of the bioaccumulation model predictions on MeHg concentrations in tributaries to the lake.

The EPA RfD for MeHg is 0.1 µg/kg-day to protect against adverse neurological effects in infants (U.S. EPA, 2000). Using equation 27 the estimated contaminant concentration with the desired consumption rate of 260 g of fish per day for MeHg would be 0.025 µg/g ww.

$$\text{contamination concentration} \left(\frac{\mu\text{g contaminant}}{\text{kg fish}} \right) = \frac{0.1 \left(\frac{\mu\text{g}}{\text{kg-day}} \right) \times 65.4 \text{ kg}}{0.260 \text{ (kg/day)}} = 25 \frac{\mu\text{g}}{\text{kg}} \quad (36)$$

The above criterion would still not be met with the 50% reduction of measured dissolved concentrations according to the model simulation. Coupling the bioaccumulation model with a mass balance model such as that of Hendricks (2018) would better depict the cycling of mercury that would impact the accumulation in fish.

4.3 The influence of fish lipid content on the PCB bioaccumulated burdens

The PCB concentrations in fish species are commonly normalized to lipid content because of the dependence of PCB concentrations on lipid content. PCBs are lipophilic substances, meaning the compounds have a greater fugacity capacity in lipid tissues. The age, size, and health of an organism influence its lipid content. The degradation of the benthic community in Torch Lake may limit the food available to Torch Lake fish, thereby causing the fish to be unhealthy and leading to the decline in lipid content shown in Figure 9. The lipid-normalized PCB concentrations shown in Figure 10, depict a statistically insignificant decrease in walleye, contrary to EGLE reports (MDEQ, 2008a; MDEQ, 2016).

The bioaccumulation model simulated the impact of walleye lipid content on the predicted walleye PCB concentration. The modeling results in Figure 22 display the 10-fold increase in PCB concentrations associated with a 100-fold increase in lipid content. The lipid content in the model simulations ranged between 0.1-9.5%; the higher lipid content was observed in the earlier studies (year 2000) of Torch Lake. Therefore, the future recovery of the benthic community in Torch Lake may cause the bioaccumulated PCB burden in the fish to increase. The increase in the complexity of food webs has been shown in other studies to increase trophic magnification of PCBs and contaminants (Lepak et al., 2019; Urban et al., 2020).

Furthermore, other ecosystem-scale changes (e.g., climate change, population and land-use change, stocking practices) can impact the health of fish species and therefore, the fish lipid content. Walleye have been stocked in Torch Lake by the MDNR since 1987, highest rates of stocking occurred in 2012. Analysis of the fish stocking data shows that lipid content peaked in the years of high stocking rates (Urban, personal communication). The limitations of the kinetics bioaccumulation model on an individual organism scale, is that the perturbations on an ecosystem scale may not be correctly modeled or identified as causes in changes in fish PCB concentrations.

4.4 Potential impacts of fish immigration to and emigration from Torch Lake

The movement of fish impacts the exposure to contaminants, and subsequently the bioaccumulated burden of contaminants. Organisms with limited mobility are likely to reflect the contaminant concentrations in their immediate environment (Gobas & Arnot, 2010). In comparison, top predator organisms are more mobile and can integrate food items from clean and contaminated areas impacting the trophic magnification. The Torch Lake connection to the Keweenaw Waterway and to Lake Superior provides fish with the capability to move large distances. The movement of fish has been examined with tag and release studies conducted by the MDNR (Hanchin, 2013). The results indicate the movement of fish back and forth between Torch Lake and the Keweenaw Waterway. A recent telemetry study conducted in collaboration with the U.S. FWS revealed that there is little migration into Torch Lake from Portage Lake, however there is a higher rate of

migration from Torch Lake into Portage Lake. In addition, the results showed minimal migration into Lake Superior from the Keweenaw Waterway (Steve Shier, USFWS, personal communication).

In order to examine the effects of immigration to and emigration from Torch Lake the bioaccumulation model was used to estimate the time to acquire unhealthy bioaccumulated burdens. The simulation reflected the migration of an individual fish into Torch Lake when the other trophic levels had constant steady-state concentrations. The other trophic levels were held constants as a conservative estimate. The time for PCB congener concentration in walleye to reach measured concentrations ranged from 0.17 years to over the 10-year modeled time-period. There was no relationship identified between the time to reach measured concentrations and chlorination level of PCB congeners. These results also indicate the disadvantages of having few measurements to calibrate the model.

The time for fish to acquire MeHg measured concentration was predicted to be 2 years. The time for fish to reach steady state conditions, represents the balance between the accumulation of chemical mass and the elimination losses. The age and fish species type impact the time it takes to reach steady state. For example, for less chlorinated PCB congeners and warm water species with fast growth kinetics may reach steady state within their lifetime (Burtnyk et al., 2009). In comparison, highly hydrophobic PCB congeners of $\log K_{ow} > 6.8$, elimination for has shown to be minimal in freshwater fish species and higher trophic level organism may never reach steady state (Paterson et al., 2007a; 2007b). The elimination half-lives for PCB congeners in fish species in the literature has ranged from 71.4 d to 820 d based on laboratory and field studies (Barber, 2008). Similarly, the thermal preference and feeding habitats of fish species has been shown to impact the recovery (Blanchfield et al., 2021). The estimated half-life for mercury ranges from 16-1030 d from laboratory studies but has been shown to be slower (1192 d) in longer term field studies in predatory fish (Van Walleghem et al., 2013).

The movement of an organism can affect the predicted bioaccumulated concentration and changes on an ecosystem scale are out of the scope of the individual bioaccumulation model used in this project. Other studies such as McLeod et al. (2015) adapt the Arnot & Gobas (2004) model that incorporates the influence of fish movements and spatial heterogeneity for chemical concentrations in water and sediments.

4.5 Future work

The non-steady state model used in this thesis project has limitations that could be improved on in the future. The simple models help limit the number of unknown variables; however, it holds unrealistic assumptions. The following section highlights areas of model improvement that includes calibration of rate constants and coupling with site-specific bioenergetics and population models.

The bioaccumulation model in this project utilized literature values and empirical equations to estimate uptake and elimination rate constants, because of the lack of

measured rates in Torch Lake. Calibration of the kinetic parameters can be adjusted to meet optimal agreement between the model calculations and independent empirical concentrations (Chapra, 2014). Two approaches for calibration methods include trial-by-error fashion and automated techniques such as least-squares regression (Chapra, 2014). Model calibration was not performed in this project because the predicted concentrations were within a reasonable range and the sparse number of observed concentrations. Future work of this model could include the calibration of the most sensitive parameters for the PCB and MeHg bioaccumulation models (i.e., dietary uptake, ingestion, fecal excretion, and total elimination rate constants). The increase in measured frequency of fish contaminant concentrations could calibrate the model to be more robust.

An alternative approach would be to couple a site-specific bioenergetics model to estimate these values. The Arnot & Gobas (2004) model coupled with a bioenergetic model was created Douillard et al. (2009) and examined the influence of temperature on the uptake and elimination rates of PCBs in fish. The bioenergetic models estimate the flow of energy with food consumption, growth, metabolism, egestion, and excretion (Kitchell et al., 1977; Stewart et al., 1983; Deslauriers et al., 2017). The mass balance model from Stewart et al. (1983) is represented in Equation 37:

$$C = R + SDA + F + E + \Delta B \quad (37)$$

Food consumption (C) is the source of energy for organisms that can be used for metabolism (R) and specific dynamic action (SDA), lost through egestion (F) and excretion (E), or leading to growth (ΔB). However, this approach would require more data. The elimination mechanisms of mercury from fish are less understood in comparison to PCBs. Future studies are needed to improve the feeding consumption estimation which in turn impacts the elimination rate constant and fish contaminant concentration predicted (Paterson et al., 2007b; Madenjian et al., 2021). The bioenergetics model should be used with caution if the values are not site specific (Trudel & Rasmussen, 2006).

The growth of fish can “dilute” the contaminant burdens by increasing biomass. This pseudo-first order elimination is predominantly seen in younger-fast growing juvenile fish (Trudel et al., 2001; Borga, 2005; Deslauriers et al., 2017). “Bloom dilution” has been observed in freshwater ecosystems in which phytoplankton growth reduce the uptake of contaminants (Pickhardt et al., 2002; Ward et al., 2010) Growth was not included in the model because of the dependence of other factors such as resource availability, age, temperature, and species- which was out of the scope of this project (Paterson et al., 2007b; Paterson et al., 2016; Li et al., 2018). In addition, the modeled assumed a constant body weight, corresponding to an 8-year-old fish. This condition represents an older species in which growth dilution is likely to be negligible. The Von Bertalanffy growth curves for walleye populations in eastern Canadian lakes indicate a slower growth rate as the fish reach this age (Simoneau et al., 2005). The faster-growing walleye were shown to have lower mercury concentrations in comparison than slower-growing fish. Intrinsic factors of the fish in each lake such as, habitats and feeding habits

may have caused the differences between mean ages and growth rates in the study (Simoneau et al., 2005).

However, as Hansen et al. (2022) explains in the literature review, “It’s complicated and it depends.” The increase in growth, may be offset by the increase in consumption of higher trophic level organisms. For example, in Schartup et al. (2018) growth dilution was not experienced in higher trophic levels in the marine environment as seen in freshwater ecosystems. The interconnection between growth and other bioenergetic parameters, may cause compounding effects. Madenjian et al. (2021) suggests other factors need to be investigated other than growth, such as differences in species and sexes (Madenjian et al., 2014b; 2016; 2021). Growth rate cannot be examined independently of chemical intake rates via food consumption.

Temperature can also influence bioaccumulated concentrations of PCBs and MeHg mainly because of fish bioenergetics (Paterson et al., 2016). The temperature was assumed to be 10°C for the ten-year period, keeping the rate constant values constant. A future improve would be to incorporate a temperature dependent bioenergetics model. However, with the constant temperature the model limits the number of unknowns. The sensitivity of the model to temperature is shown in A.3. The mercury mass balance model of Hendricks (2018) predicted the annual divalent, methyl, and elemental mercury concentrations in Torch Lake. The 2021 measured concentration used to drive the MeHg model in phytoplankton and zooplankton bioaccumulation model falls within the estimated concentrations. The MeHg concentrations are lowest in the spring during snowmelt and highest in hypolimnion in the summer. However, the range of MeHg dissolved concentrations in the hypolimnion is relatively small (see A.4).

Bioaccumulation is a whole-ecosystem process, but the kinetics are viewed on an individual organism scale. Other bioaccumulation models have been coupled with population models. For example, the Bioaccumulation and Aquatic System Simulator (BASS) model combines population, bioenergetics, and bioaccumulation models to estimate steady state concentrations in fish (Barber, 2008b). Other models such as Ecopath with Ecosim (EwE) model impacts of fishing and environmental disturbances (Christensen and Walters, 2004). Stable isotopic analyses provide an empirical method to determine the food web structure and examine eco-system scale changes. The kinetic bioaccumulation models for PCBs and MeHg developed in this thesis project can be used as a complementary tool for future analyses in Torch Lake. The model was implemented to see analyze the changes in fish concentrations due to remediation activities such as source elimination, and changing lipid concentrations. However, the bioaccumulation model coupled with bioenergetic and population models can be used to examine changes on an ecosystem scale such as climate change responses, population and land-use change, and stocking practices. The results from the bioaccumulation model suggest that the remediation of elevated PCB lake sediments, especially for the Hubbell Processing Area would greatly reduce the fish PCB concentrations and may lead to the delisting from the State’s consumption advisory. Similarly, remediation of the in-lake MeHg sources would reduce the fish MeHg concentrations and would likely lead to the removal of the fish consumption advisory not based on the tribal consumption rate. still exceed

the safe amount for fish Hg concentrations and thus consumption advisories. However, such efforts (sediment capping or dredging) could remove the benthic community BUI. Subsequently, efforts to delist Torch Lake may be much more complicated than just cleaning up sediment/in-lake sources. This research project does point to the value of remediation for removing one of the BUIs for Torch Lake.

5 Reference List

Amos, H. M., Jacob, D. J., Streets, D. G., & Sunderland, E. M. (2013). Legacy impacts of all-time anthropogenic emissions on the global mercury cycle. *Global Biogeochemical Cycles*, 27(2), 410-421.

Arnot, J. A., & Gobas, F. (2004). A food web bioaccumulation model for organic chemicals in aquatic ecosystems. *Environmental Toxicology and Chemistry*, 23(10), 2343-2355.

Arnot Research and Consulting (ARC). "AQUAWEB."
<https://arnotresearch.com/AQUAWEB/>

Asher Consulting, LLC, & Ad Hoc Analytics, LLC.(2016). Assessment of the Keweenaw Bay Indian Community's Fish Consumption. Prepared for: the Keweenaw Bay Indian Community (KBIC) Natural Resources Department.

Back, R. C., & Watras, C. J. (1995). MERCURY IN ZOOPLANKTON OF NORTHERN WISCONSIN LAKES - TAXONOMIC AND SITE-SPECIFIC TRENDS. *Water Air and Soil Pollution*, 80(1-4), 931-938.

Barber, M.C. (2008a). "Dietary uptake models used for modeling the bioaccumulation of organic contaminants in fish." *Environmental Toxicology and Chemistry* 27 (4): 755-777.

Barber, M.C. (2008b). "Bioaccumulation and Aquatic System Simulator (BASS) User's Manual Version 2.2." Ecosystems Research Division, U.S. Environmental Protection Agency.

Blanchard, P., Audette, C. V., Hulting, M. L., Basu, I., Brice, K. A., Backus, S. M., . . . Wu, R. (2021). *Atmospheric Deposition of Toxic Substances to the Great Lakes: IADN Results through 2021*.

Blanchfield, P. J., Rudd, J. W. M., Hrenchuk, L. E., Amyot, M., Babiarz, C. L., Beaty, K. G., et al. (2022). Experimental evidence for recovery of mercury-contaminated fish populations. *Nature*, 601(7891), 74-+.

Borga, K., Fisk, A. T., Hargrave, B., Hoekstra, P. F., Swackhamer, D., & Muir, D. C. G. (2005). Bioaccumulation factors for PCBs revisited. *Environmental Science & Technology*, 39(12), 4523-4532.

Burtnyk, M. D., Paterson, G., Drouillard, K. G., & Haffner, G. D. (2009a). Steady and non-steady state kinetics describe polychlorinated biphenyl bioaccumulation in natural populations of bluegill (*Lepomis macrochirus*) and cisco (*Coregonus artedii*). *Canadian Journal of Fisheries and Aquatic Sciences*, 66(12), 2189-2198.

- Chapra, S. C. (2014). "Surface water-quality modeling." Waveland Press, Inc. Long Grove, IL.
- Chen, C. Y., Stemberger, R. S., Kamman, N. C., Mayes, B. M., & Folt, C. L. (2005). Patterns of Hg bioaccumulation and transfer in aquatic food webs across multi-lake studies in the northeast US. *Ecotoxicology*, 14(1-2), 135-147.
- Christensen, V., & Walters, C. J. (2004). Ecopath with Ecosim: methods, capabilities and limitations. *Ecological Modelling*, 172(2-4), 109-139.
- Clayden, M. G., Kidd, K. A., Wyn, B., Kirk, J. L., Muir, D. C. G., & O'Driscoll, N. J. (2013). Mercury Biomagnification through Food Webs Is Affected by Physical and Chemical Characteristics of Lakes. *Environmental Science & Technology*, 47(21), 12047-12053.
- Clayden, M. G., Kidd, K. A., Wyn, B., Kirk, J. L., Muir, D. C. G., & O'Driscoll, N. J. (2014). Response to Comment on "Mercury Biomagnification through Food Webs Is Affected by Physical and Chemical Characteristics of Lakes". *Environmental Science & Technology*, 48(17), 10526-10527.
- Degraeve, M., McCauley, D., 2003. Low Level Mercury Concentrations in Selected Michigan Surface Waters, Summer/Fall 2002. Great Lakes Environmental Center, Traverse City, MI, p. 9.
- Depew, D.C., Burgess, N.M. and Campbell, L.M. (2013) Modelling Mercury Concentrations in Prey Fish: Derivation of a National-Scale Common Indicator of Dietary Mercury Exposure for Piscivorous Fish and Wildlife. *Environmental Pollution*, 176, 234-243.
- Deslauriers, D., Chipps, S. R., Breck, J. E., Rice, J. A., & Madenjian, C. P. (2017). Fish Bioenergetics 4.0: An R-Based Modeling Application. *Fisheries*, 42(11), 586-596.
- Dittman, J. A., Shanley, J. B., Driscoll, C. T., Aiken, G. R., Chalmers, A. T., Towse, J. E., et al. (2010). Mercury dynamics in relation to dissolved organic carbon concentration and quality during high flow events in three northeastern US streams. *Water Resources Research*, 46.
- Driscoll, C. T., Han, Y. J., Chen, C. Y., Evers, D. C., Lambert, K. F., Holsen, T. M., et al. (2007). Mercury contamination in forest and freshwater ecosystems in the Northeastern United States. *Bioscience*, 57(1), 17-28.
- Driscoll, C. T., Mason, R. P., Chan, H. M., Jacob, D. J., & Pirrone, N. (2013). Mercury as a Global Pollutant: Sources, Pathways, and Effects. *Environmental Science & Technology*, 47(10), 4967-4983.

Donohue and Associates, Inc. Volume 1a: Final Work Plan: Torch Lake Remedial Investigation/Feasibility Study Houghton County, Michigan Revision 1; U.S. EPA: June 1989.

Driscoll, C.T.; Han, Y.; Chen, C.Y.; Evers, D.C.; Lambert, K.F.; Holsen, T.M.; Kamman, N.C.; & Munson, R.K. (2007). "Mercury Contamination in forest and freshwater ecosystems in the northeastern United States." *BioScience* 57 (1): 17-28.

Evers, D. C., Han, Y. J., Driscoll, C. T., Kamman, N. C., Goodale, M. W., Lambert, K. F., et al. (2007). Biological mercury hotspots in the northeastern United States and southeastern Canada. *Bioscience*, 57(1), 29-43.

Figueiredo, K., Maenpaa, K., Leppanen, M. T., Kiljunen, M., Lyytikainen, M., Kukkonen, J. V. K., et al. (2014). Trophic transfer of polychlorinated biphenyls (PCB) in a boreal lake ecosystem: Testing of bioaccumulation models. *Science of the Total Environment*, 466, 690-698.

Frame, G. M., Cochran, J. W., & Bowadt, S. S. (1996). Complete PCB congener distributions for 17 aroclor mixtures determined by 3 HRGC systems optimized for comprehensive, quantitative, congener-specific analysis. *Hrc-Journal of High Resolution Chromatography*, 19(12), 657-668.

Gagnon, Valoree S. 2014. Synthesis and Community Brief: A Talking Circles Event. Proceedings. Keweenaw Bay Ojibwa Community College. Contribution No. 15 of the Great Lakes Research Center at Michigan Tech. Available at: <http://asep.mtu.edu/Publications/asep-publications.htm> (March 2015)

Gagnon, V.S., Gorman H. S. and Norman, E. S. Gateways: *International Journal of Community Research and Engagement*, 2017, 10, 164–184.

Gagnon, V.S., Gorman H. S. and Norman, E. S. (2018). A Policy Brief: Eliminating the Need for Fish Consumption Advisories in the Great Lakes Region. Contribution No. 15 of the Great Lakes Research Center at Michigan Tech.

GLIFWC Climate Change Team. 2023. Aanji-bimaadiziimagak o'ow aki. Great Lakes Indian Fish and Wildlife Commission, Odanah, Wisconsin. 332 p.

Great Lakes Environmental Center (2003). "Low level mercury concentrations in selected Michigan surface waters, summer/fall 2002." Michigan Department of Environmental Quality. MI/DEQ/WD-03/082.

Gobas, F., Muir, D. C. G., & Mackay, D. (1988). DYNAMICS OF DIETARY BIOACCUMULATION AND FECAL ELIMINATION OF HYDROPHOBIC ORGANIC CHEMICALS IN FISH. *Chemosphere*, 17(5), 943-962.

Gobas, F., Wilcockson, J. B., Russell, R. W., & Haffner, G. D. (1999). Mechanism of biomagnification in fish under laboratory and field conditions. *Environmental Science & Technology*, 33(1), 133-141.

Gobas, F., & Arnot, J. A. (2010). FOOD WEB BIOACCUMULATION MODEL FOR POLYCHLORINATED BIPHENYLS IN SAN FRANCISCO BAY, CALIFORNIA, USA. *Environmental Toxicology and Chemistry*, 29(6), 1385-1395.

Gobas, F., Burkhard, L. P., Doucette, W. J., Sappington, K. G., Verbruggen, E. M. J., Hope, B. K., et al. (2016). Review of Existing Terrestrial Bioaccumulation Models and Terrestrial Bioaccumulation Modeling Needs for Organic Chemicals. *Integrated Environmental Assessment and Management*, 12(1), 123-134.

Great Lakes Environmental Center (GLEC). (2006). *PCB study using semipermeable membrane devices in Torch Lake, Houghton County (MDEQ project number 05-25)*.

Green, M. and Urban, N. (2022). "Mercury and Copper in Torch Lake." ArcGIS StoryMaps. <https://storymaps.arcgis.com/stories/53afe85e2ab447faa52c06a316b939f6>

Guo, L., Zhang, B., Xiao, K., Zhanf, Q., Zheng, M. (2009). Levels and distribution of polychlorinated biphenyls in sewage sludge of urban wastewater treatment plants. *Journal of Environmental Sciences*, 21, 468-473

Hall, B. D., et al. (1997). Food as the dominant pathway of methylmercury uptake by fish. *Water Air and Soil Pollution*, 100(1-2): 13-24.

Hanchin, P.A., 2013. The fish community and fishery of the Portage-Torch lake system, Houghton County, Michigan in 2007-08. Michigan Department of Natural Resources, Lansing, MI, p. 63.

Hansen, G. J. A., Ruzich, J., Krabbenhoft, C. A., Kundel, H., Mahlum, S., Rounds, C. I., et al. (2022). It's Complicated and It Depends: A Review of the Effects of Ecosystem Changes on Walleye and Yellow Perch Populations in North America. *North American Journal of Fisheries Management*, 42(3), 484-506.

Harris, R. C., Rudd, J. W. M., Amyot, M., Babiarz, C. L., Beaty, K. G., Blanchfield, P. J., et al. (2007b). Whole-ecosystem study shows rapid fish-mercury response to changes in mercury deposition. *Proceedings of the National Academy of Sciences of the United States of America*, 104(42), 16586-16591.

Hendricks, Ashley, "A model to predict concentrations and uncertainty for mercury species in lakes", Open Access Master's Thesis, Michigan Technological University, 2018. <https://doi.org/10.37099/mtu.edu/dc.etr/585>

- Hoover, E. (2013). "Cultural and health implications of fish advisories in a Native American community." *Ecological Processes*, 2:4.
- Horowitz, H. M., Jacob, D. J., Zhang, Y., Dibble, T. S., Slemr, F., Amos, H. M., Schmidt, J. A., Corbitt, E. S., Marais, E. A., and Sunderland, E. M.: A new mechanism for atmospheric mercury redox chemistry: implications for the global mercury budget, *Atmos. Chem. Phys.*, 17, 6353–6371, <https://doi.org/10.5194/acp-17-6353-2017>, 2017.
- Kerfoot, C.W., Harting, S.L., Rossmann, R., Robbins, J.A., 2002. Elemental mercury in copper, silver, and gold ores: an unexpected contribution to Lake Superior sediments with global implications. *Geochemistry: Exploration, Environment, Analysis* 2, 185-202
- Kerfoot, C. W.; Urban, N. R.; McDonald, C. P.; Rossman, R.; & Zhang, H. (2016). "Legacy mercury releases during copper mining near Lake Superior." *Journal of Great Lakes Research* 42: 50-61.
- Kerfoot, W.; Urban, N.; McDonald, C.; Zhang, H.; Rossmann, R.; Perlinger, J.; Khan, T.; Hendricks, A.; Priyadarshini, M.; & Bolstad, M. (2018). "Mining Legacy Across a Wetland Landscape: High Mercury in Upper Peninsula (Michigan) Rivers, Lakes, and Fish." *Environmental Sciences: Processes and Impacts*
- Khan, Tanvir, "EVALUATION, IMPROVEMENT, AND APPLICATION OF MODELS OF ENVIRONMENTAL FATE AND TRANSPORT OF ATMOSPHERE-SURFACE EXCHANGEABLE POLLUTANTS (ASEPs)", Open Access Dissertation, Michigan Technological University, 2018.<https://doi.org/10.37099/mtu.dc.etr/593>
- Kitchell, J. F., Stewart, D. J., & Weininger, D. (1977a). APPLICATIONS OF A BIOENERGETICS MODEL TO YELLOW PERCH (*PERCA-FLAVESCENS*) AND WALLEYE (*STIZOSTEDION-VITREUM-VITREUM*). *Journal of the Fisheries Research Board of Canada*, 34, 1922-1935.
- Knauer, D., Pelkola, G., Casey, S., Krabbenhoft, D., Dewild, J.F. (2011) The distribution of total and methyl mercury in Michigan's Upper Peninsula Lakes. Michigan Dept. Environmental Quality, Lansing, MI, p. 76.
- Knights, C. D. (2008). Development and test application of a screening-level mercury fate model and tool for evaluating wildlife exposure risk for surface waters with mercury-contaminated sediments (SERAFM). *Environmental Modelling & Software*, 23(4), 495-510.
- Kruger, G.W., Bartelt, R.E., 1992. Final Drum Removal Report. Geraghty & Miller, INC., , Chicago, IL, p. 365.
- Lee, C. S., Lutcayage, M. E., Chandler, E., Madigan, D. J., Cerrato, R. M., & Fisher, N. S. (2016). Declining Mercury Concentrations in Bluefin Tuna Reflect Reduced Emissions

to the North Atlantic Ocean. *Environmental Science & Technology*, 50(23), 12825-12830.

Lepak, R. F., Hoffman, J. C., Janssen, S. E., Krabbenhoft, D. P., Ogorek, J. M., DeWild, J. F., et al. (2019). Mercury source changes and food web shifts alter contamination signatures of predatory fish from Lake Michigan. *Proceedings of the National Academy of Sciences of the United States of America*, 116(47), 23600-23608.

Li, J. J., Drouillard, K. G., Branfireun, B., & Haffner, G. D. (2015). Comparison of the Toxicokinetics and Bioaccumulation Potential of Mercury and Polychlorinated Biphenyls in Goldfish (*Carassius auratus*). *Environmental Science & Technology*, 49(18), 11019-11027.

Li, J. J., Haffner, G. D., Paterson, G., Walters, D. M., Burtnyk, M. D., & Drouillard, K. G. (2018). Importance of growth rate on mercury and polychlorinated biphenyl bioaccumulation in fish. *Environmental Toxicology and Chemistry*, 37(6), 1655-1667.

Lombard, N. J., Bokare, M., Harrison, R., Yonkos, L., Pinkney, A., Murali, D., et al. (2023). Codeployment of Passive Samplers and Mussels Reveals Major Source of Ongoing PCB Inputs to the Anacostia River in Washington, DC. *Environmental Science & Technology*, 57(3), 1320-1331.

Madenjian, C. P., O'Connor, D. V., Rediske, R. R., O'Keefe, J. P., & Pothoven, S. A. (2008). Net trophic transfer efficiencies of polychlorinated biphenyl congeners to lake whitefish (*Coregonus clupeaformis*) from their food. *Environmental Toxicology and Chemistry*, 27(3), 631-636.

Madenjian, C. P., David, S. R., & Krabbenhoft, D. P. (2012). Trophic Transfer Efficiency of Methylmercury and Inorganic Mercury to Lake Trout *Salvelinus namaycush* from Its Prey. *Archives of Environmental Contamination and Toxicology*, 63(2), 262-269.

Madenjian, C. P., Rediske, R. R., O'Keefe, J. P., & David, S. R. (2014a). Laboratory Estimation of Net Trophic Transfer Efficiencies of PCB Congeners to Lake Trout (*Salvelinus namaycush*) from Its Prey. *Jove-Journal of Visualized Experiments*(90).

Madenjian, C. P., Blanchfield, P. J., Hrenchuk, L. E., & Van Walleggem, J. L. A. (2014b). Mercury Elimination Rates for Adult Northern Pike *Esox lucius*: Evidence for a Sex Effect. *Bulletin of Environmental Contamination and Toxicology*, 93(2), 144-148.

Madenjian, C. P., Chipps, S. R., & Blanchfield, P. J. (2021). Time to refine mercury mass balance models for fish. *Facets*, 6, 272-286.

Mandelia, Ankita, "Polychlorinated Biphenyl Compound and Metal Contamination and Remediation in Torch Lake, Houghton County, MI" Master's Thesis, Michigan Technological University, 2016.

MathWorks, (2023a). “Choose an ODE Solver- MATLAB & Simulink.”
<https://www.mathworks.com/help/matlab/math/choose-an-ode-solver.html>

MathWorks, (2023b). “MATLAB normrnd-Normal random numbers.”
<https://www.mathworks.com/help/stats/normrnd.html>

McDonald, C.P. & Urban, N.R. (2009). “Using a model selection criterion to identify appropriate complexity in aquatic biogeochemistry models.” *Ecological Modeling* 221 (3): 428-432.

McDonald, C. P.; Urban, N. R.; Barkach, J. H.; & McCauley, D. (2010). “Copper profiles in the sediments of a mining-impacted lake.” *Journal of Soils and Sediments* 10 (3): 343-348.

McLeod, A. M., Paterson, G., Drouillard, K. G., & Haffner, G. D. (2016). Ecological Implications of Steady State and Nonsteady State Bioaccumulation Models. *Environmental Science & Technology*, 50(20), 11103-11111.

MDCH, (1995). Site Review and Update: Torch Lake, Hubbell, Houghton County, Michigan. U.S. Dept. Health & Human Services, Public Health Services, Atlanta, GA, p. 24.

MDNR Michigan Department of Natural Resources Remedial Action Plan for Torch Lake Area of Concern; October 27, 1987, p 59.

MDNR, (1990). Fish growth anomalies in Torch and Portage Lakes 1974-1988, Houghton County, Michigan. Michigan Department of Natural Resources, Lansing, MI, p. 49.

MDEQ, (2001). Michigan Fish Contaminant Monitoring Report, 2001 Annual Report. Michigan Dept. Environmental Qual., Lansing, MI, p. 123.

MDEQ, (2006). *PCB concentrations in Torch Lake using semi-permeable membrane devices.*

MDEQ, (2007a). The Michigan Department of Environmental Quality Biennial Remedial Action Plan Update for the Torch Lake Area of Concern; Michigan Department of Environmental Quality: Lansing, MI, October 29, 2007.

MDEQ, (2007b). Michigan Fish Contaminant Monitoring Report, 2007 Annual Report. Mich. Dept. Environmental Quality, Lansing, MI, p. 218.

MDEQ, (2008a). Michigan Fish Contaminant Monitoring Report, 2008 Annual Report. Michigan Dept. Environmental Quality, Lansing, MI, p. 189.

- MDEQ, (2008b). A sediment chemistry survey of Torch Lake. Michigan Dept. Environmental Quality, Lansing, MI.
- MDEQ, (2016). Status of Fish Contaminant Levels in the Torch Lake Area of Concern 2013, STAFF REPORT. Michigan Dept. Environmental Quality, Lansing, Michigan, p. 24.
- MDEQ (2018), Abandoned Mining Wastes. Torch Lake Non-Superfund Site. STAFF REPORT. Michigan Dept. Environmental Quality: Calumet, Michigan, August 2018.
- MDEQ, Michigan Dept. of Environ.Qual., 2019. Supplemental Site Investigation Report, Abandoned Mining Wastes – Torch Lake Non-Superfund Site, Calumet and Hecla Lake Linden Operations Area, Houghton County, Michigan. Michigan Dept. Environmental Quality, Remediation and Redevelopment Division, Lansing, MI, p. 160.
- Michigan Department of Community Health (November, 2012). “Health Consultation: Technical Support Document for a Polychlorinated Biphenyl Reference Dose (RfD) as a Basis for Fish Consumption Screening Values (FCSVs).” State of Michigan.
- Niimi, A. J. and B. G. Oliver (1983). BIOLOGICAL HALF-LIVES OF POLYCHLORINATED BIPHENYL (PCB) CONGENERS IN WHOLE FISH AND MUSCLE OF RAINBOW-TROUT (*SALMO-GAIRDNERI*). *Canadian Journal of Fisheries and Aquatic Sciences*, 40(9): 1388-1394.
- Niu, S., Chen, R. W., Hageman, K. J., McMullin, R. M., Wing, S. R., & Ng, C. A. (2023). Understanding impacts of organic contaminants from aquaculture on the marine environment using a chemical fate model. *Journal of Hazardous Materials*, 443.
- Norman, E. S. (2013a). Who's counting? Spatial politics, ecocolonisation and the politics of calculation in Boundary Bay. *Area*, 45(2), 179-187.
- Paterson, G., Drouillard, K. G., & Haffner, G. D. (2007a). PCB elimination by yellow perch (*Perca flavescens*) during an annual temperature cycle. *Environmental Science & Technology*, 41(3), 824-829.
- Paterson, G., Drouillard, K. G., Leadley, T. A., & Haffner, G. D. (2007b). Long-term polychlorinated biphenyl elimination by three size classes of yellow perch (*Perca flavescens*). *Canadian Journal of Fisheries and Aquatic Sciences*, 64(9), 1222-1233.
- Paterson, G., Ryder, M., Drouillard, K. G., & Haffner, G. D. (2016). CONTRASTING PCB BIOACCUMULATION PATTERNS AMONG LAKE HURON LAKE TROUT REFLECT BASIN-SPECIFIC ECOLOGY. *Environmental Toxicology and Chemistry*, 35(1), 65-73.

Perlinder, J. A., Gorman, H. S., Norman, E. S., Obrist, D., Selin, N. E., Urban, N. R., et al. (2016). Measurement and Modeling of Atmosphere-Surface Exchangeable Pollutants (ASEPs) To Better Understand their Environmental Cycling and Planetary Boundaries. *Environmental Science & Technology*, 50(17), 8932-8934.

Perlinder, J. A.; Urban, N. R.; Giang, A.; Selin, N.E.; Hendricks, A. N.; Zhang, H.; Kumar, A.; Wu, S.; Gagnon, V. S. Gorman, H. S., & Norman, E. S. (2018). "Responses of deposition and bioaccumulation in the Great Lakes region to policy and other large-scale drivers of mercury emissions." *Environmental Science: Processes & Impacts* 20 (1): 195- 209.

Pickhardt, P. C., Folt, C. L., Chen, C. Y., Klaue, B., & Blum, J. D. (2002). Algal blooms reduce the uptake of toxic methylmercury in freshwater food webs. *Proceedings of the National Academy of Sciences of the United States of America*, 99(7), 4419-4423.

Pickhardt, P. C., Stepanova, M., & Fisher, N. S. (2006). Contrasting uptake routes and tissue distributions of inorganic and methylmercury in mosquitofish (*Gambusia affinis*) and redear sunfish (*Lepomis microlophus*). *Environmental Toxicology and Chemistry*, 25(8), 2132-2142.

Raymond, B., & Rossmann, R. (2009). Total and methyl mercury accumulation in 1994-1995 Lake Michigan lake trout and forage fish. *Journal of Great Lakes Research*, 35(3), 438-446.

René P. Schwarzenbach, P. M. G., Dieter M. Imboden (2017). *Environmental Organic Chemistry*.

Schartup, A. T., Qureshi, A., Dassuncao, C., Thackray, C. P., Harding, G., & Sunderland, E. M. (2018). A Model for Methylmercury Uptake and Trophic Transfer by Marine Plankton. *Environmental Science & Technology*, 52(2), 654-662.

Schwarzenbach, P. M. G., Dieter M. Imboden (2017). *Environmental Organic Chemistry*.

Shaw, E. L., & Urban, N. R. (2023a). What can we learn from 28 years of monitoring of fish tissue polychlorinated biphenyls in Michigan's rivers? *Integrated Environmental Assessment and Management*, 19(1), 152-162.

Simoneau, M., Lucotte, M., Garceau, S., and Laliberté, D. (2005). Fish growth rates modulate mercury concentrations in walleye (*Sander vitreus*) from eastern Canadian lakes. *Environmental Research*, 98, 73-82.

Sokol, Emily, "An Assessment of Polychlorinated Biphenyl Contamination in Fish from the Inland and Great Lakes of Michigan", Open Access Master's Thesis, Michigan Technological University, 2015.<http://digitalcommons.mtu.edu/etdr/48>

- Stewart, D. J., Weininger, D., Rottiers, D. V., & Edsall, T. A. (1983). AN ENERGETICS MODEL FOR LAKE TROUT, SALVELINUS-NAMAYCUSH - APPLICATION TO THE LAKE-MICHIGAN POPULATION. *Canadian Journal of Fisheries and Aquatic Sciences*, 40(6), 681-698.
- Thomas, G. O. (2008). Polychlorinated Biphenyls. In J. Editors-in-Chief: Sven Erik & F. Brian (Eds.), *Encyclopedia of Ecology* (pp. 2872-2881). Oxford: Academic Press.
- Trudel, M., & Rasmussen, J. B. (1997). Modeling the elimination of mercury by fish. *Environmental Science & Technology*, 31(6), 1716-1722.
- Trudel, M., & Rasmussen, J. B. (2001). Predicting mercury concentration in fish using mass balance models. *Ecological Applications*, 11(2), 517-529.
- Trudel, M., & Rasmussen, J. B. (2006). Bioenergetics and mercury dynamics in fish: a modelling perspective. *Canadian Journal of Fisheries and Aquatic Sciences*, 63(8), 1890-1902.
- U.S. Environmental Protection Agency (1992) Declaration of the record of decision for operable units I & III, EPA/RODR05-92/ 215. Chicago (IL): USEPA Region 5
- U.S. Environmental Protection Agency (1994) Declaration of the record of decision for operable unit II, EPA/ROD/R05-94/264. Chicago (IL): USEPA Region 5
- U.S. EPA. Reference Dose for Methylmercury (External Review Draft, 2000). U.S. Environmental Protection Agency, Washington, D.C., NCEA-S-0930.
- U.S. Environmental Protection Agency (EPA). 2000. Guidance for Assessing Chemical Contaminant Data for Use in Fish Advisories Volume 2 Risk Assessment and Fish Consumption Limits, Third Edition. Washington DC: U.S. Environmental Protection Agency, Office of Science and Technology, Office of Water. EPA 823-B- 00-008.
- U.S. EPA. Reference Dose for Methylmercury (External Review Draft, 2000). U.S. Environmental Protection Agency, Washington, D.C., NCEA-S-0930.
- U.S.EPA, 2009. Aroclor Sediment Investigation Torch Lake Area Of Concern, Houghton County, Michigan. U.S. EPA, Great Lakes National Program Office, Chicago, IL, p. 15.
- U.S. EPA, 2019a. Final Report - Time Critical Removal Action, Lake Linden Recreation Area – Area A. U.S. Environmental Protection Agency, Region 5, Chicago, IL, p. 63.
- U.S. EPA, 2019b. Remedial Action Work Plan: Mineral Building, Torch Lake Area of Concern, Houghton County, Michigan. U.S. Environmental Protection Agency, Great Lakes National Program Office, Chicago, IL, p. 118.

U.S. Fish and Wildlife Service (FWS). "National Wetlands Inventory (NWI)." from <https://www.fws.gov/wetlands/data/state-downloads.html>.

U.S. Geological Survey (2016). "NLCD 2011 Land Cover (2011 Edition, amended 2016), by State: NLCD2016_LC_Michigan: U.S. Geological Survey."

Urban, N.R., MacLennan, C.A., Perlinger, J.A., 2018. Integrated Assessment of Torch Lake Area of Concern. Sea Grant, Lansing, MI, p. 267.

Urban, N. R., Lin, H., & Perlinger, J. A. (2020a). Temporal and spatial variability of PCB concentrations in lake trout (*Salvelinus namaycush*) in Lake Superior from 1995 to 2016. *Journal of Great Lakes Research*, 46(2), 391-401.

Urban, N.R. and Perlinger, J.A. (2022). Data Gap on Responses of Fish PCB Content to Remedial Actions Project 2021-2502. Final Project Report. August 31, 2022. Michigan Technological University.

Van Wallegghem, J. L. A., Blanchfield, P. J., & Hintelmann, H. (2007). Elimination of mercury by yellow perch in the wild. *Environmental Science & Technology*, 41(16), 5895-5901.

Van Wallegghem, J. L. A., Banchfied, P. J., Hrenchuk, L. E., & Hintelmann, H. (2013). Mercury Elimination by a Top Predator, *Esox lucius*. *Environmental Science & Technology*, 47(9), 4147-4154.

Ward, D. M., Nislow, K. H., & Folt, C. L. (2010). Bioaccumulation syndrome: identifying factors that make some stream food webs prone to elevated mercury bioaccumulation. *Year in Ecology and Conservation Biology 2010*, 1195, 62-83.

Wang, X. and W. X. Wang (2015). Physiologically Based Pharmacokinetic Model for Inorganic and Methylmercury in a Marine Fish. *Environmental Science & Technology*, 49(16): 10173-10181.

Wang, X., et al. (2017). In Vivo Mercury Demethylation in a Marine Fish (*Acanthopagrus schlegeli*). *Environmental Science & Technology* 51(11): 6441-6451.

Wellman, S. T., & Haynes, J. M. (2022). Two Congener-specific Models Estimate PCB TEQ Hazard to American Mink (*Neovison vison*) Living near a Western New York Creek. *Archives of Environmental Contamination and Toxicology*, 83(4), 313-325.

Weston Solutions, Inc. (2007). *Summary Report for the Torch Lake Area Assessment Torch Lake NPL Site and Surrounding Areas Keweenaw Peninsula, Michigan*. Retrieved from Okemos, Michigan.

Wiener, J. G., Sandheinrich, M. B., Bhavsar, S. P., Bohr, J. R., Evers, D. C., Monson, B. A., et al. (2012). Toxicological significance of mercury in yellow perch in the Laurentian Great Lakes region. *Environmental Pollution*, 161, 350-357.

Yao, S. F., & Drouillard, K. G. (2019). Prediction of Mercury Elimination Rate Coefficients of Fish is Improved by Incorporating Fish Temperature Classification into Models. *Bulletin of Environmental Contamination and Toxicology*, 103(5), 657-662.

Zawisza, Emma, "Powering an Industry: The History of the Calumet and Hecla Electrical System and the Environmental Consequences Left Behind" Master's Thesis, Michigan Technological University, 2016.

A Title of Appendix

A.1 Matlab model code

A.1.1 PCB bioaccumulation model

```
% Function to define mass balance of PCB congeners in Torch Lake
aquatic
% food web. Following bioaccumulation model developed by Arnot and
Gobas
% 2004.

function
dMdt=PCBfun(t,M,W,k1,i,n,mo,mp,CwdO,CwdS,kD,Pi,k2,kE,kG,kM,Cd,tspan)
Cd_time = interp1(tspan(:),Cd(:,n),t);
dMdt =
(W(n).*((k1(i,n).*(mo(n).*CwdO(i)))+(mp(n).*CwdS)))+(kD(i,n).*Pi(n).*Cd_
ime))-(k2(i,n)+kE(i,n)+kG(n)+kM(i))*M;
dMdt = dMdt';
end

% Variables
% M (g) = mass of chemical in organism
% k1 (L/kg*d) = clearance rate constant for chemical uptake via
respiratory area
% W (kg) = weight of organism
% mo (unitless) = fraction of the respiratory ventilation that
involves overlying water
% mp (unitless) = fraction of the respiratory ventilation that
involves sediment-associated pore water
% phi(unitless) = fraction of total freely dissolved chemical conc.
in overlying water
% CwdO (g/L) = dissolved chemical conc. in water above sediments
% kD (kg/kg*d) = clearance rate constant for chemical via ingestion
of diet
% Pi (unitless) = fraction of diet consisting of prey
% Cd (g/kg) = chemical conc. in prey item
% k2 (1/d) = rate constant for chemical elimination via
respiratory area
% kE (1/d) = rate constant for chemical elimination via
excretion into egested feces
% kM (1/d) = rate constant for metabolic transformation of the chemical

clearvars; close all; clc;
%% BIOLOGICAL PARAMETERS
W = [5.7e-10 5.7e-8 0.5 1.45]; %wet-weight of organism (kg)
mo = [1 1 1 1]; %fraction respiration in overlying water (unitless)
mp = [0 0 0 0]; %fraction respiration in sediment pore water
(unitless)
eL = [0 0.75 0.92 0.92]; %absorption efficiency of lipids (unitless)
eN = [0 0.75 0.60 0.60]; %absorption efficiency of NLOM (unitless)
eW = [0 0.50 0.50 0.50]; %absorption efficiency of water (unitless)
```

```

f_LB = [0.01 0.007 0.056 0.01]; %fraction lipid in biota (unitless)
f_NB = [0.195 0.20 0.20 0.20]; %fraction NLOM in biota (unitless)
f_WB = [0.80 0.793 0.744 0.79]; %fraction water in biota (unitless)
f_LD = [0 0.005 0.007 0.056]; %fraction lipid in diet (unitless)
f_ND = [0 0.195 0.20 0.20]; %fraction NLOM in diet (unitless)
f_WD = [0 0.80 0.793 0.744]; %fraction water in diet (unitless)
%% CHEMICAL PARAMETERS
PCB_congeners = [33 52 99 101 149 158 180];
Kow = [2.936e+05 4.063e+05 1.315e+06 1.262e+06 3.088e+06 3.897e+06
1.341e+07]; %octanol-water coefficient (unitless)
CwdO = [1.5e-12 1.06e-11 5.2e-12 8.3e-12 1.2E-12 7.5e-12 2.2e-12];
%SPMD dissolved conc in water (g/L)
CwdS = 8.63; %dissolved conc in sediment (g/L)
%% ENVIRONMENTAL PARAMETERS
T = 10; %water temperature (degree celsius)
S = 90; % degree of oxygen saturation in water (% saturation)
Cox = (-0.24*T+14.04)*(S/100); %dissolved oxygen conc (mg/L)
%% BIOENERGETICS EQUATIONS (ARNOT & GOBAS 2004)

%calculate aqueous clearance uptake rate:
Ew = (1.85+(155./Kow(:)).^-1); %efficiency of transfer via
gills (unitless)
Gv = (1400.*W(:).^0.65)/Cox; %gill ventilation rate (L/d)

k1(:,1) = ((6.0e-5)+(5.5./Kow(:)).^-1); %TL 1 aqueous uptake rate
(L/kg*d^-1)
k1(:,2) = Ew(:).*Gv(2)/W(2); %TL 2 aqueous uptake rate
(L/kg*d^-1)
k1(:,3) = Ew(:).*Gv(3)/W(3); %TL 3 aqueous uptake rate
(L/kg*d^-1)
k1(:,4) = Ew(:).*Gv(4)/W(4); %TL 4 aqueous uptake rate
(L/kg*d^-1)

%calculate aqueous elimination rate:
K_BW(:,1) = f_LB(1).*Kow(:) + f_NB(1).*0.35.*Kow(:) + f_WB(1); %TL 1
biota-water coefficient (unitless)
K_BW(:,2) = f_LB(2).*Kow(:) + f_NB(2).*0.035.*Kow(:) + f_WB(2); %TL 2
biota-water coefficient (unitless)
K_BW(:,3) = f_LB(3).*Kow(:) + f_NB(3).*0.035.*Kow(:) + f_WB(3); %TL 3
biota-water coefficient (unitless)
K_BW(:,4) = f_LB(4).*Kow(:) + f_NB(4).*0.035.*Kow(:) + f_WB(4); %TL 4
biota-water coefficient (unitless)

k2(:,1) = k1(:,1)./K_BW(:,1); %TL 1 aquaous elimination rate (1/d)
k2(:,2) = k1(:,2)./K_BW(:,2); %TL 2 aquaous elimination rate (1/d)
k2(:,3) = k1(:,3)./K_BW(:,3); %TL 3 aquaous elimination rate (1/d)
k2(:,4) = k1(:,4)./K_BW(:,4); %TL 4 aquaous elimination rate (1/d)

%calculate dietary clearance uptake rate:
ED = (3.0e-7.*Kow(:)+2.0).^(-1); %efficiency of transfer via
intestinal tract (unitless)

```

```

GD = 0.022*(W(:).^0.85)*exp(0.06*T); %feeding rate (kg/d)

kD(:,1) = [0;0;0;0;0;0;0]; %TL 1 dietary uptake rate (kg food/kg
organism*d^-1)
kD(:,2) = ED(:)*GD(2)/W(2); %TL 2 dietary uptake rate (kg food/kg
organism*d^-1)
kD(:,3) = ED(:)*GD(3)/W(3); %TL 3 dietary uptake rate (kg food/kg
organism*d^-1)
kD(:,4) = ED(:)*GD(4)/W(4); %TL 4 dietary uptake rate (kg food/kg
organism*d^-1)

Pi(:,1) = [1,1,1,1]; %TL 1 fraction of diet (unitless)
Pi(:,2) = [1,1,1,1]; %TL 2 fraction of diet (unitless)
Pi(:,3) = [1,1,1,1]; %TL 3 fraction of diet (unitless)
Pi(:,4) = [1,1,1,1]; %TL 4 fraction of diet (unitless)

%calculate fecal elimination rate:
GF = ((1-eL(:)).*f_LD(:))+((1-eN(:)).*f_ND(:))+((1-
eW(:)).*f_WD(:)).*GD(:); %fecal egestion rate (kg feces/kg organism
*d^-1)
f_LG = ((1-eL(:)).*f_LD(:))./(((1-eL(:)).*f_LD(:))+((1-
eN(:)).*f_ND(:))+((1-eW(:)).*f_WD(:))); %fraction lipid in gut
(unitless)
f_NG = ((1-eN(:)).*f_ND(:))./(((1-eL(:)).*f_LD(:))+((1-
eN(:)).*f_ND(:))+((1-eW(:)).*f_WD(:))); %fraction NLOM in gut
(unitless)
f_WG = ((1-eW(:)).*f_WD(:))./(((1-eL(:)).*f_LD(:))+((1-
eN(:)).*f_ND(:))+((1-eW(:)).*f_WD(:))); %fraction water in gut
(unitless)

K_GB(:,1) = [0 0 0 0 0 0 0];
%TL 1 gut-biota coefficient (unitless)
K_GB(:,2) = ((f_LG(2).*
Kow(:))+(f_NG(2).*0.35*Kow(:))+f_WG(2))./K_BW(:,2); %TL 2 gut-biota
coefficient (unitless)
K_GB(:,3) = ((f_LG(3).*
Kow(:))+(f_NG(3).*0.035*Kow(:))+f_WG(3))./K_BW(:,3); %TL 3 gut-biota
coefficient (unitless)
K_GB(:,4) = ((f_LG(4).*
Kow(:))+(f_NG(4).*0.035*Kow(:))+f_WG(4))./K_BW(:,4))*0.9; %TL 4 gut-
biota coefficient (unitless)

kE(:,1) = [0;0;0;0;0;0;0]; %TL 1 fecal elimination rate
(1/d)
kE(:,2) = (ED(:).*K_GB(:,2).*GF(2))/W(2); %TL 2 fecal elimination rate
(1/d)
kE(:,3) = (ED(:).*K_GB(:,3).*GF(3))/W(3); %TL 3 fecal elimination rate
(1/d)
kE(:,4) = (ED(:).*K_GB(:,4).*GF(4))/W(4); %TL 4 fecal elimination rate
(1/d)

```

```

%calculate growth rate constant:
kG = [0 0 0 0];

%calculate metabolic transformation rate constant:
kM = [0 0 0 0 0 0 0]; %metabolic rate (1/d)

%% BIOACCUMULATION ODE SOLVE
%time span:
tspan = 0:1:3650; % daily time step for 10 year period

%inital PCB mass (g):
M0_33 = [1e-17 1e-17 1e-17 1e-17];
M0_52 = [1e-17 1e-17 1e-17 1e-17];
M0_99 = [1e-17 1e-17 1e-17 1e-17];
M0_101 = [1e-17 1e-17 1e-17 1e-17];
M0_149 = [1e-17 1e-17 1e-17 1e-17];
M0_153 = [1e-17 1e-17 1e-17 1e-17];
M0_180 = [1e-17 1e-17 1e-17 1e-17];

opts = odeset('RelTol',1e-2,'AbsTol',1e-20); %settings of ode15s
Cd = zeros(length(tspan),5); %pre-allocate diet conc
for i = 1:length(PCB_congeners)
switch i
case 1 %PCB 33
C33 = zeros (length(tspan),4);
for n = 1:4
[t_out,M_out] =
ode15s(@(t,M)PCBfun(t,M,W,k1,i,n,mo,mp,CwdO,CwdS,kD,Pi,k2,kE,kG,kM,Cd,t
span),tspan,M0_33(n),opts);
M33_out(:,n) = M_out; %PCB mass in organism (g)
C33(:,n) = M33_out(:,n)./W(n); %PCB conc in organism (g/kg)
Cd(:,n+1) = C33(:,n); %PCB diet conc (g/kg)
end
case 2 %PCB 52
C52 = zeros (length(tspan),4);
for n = 1:4
[t_out,M_out] =
ode15s(@(t,M)PCBfun(t,M,W,k1,i,n,mo,mp,CwdO,CwdS,kD,Pi,k2,kE,kG,kM,Cd,t
span),tspan,M0_52(n),opts);
M52_out(:,n) = M_out; %PCB mass in organism (g)
C52(:,n) = M52_out(:,n)./W(n); %PCB conc in organism (g/kg)
Cd(:,n+1) = C52(:,n); %PCB diet conc (g/kg)
end
case 3 %PCB 99
C99 = zeros (length(tspan),4);
for n =1:4
[t_out,M_out] =
ode15s(@(t,M)PCBfun(t,M,W,k1,i,n,mo,mp,CwdO,CwdS,kD,Pi,k2,kE,kG,kM,Cd,t
span),tspan,M0_99(n),opts);
M99_out(:,n) = M_out; %PCB mass in organism (g)
C99(:,n) = M99_out(:,n)./W(n); %PCB conc in organism (g/kg)
Cd(:,n+1) = C99(:,n); %PCB diet conc (g/kg)
end
case 4 %PCB 101
C101 = zeros (length(tspan),4);

```

```

        for n = 1:4
            [t_out,M_out] =
ode15s(@ (t,M) PCBfun(t,M,W,k1,i,n,mo,mp,CwdO,CwdS,kD,Pi,k2,kE,kG,kM,Cd,t
span),tspan,M0_101(n),opts);
            M101_out(:,n) = M_out;           %PCB mass in organism (g)
            C101(:,n) = M101_out(:,n)./W(n); %PCB conc in organism (g/kg)
            Cd(:,n+1) = C101(:,n);         %PCB diet conc (g/kg)
        end
    case 5 %PCB 149
        C149 = zeros (length(tspan),4);
        for n =1:4
            [t_out,M_out] =
ode15s(@ (t,M) PCBfun(t,M,W,k1,i,n,mo,mp,CwdO,CwdS,kD,Pi,k2,kE,kG,kM,Cd,t
span),tspan,M0_149(n),opts);
            M149_out(:,n) = M_out;           %PCB mass in organism (g)
            C149(:,n) = M149_out(:,n)./W(n); %PCB conc in organism (g/kg)
            Cd(:,n+1) = C149(:,n);         %PCB diet conc (g/kg)
        end
    case 6 %PCB 153
        C153 = zeros (length(tspan),4);
        for n =1:4
            [t_out,M_out] =
ode15s(@ (t,M) PCBfun(t,M,W,k1,i,n,mo,mp,CwdO,CwdS,kD,Pi,k2,kE,kG,kM,Cd,t
span),tspan,M0_153(n),opts);
            M153_out(:,n) = M_out;           %PCB mass in organism (g)
            C153(:,n) = M153_out(:,n)./W(n); %PCB conc in organism (g/kg)
            Cd(:,n+1) = C153(:,n);         %PCB diet conc (g/kg)
        end
    case 7 %PCB 180
        C180 = zeros (length(tspan),4);
        for n =1:4
            [t_out,M_out] =
ode15s(@ (t,M) PCBfun(t,M,W,k1,i,n,mo,mp,CwdO,CwdS,kD,Pi,k2,kE,kG,kM,Cd,t
span),tspan,M0_180(n),opts);
            M180_out(:,n) = M_out;           %PCB mass in organism (g)
            C180(:,n) = M180_out(:,n)./W(n); %PCB conc in organism (g/kg)
            Cd(:,n+1) = C180(:,n);         %PCB diet conc (g/kg)
        end
    end
end
end

%% RESULTS
% concentration in organism - (ppb):
PhytoConc =
[C33(end,1);C52(end,1);C99(end,1);C101(end,1);C149(end,1);C153(end,1);C
180(end,1)]*1e6;
ZooConc =
[C33(end,2);C52(end,2);C99(end,2);C101(end,2);C149(end,2);C153(end,2);C
180(end,2)]*1e6;
ForageConc =
[C33(end,3);C52(end,3);C99(end,3);C101(end,3);C149(end,3);C153(end,3);C
180(end,3)]*1e6;
WalleyeConc =
[C33(end,4);C52(end,4);C99(end,4);C101(end,4);C149(end,4);C153(end,4);C
180(end,4)]*1e6;

```

```

results = [PhytoConc ZooConc ForageConc WalleyeConc];

TMF = [PhytoConc(:)./Cwd0(:), ZooConc(:)./PhytoConc(:),
ForageConc(:)./ZooConc(:), WalleyeConc(:)./ForageConc(:)]; %trophic
magnification factor (unitless)
AQUAWEB = [5.42e-2 6.99e-1 2.99 4.41 2.82 2.46e1 2.76e1] %PCB conc in
walleye (ng/g)

%% PLOTTING
%plot results
figure; % plot of trophic level 1 results
plot(t_out,C33(:,1)*1e6,t_out,C52(:,1)*1e6,t_out,C99(:,1)*1e6,t_out,C10
1(:,1)*1e6,t_out,C149(:,1)*1e6,t_out,C153(:,1)*1e6,t_out,C180(:,1)*1e6)
legend('PCB 33','PCB 52','PCB 99','PCB 101','PCB 149','PBC 153','PCB
180')
title('PCB concentration in phytoplankton')
xlabel('Time (day)')
ylabel('Concentration (ng/g)')

figure; % plot of trophic level 2 results
plot(t_out,C33(:,2)*1e6,t_out,C52(:,2)*1e6,t_out,C99(:,2)*1e6,t_out,C10
1(:,2)*1e6,t_out,C149(:,2)*1e6,t_out,C153(:,2)*1e6,t_out,C180(:,2)*1e6)
legend('PCB 33','PCB 52','PCB 99','PCB 101','PCB 149','PBC 153','PCB
180')
title('PCB concentration in zooplankton')
xlabel('Time (day)')
ylabel('Concentration (ng/g)')

figure; % plot of trophic level 3 results
plot(t_out,C33(:,3)*1e6,t_out,C52(:,3)*1e6,t_out,C99(:,3)*1e6,t_out,C10
1(:,3)*1e6,t_out,C149(:,3)*1e6,t_out,C153(:,3)*1e6,t_out,C180(:,3)*1e6)
legend('PCB 33','PCB 52','PCB 99','PCB 101','PCB 149','PBC 153','PCB
180')
title('PCB concentration in forage fish')
xlabel('Time (day)')
ylabel('Concentration (ng/g)')

figure; % plot of trophic level 4 results
plot(t_out,C33(:,4)*1e6,'-',t_out,C52(:,4)*1e6,'--
',t_out,C99(:,4)*1e6,':',t_out,C101(:,4)*1e6,'-
.',t_out,C149(:,4)*1e6,'-',t_out,C153(:,4)*1e6,'--
',t_out,C180(:,4)*1e6,'-.')
legend('PCB 33','PCB 52','PCB 99','PCB 101','PCB 149','PBC 153','PCB
180')
% title('PCB concentration in walleye')
xlabel('Time (day)')
ylabel('Fish Concentration (ng/g)')

%% VALIDATION
%validate model to measured data:
MDEQ_obs = [0.00 2.23 5.19 7.41 4.89 11.93 5.56]; %MDEQ walleye
measured PCB conc (ppb or ng/g) (1988-2018)

```

```

TLPAC_obs = [0.05 0.00 0.88 3.97 3.03 7.29 3.39]; %TLPAC walleye
measured PCB conc (ppb or ng/g) (2018-2022)

percent_error = (WalleyeConc - MDEQ_obs)/MDEQ_obs*100;

%plot results:
figure;
scatter(PCB_congeners(:),PCB_obs(:), PCB_congeners(:),WalleyeConc(:))
hold on
bar(PCB_congeners,WalleyeConc)
hold off
legend('MDHHS measured','Model')
title('Model vs. Measured Concentration')
xlabel('PCB Congeners')
ylabel('Concentration (ppb)')

```

A.1.2 MeHg bioaccumulation model

```

% Function to define mass balance of MeHg in Torch Lake aquatic
zooplankton.
%Following bioaccumulation model developed by Schartup et al. (2018)

function dMdt=MeHgzoo(t,M,W,n,k1,CwdO,kD,kTOT,Cd,tspan)
Cd_time = interp1(tspan(:),Cd(:,n),t);
dMdt = (W(n)*(k1(n)*CwdO)+(kD(n)*Cd_time))-kTOT(n)*M;
dMdt = dMdt';
end

% Variables
% M (ng) = mass of chemical in organism
% k1 (L/g/d) = clearance rate constant for chemical uptake via
respiratory area
% W (kg) = weight of organism
% CwdO (g/L) = total chemical conc. in water above sediments
% kD (1/d) = clearance rate constant for chemical via ingestion
of diet
% Pi (unitless) = fraction of diet consisting of prey
% Cd (ng/g) = chemical conc. in prey item
% kTOT (1/d) = rate constant for chemical elimination via
excretion into egested feces

% Function to define mass balance of MeHg in Torch Lake fish.
%Following bioaccumulation model developed by Trudel and
Rasmussen(2001).

function dMdt=MeHgfish(t,M,I,ED,n,Cd,kTOT,W,tspan)
Cd_time = interp1(tspan(:),Cd(:,n),t);
dMdt = (I(n)*ED(n)*Cd_time*W(n))-(kTOT(n)*M);
dMdt = dMdt'; %transpose to column vector
end

% Variables
% M (ng) = mass of chemical in organism

```

```

% ED (unitless) = assimilation efficiency
% Cd (ng/g)     = concentration in diet
% kD (1/day)   = ingestion rate
% W (g)        = wet-weight of organism
% kTOT (1/day) = elimination rate constant
% phi(unitless) = fraction of total freely dissolved chemical conc.
in overlying water
% CwtO (g/L)   = total chemical conc. in water above sediments
% CwdS (g/L)   = freely dissolved conc. in sediment pore water
% kD (g/g*d)   = clearance rate constant for chemical via ingestion
of diet
% kTOT (1/d)   = rate constant for total chemical elimination

```

```
clearvars; close all; clc;
```

```
%% BIOLOGICAL PARAMETERS
```

```

W      = [5.7e-7 5.7e-5 500 1450]; %wet-weight of organism (g)
ED     = [0 0.6 0.8 0.8]; %assimilation efficiency (unitless)
U      = 2.92e-4; %phytoplankton empirical parameter(amol*um^-3/nmol)
r      = 25; %phytoplankton cell radius (um)
V      = 6.54e4; %phytoplankton cell volume (um^3)

```

```
%% CHEMICAL PARAMETERS
```

```

Kow    = 50.12; %octanol-water partition coefficient (unitless)
CwdO_M = 7.51e-1; %MeHg water concentration(pM)
CwdO   = 1.51e-1; %MeHg water concentration (ng/L)

```

```
%% ENVIRONMENTAL PARAMETERS
```

```

T      = 10; %water temperature (degree celsius)
S      = 90; %water oxygen saturation (percent)
Cox    = (-0.24*T+14.04)*(S/100); %water oxygen concentration (mg/L)
DOC    = 658; %water dissolved organic C (uM)
SPM    = 9.4e-4; %suspended particulate matter concentration (g/L)
Chla   = 50; %water chla concentration (ug/L)

```

```
%% PHYTOPLANKTON EQUATIONS (Schartup et al. 2018)
```

```
%calculate MeHg concentration in phytoplankton size class
```

```
%time span:
```

```

tspan  = 0:1:3650; % daily time step for 10 year period
Cd     = zeros(length(tspan),5); %pre-allocate diet concentration
C_Hg   = zeros(length(tspan),4); %pre-allocate Hg concentration
C_Hg(:,1) = (U*CwdO_M*V/W(1))*200.59*1e-12; %wet-weight conc(ng/g)
Cd(:,2) = C_Hg(:,1); %diet wet-weight conc (ng/g)

```

```
%% ZOOPLANKTON EQUATIONS (Schartup et al. 2018)
```

```
%calculate aqueous clearance uptake rate:
```

```

Gv     = zeros(4,1); %pre-allocate gill ventilation rate
Ew     = (1.85+(155/Kow))^-1; %absorption efficiency (unitless)
(Arnot & Gobas 2004)
Gv(2)  = (1400*(W(2)*1e-3)^0.65)/Cox; %gill ventilation rate (L/d)
(Arnot & Gobas 2004)
k1     = zeros(4,1); %pre-allocate aqueous uptake rate
k1(2)  = Ew*Gv(2)/W(2); %TL 2 aqueous uptake rate (L/g*d^-1)

```

```

%calculate aqueous elimination rate:
kTOT      = zeros(4,1);           %pre-allocate total
elimination constant
kTOT(2)   = 0.00335*(W(2)^-0.195)*exp(0.0066*T); %TL 2 total elimination
rate constnat (1/d)

%calculate dietary clearance uptake rate:
E_SPM = 0.75*SPM;           %efficient SPM (unitless)
kD     = zeros(4,1);       %pre-allocate diet uptake constant
kD(2)  = Gv(2)*E_SPM*ED(2); %TL 2 dietarty uptake rate (g SPM/g organism
*d^-1)

%% FISH EQUATIONS (Trudel & Rasmussen 2006)
%ingestion rate (g/g*d)
I = zeros(1,4);           %pre-allocate ingestion rate
I(3) = 0.0100;           %TL 3 from Hartman (2017)
I(4) = 0.0201;           %TL 4 from Trudel & Rasmussen (2001)

%Elimination rate
kTOT(3) = 0.0058; %TL 3 total elimination rate constant (1/d) (Yoa &
Drouillard 2019)
kTOT(4) = 0.0013; %TL 4 total elimination rate constant (1/d) (Yoa &
Drouillard 2019)
%% BIOACCUMULATION ODE SOLVE
%inital MeHg burden mass:
MeHg0 = [1e-17 1e-17 1e-17 1e-17]; %inital mass of MeHg (ng)
opts = odeset('RelTol',1e-2,'AbsTol',1e-20); %settings of ode15s
MeHg_out = zeros(length(tspan),4); %pre-allocate mass out

%zooplankton ode
n = 2;
[t_out,M_out] =
ode15s(@ (t,M)MeHgzoo(t,M,W,n,k1,Cwd0,kD,kTOT,Cd,tspan),tspan,MeHg0(2),o
pts);
MeHg_out(:,2) = M_out; %MeHg mass (ng)
C_Hg(:,2) = MeHg_out(:,2)./W(2); %MeHg conc ng/g wet-weight
Cd(:,3) = C_Hg(:,2); %diet conc ng/g wet-weight

%forage and predatory fishes ode
opts = odeset('RelTol',1e-2,'AbsTol',1e-20); %settings of ode15s
for n = 3:4
    [t_out,M_out] =
ode15s(@ (t,M)MeHgfish(t,M,I,ED,n,Cd,kTOT,W,tspan),tspan,MeHg0(n),opts);
    MeHg_out(:,n) = M_out; %MeHg mass (ng)
    C_Hg(:,n) = MeHg_out(:,n)./W(n); %MeHg conc ng/g wet-weight
    Cd(:,n+1) = C_Hg(:,n); %diet conc ng/g wet-weight
end

%% RESULTS
%concentration in organism - (ug/g ww):
PhytoConc = C_Hg(end,1)*1e-3;
ZooConc = C_Hg(end,2)*1e-3;
ForageConc = C_Hg(end,3)*1e-3;

```

```

WalleyeConc = C_Hg(end,4)*1e-3;
results      = [PhytoConc ZooConc ForageConc WalleyeConc];

%Biomagnification factor (ug/kg):
BMF(1) = (PhytoConc/Cwd0)*1e6;
BMF(2) = (ZooConc/Cwd0)*1e6;
BMF(3) = (ForageConc/Cwd0)*1e6;
BMF(4) = (WalleyeConc/Cwd0)*1e6;

% %% PLOTTING
% %plot results
figure; % plot of trophic level 1 results
plot(t_out,C_Hg(:,1)*1e-3)
title('MeHg concentration in phytoplankton')
xlabel('Time (day)')
ylabel('Concentration (ug/g ww)')

figure; % plot of trophic level 2 results
plot(t_out,C_Hg(:,2)*1e-3)
title('MeHg concentration in zooplankton')
xlabel('Time (day)')
ylabel('Concentration (ug/g ww)')

figure; % plot of trophic level 3 results
plot(t_out,C_Hg(:,3)*1e-3)
title('MeHg concentration in forage fish')
xlabel('Time (day)')
ylabel('Concentration (ug/g ww)')

figure; % plot of trophic level 4 results
plot(t_out,C_Hg(:,4)*1e-3)
title('MeHg concentration in walleye')
xlabel('Time (day)')
ylabel('Walleye Concentration (ug/g ww)')

figure; % plot of trophic level results
plot(t_out,C_Hg(:,1)*1e-3,t_out,C_Hg(:,2)*1e-3,'-',t_out,C_Hg(:,3)*1e-3,':',t_out,C_Hg(:,4)*1e-3,'-.')
title('MeHg concentration in Torch Lake')
legend('Trophic Level 1','Trophic Level 2','Trophic Level 3','Trophic Level 4')
xlabel('Time (day)')
ylabel('MeHg Concentration (ug/g ww)')

%% VALIDATION
%validate model to measured data:
MeHgObs = 0.55; %GLIFWC walleye measured PCB conc 2018, 2019 average (ug/g ww)
percent_error = (WalleyeConc - MeHgObs)/MeHgObs*100

%% SENSITIVITY ANALYSIS
% change sediment area over a fixed range (factor of 10)

```

% predicted top predator concentration by changing parameter +/- 10% to see
 % which parameters have the greatest output on the model.

A.2 Fish measurement data

A.2.1 PCB fish measurement data

Table 22. MDEQ Fish Contaminant Monitoring Program walleye PCB congener concentrations (2000-2018).

MDEQ Fish Contaminant Monitoring Program							
Collection Date	Walleye PCB congener concentration (ng/g ww)						
	33	52	99	101 (90-101)	149	153	180
5/14/18	-	-	1	1.5	-	2.7	0.7
5/14/18	-	-	-	-	-	0.8	0.4
5/14/18	-	-	1.1	1.7	-	3.2	0.9
5/14/18	-	0.8	4.4	7	-	12.1	4.8
5/14/18	-	-	-	-	-	2.1	0.8
8/1/13	-	-	-	-	-	0.3	-
8/1/13	-	-	-	-	-	0.7	0.2
8/1/13	-	-	-	-	-	0.3	-
8/1/13	-	-	0.9	1.6	-	3	1.1
8/1/13	-	2.9	16.1	23.4	-	42.3	20.7
5/23/13	-	1.4	4.1	6.5	-	10.8	4.4
5/23/13	-	-	-	-	-	1.8	0.7
5/23/13	-	2.5	6.5	9.9	-	17.4	7.9
5/23/13	-	1.8	5.3	8.4	-	14.2	6
5/23/13	-	0.6	2.8	4.1	-	8	3.8
4/25/07	-	-	2.4	3.2	1.6	5.9	2.3
4/25/07	-	-	0.6	0.7	0.5	2	0.9
4/25/07	-	-	0.8	1.4	0.6	2.3	1
4/25/07	-	-	0.6	0.7	-	2	1
4/25/07	-	-	1.1	1.5	1.1	3.6	1.8
4/25/07	-	1.9	5	8	4	12	5.1
4/25/07	-	-	1	1.2	0.7	3.5	1.5
4/25/07	-	-	3	4.4	2.8	8.5	4
4/25/07	-	-	2.2	3.3	1.8	5.6	2.4
4/25/07	-	3.7	10.1	15.5	7.8	20.1	7.1
4/25/07	-	-	1.8	2.7	1.5	4.2	1.6
4/25/07	-	2.5	8.8	12.2	6.7	22.9	9.5

4/25/07	-	3.5	18	26.8	15.1	47.7	22.1
4/25/07	-	1.2	8.1	11.1	6.5	22.1	11.2
4/25/07	-	1.2	6.7	9.7	5.5	18.9	9.3
4/25/07	-	-	5.4	8	5.4	17.1	9.3
4/25/07	-	1.8	10.4	14.3	8.3	28.2	14.3
4/25/07	-	1.9	7.6	10.8	5.7	18.6	9.2
4/25/07	-	2.7	13	18.1	10.3	34.6	17.6
4/25/07	-	1	8	10.9	6.3	23.5	11.4
5/3/00	-	-	1.8	2.7	2.8	5.4	2
5/3/00	-	-	2	2.1	2	4.3	1.6
5/3/00	-	-	2.7	2.3	2.4	5.6	2.1
5/3/00	-	-	1.7	1.3	1.4	3.6	1.4
5/3/00	-	-	2.4	3.5	2.8	5.6	2
5/3/00	-	4.1	15.7	21.4	17.1	39.5	16.5
5/3/00	-	2.8	7.1	10.9	8.2	20.3	7.7
5/3/00	-	-	2.4	1.7	1.8	4.9	1.7
5/3/00	-	-	2.3	2.9	2.5	5.4	2
5/3/00	-	2.9	7.4	11.5	8.6	19.1	7.1

Table 23. Torch Lake Public Council (TLPAC) measured PCB congeners (2018-2022).

Date Collected	PCB 21+33	PCB 52	PCB 99	PCB 90+101 +113	PCB 147 +149	PCB 153 +168	PCB 180+ 193
6/17/18	0.04	0.00	0.06	0.10	0.10	0.23	0.11
6/17/18	0.07	0.00	0.43	0.57	0.62	2.04	1.05
6/17/18	0.04	0.00	0.38	0.58	0.57	1.22	0.61
6/17/18	0.05	0.00	0.21	0.32	0.32	0.66	0.32
6/17/18	0.03	0.00	0.09	0.16	0.17	0.35	0.13
6/17/18	0.05	0.00	6.01	11.04	8.24	17.43	7.45
6/17/18	0.06	0.00	0.13	33.38	25.12	65.64	30.49
6/17/18	0.04	0.00	0.01	1.01	0.77	1.53	0.57
6/17/18	0.03	0.00	0.00	0.00	0.01	0.01	0.00
5/5/19	0.04	0.00	0.12	0.19	0.18	0.40	0.19
5/5/19	0.05	0.00	0.00	0.76	0.80	1.68	0.90
5/5/19	0.04	0.00	0.69	1.09	0.85	1.89	0.83
5/5/19	0.04	0.00	0.08	0.16	0.18	0.39	0.14
5/7/19	0.20	0.00	0.00	0.00	0.04	0.05	0.00
5/7/19	0.05	0.00	0.00	0.03	0.04	0.17	0.05
5/7/19	0.05	0.00	0.01	3.15	2.61	6.65	2.58

5/10/19	0.04	0.00	0.01	0.03	0.05	0.15	0.05
5/13/19	0.05	0.00	0.00	1.45	1.53	3.76	1.73
5/16/19	0.03	0.00	0.02	0.03	0.05	0.11	0.04
5/16/19	0.03	0.00	0.02	0.03	0.04	0.09	0.03
4/21/20	0.02	0.00	1.06	1.75	1.35	2.70	1.52
4/21/20	0.04	0.00	0.85	1.31	0.89	2.06	0.81
4/21/20	0.06	0.00	1.87	3.48	2.42	5.24	1.99
4/21/20	0.03	0.00	1.13	1.93	1.38	2.93	1.28
4/21/20	0.05	0.00	7.82	12.39	8.70	22.38	11.27
4/21/20	0.06	0.00	3.49	6.06	4.50	12.39	5.51
4/21/20	0.03	0.00	0.00	0.14	0.15	0.42	0.14
4/21/20	0.05	0.00	0.02	2.31	1.72	4.11	1.75
4/21/20	0.08	0.00	0.00	0.88	0.87	1.70	0.80
4/21/20	0.22	0.00	0.00	4.01	3.89	9.66	3.53
4/21/20	0.05	0.00	0.00	0.00	0.00	0.00	0.00
4/21/20	0.05	0.00	0.00	2.72	2.04	4.19	1.44
4/21/20	0.04	0.00	0.04	6.99	5.33	13.26	6.18
4/21/20	0.08	0.00	0.00	22.97	16.79	39.57	17.97
2022	0.05	0.00	0.00	18.45	14.02	33.36	15.67
2022	0.05	0.00	0.00	19.69	15.02	35.04	16.21
2022	0.05	0.00	2.50	3.94	2.83	6.53	3.12
2022	0.05	0.00	2.12	3.34	2.39	5.54	2.68
2022	0.04	0.00	1.44	2.32	1.71	3.77	1.83
2022	0.04	0.00	1.49	2.42	1.78	3.98	1.88
2022	0.05	0.01	5.35	8.40	6.76	14.19	9.24
2022	0.05	0.01	6.02	9.45	7.58	16.17	9.85
2022	0.03	0.00	0.51	0.78	0.61	1.41	0.71
2022	0.04	0.00	0.93	1.41	1.07	2.67	1.49

A.2.2 Hg fish measurement data

Table 24. MDEQ Fish Contaminant Monitoring Program Walleye Hg concentration (1988-2018) and biological characteristics.

MDEQ Fish Contaminant Monitoring Program				
Collection Date	Length (cm)	Weight (kg)	Sex	Hg Measured Conc. (µg/ g ww)
5/14/18	53.2	1.0	F	0.54
5/14/18	60	2.0	F	0.61

5/14/18	61.1	2.1	F	0.93
5/14/18	61.4	2.0	F	1.3
5/14/18	66.5	3.0	F	0.69
8/1/13	40.7	0.7	M	0.22
8/1/13	41.6	0.8	F	0.29
8/1/13	41.8	0.8	M	0.24
8/1/13	44	0.9	M	0.42
8/1/13	58.1	2.0		1.7
5/23/13	52.4	1.5	M	0.72
5/23/13	53	1.7	M	0.42
5/23/13	55.8	1.6	M	0.81
5/23/13	56	1.8	M	0.96
5/23/13	56.2	2.0	M	0.66
4/25/07	39.116	0.6	M	0.266
4/25/07	39.37	0.5	M	0.204
4/25/07	44.196	0.7	M	0.172
4/25/07	45.212	0.9	M	0.249
4/25/07	45.212	0.7	M	0.371
4/25/07	47.752	1.1	M	0.44
4/25/07	50.038	0.9	M	0.313
4/25/07	52.832	1.4	M	0.917
4/25/07	53.086	1.2	F	0.611
4/25/07	54.61	1.8	M	0.811
4/25/07	54.61	1.7	F	0.698
4/25/07	54.864	1.6		0.775
4/25/07	57.912	1.8	M	1.18
4/25/07	58.928	2.0	M	1.708
4/25/07	59.69	1.9	M	1.376
4/25/07	60.198	1.8		1.068
4/25/07	61.722	2.2	M	1.269
4/25/07	61.722	2.2	M	1.388
4/25/07	63.246	2.1		1.518
4/25/07	63.246	2.6		2.338
5/3/00	43.4	0.8	M	0.21
5/3/00	46	1.0	M	0.3
5/3/00	46.7	0.9	M	0.36
5/3/00	47	0.9	M	0.34
5/3/00	47.8	1.0	M	0.33

5/3/00	52.1	1.2	M	0.87
5/3/00	54.1	1.5	M	0.55
5/3/00	54.1	1.6	M	0.25
5/3/00	55.4	1.9	F	0.39
5/3/00	55.9	1.6	M	0.56
8/23/88	33.782	0.3		0.13
8/23/88	37.338	0.5		0.13
8/23/88	42.926	0.7		0.28
8/23/88	43.688	0.7		0.33
8/23/88	46.736	1.0		0.27
8/23/88	49.53	1.0		0.32

Table 25. GLIFWC Hg Monitoring Program walleye concentrations and biological characteristics (2018-2020).

GLIFWC Hg Monitoring Program				
Date	Length (cm)	Wt (kg)	Sex	Hg Measured Conc. ($\mu\text{g/g ww}$)
6/17/18	41.402	18.78	M	0.283
6/17/18	63.246	28.68	M	1.19
6/17/18	56.642	25.69	F	0.632
6/17/18	38.608	17.51	M	0.242
6/17/18	49.784	22.58	M	0.457
6/17/18	61.214	27.76	M	1.01
6/17/18	37.592	17.05	M	0.183
6/17/18	49.784	22.58	M	0.243
6/17/18	49.784	22.58	F	0.449
5/5/19	53.848	24.42	F	0.842
5/5/19	51.054	23.15	F	0.439
5/5/19	49.022	22.23	M	0.449
5/5/19	61.214	27.76	F	0.786
5/7/19	64.008	29.03	F	0.846
5/7/19	63.5	28.80	M	1.15
5/10/19	37.592	17.05	M	0.232
5/13/19	41.148	18.66	M	0.257
5/16/19	35.052	15.90	M	0.198
4/21/20	62.738	28.45	M	-
4/21/20	49.784	22.58	M	-

4/21/20	56.642	25.69	M	-
4/21/20	59.436	26.96	M	-
4/21/20	47.244	21.43	M	-
4/21/20	67.31	30.53	M	-
4/21/20	60.452	27.42	F	-
4/21/20	55.118	25.00	M	-
4/21/20	60.452	27.42	M	-
4/21/20	55.118	25.00	M	-
4/21/20	65.532	29.72	M	-
4/21/20	59.944	27.19	M	-

A.3 Sensitivity analysis results

A.3.1 PCB sensitivity analysis

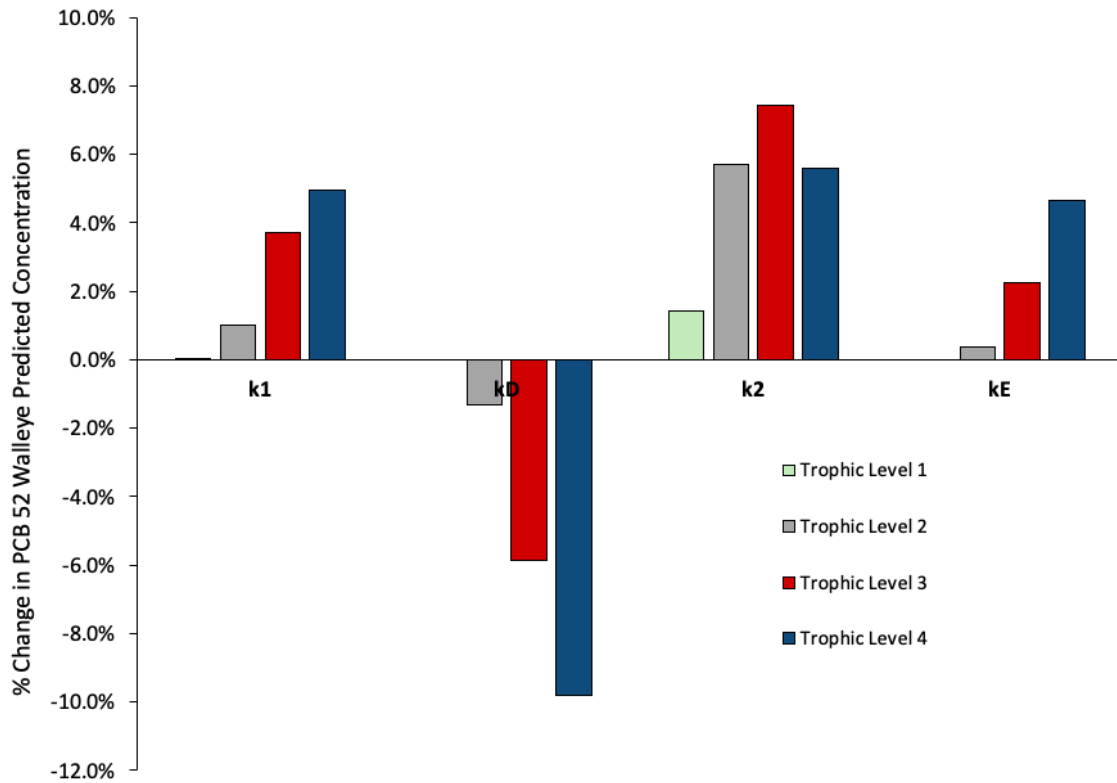


Figure 27. Change in walleye PCB 52 concentration caused by decreasing the model rate constants for trophic levels 1 (green), 2(gray), 3 (red), and 4 (blue) by 10%.

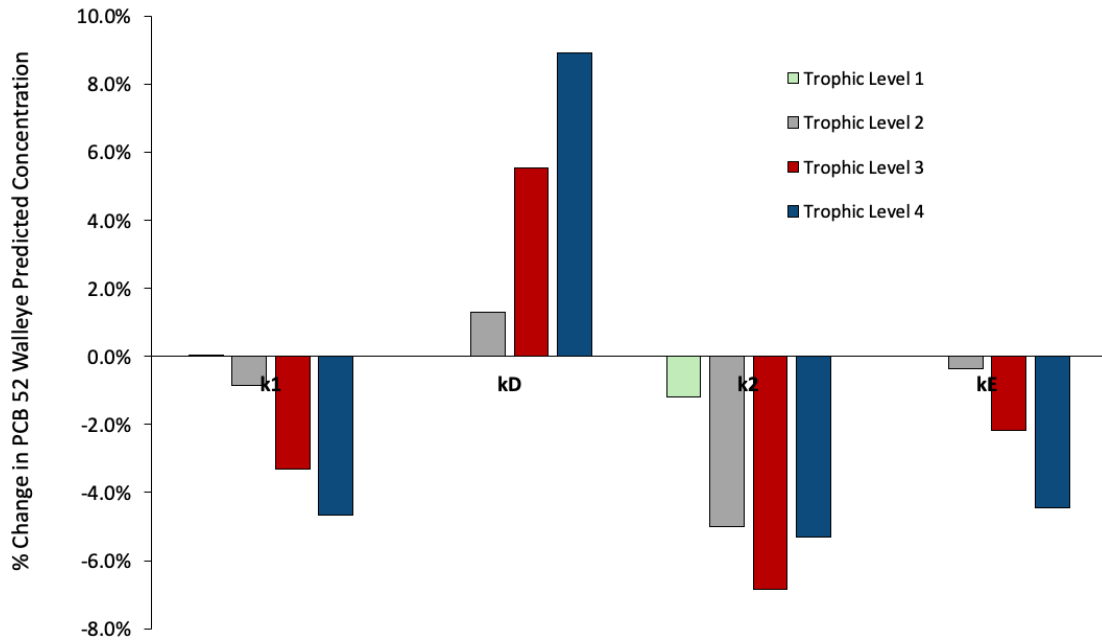


Figure 28. Change in walleye PCB 52 concentration caused by increasing the model rate constants for trophic levels 1 (green), 2(gray), 3 (red), and 4 (blue) by 10%.

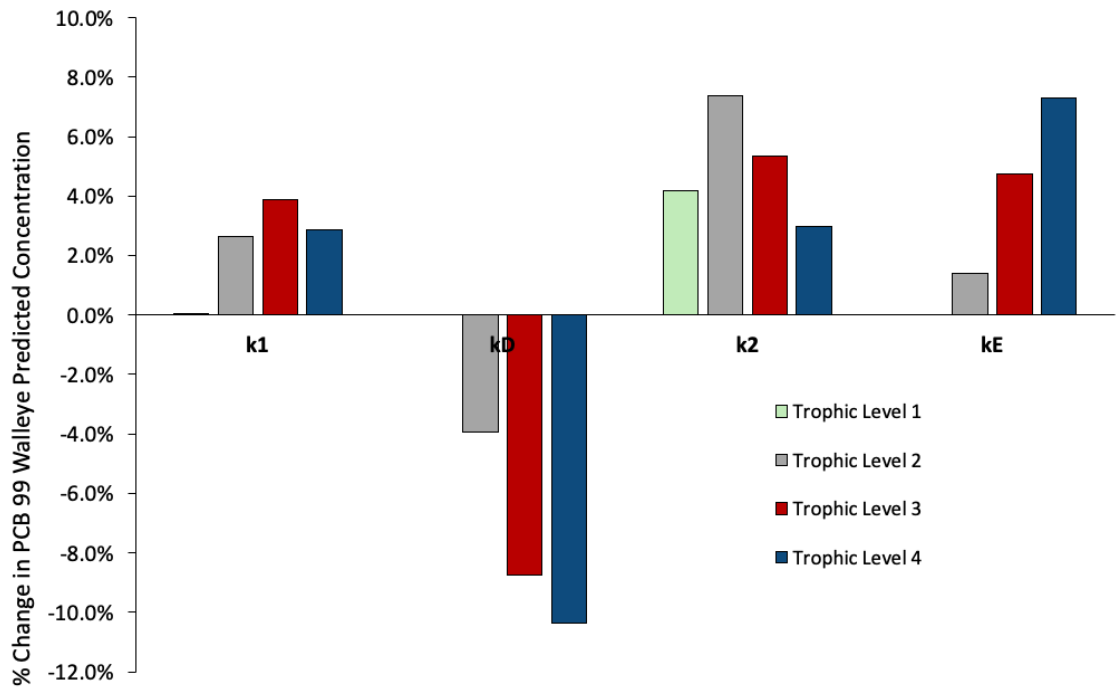


Figure 29. Change in walleye PCB 99 concentration caused by decreasing the model rate constants for trophic levels 1 (green), 2(gray), 3 (red), and 4 (blue) by 10%.

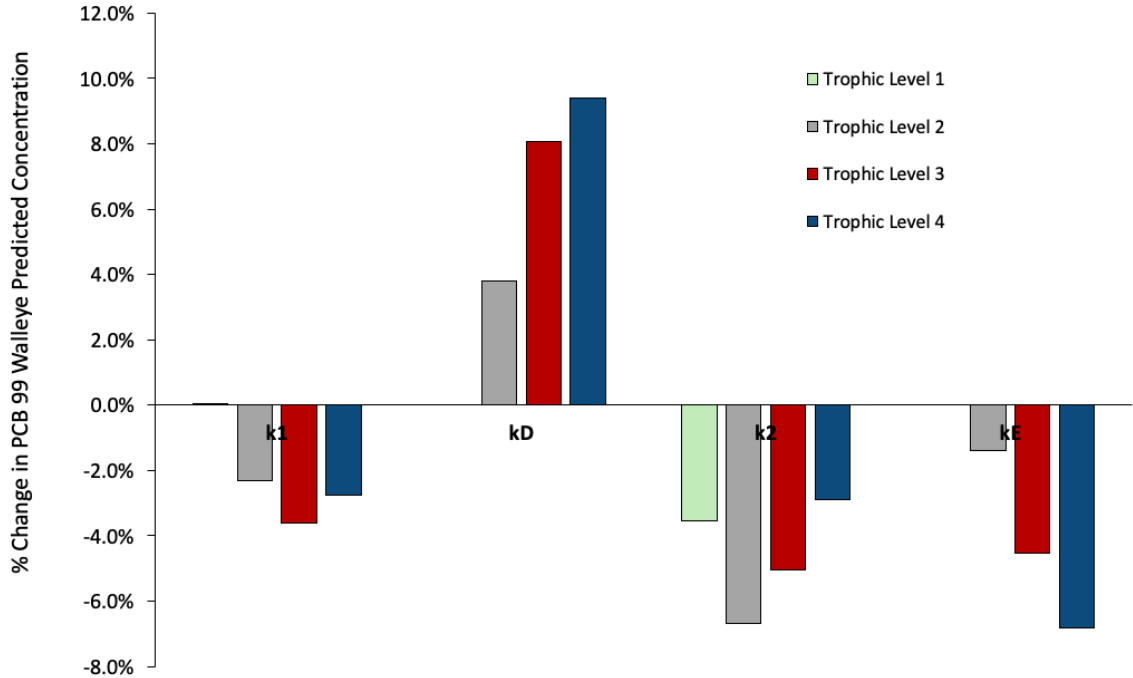


Figure 30. Change in walleye PCB 99 concentration caused by increasing the model rate constants for trophic levels 1 (green), 2 (grey), 3 (red), and 4 (blue) by 10%.

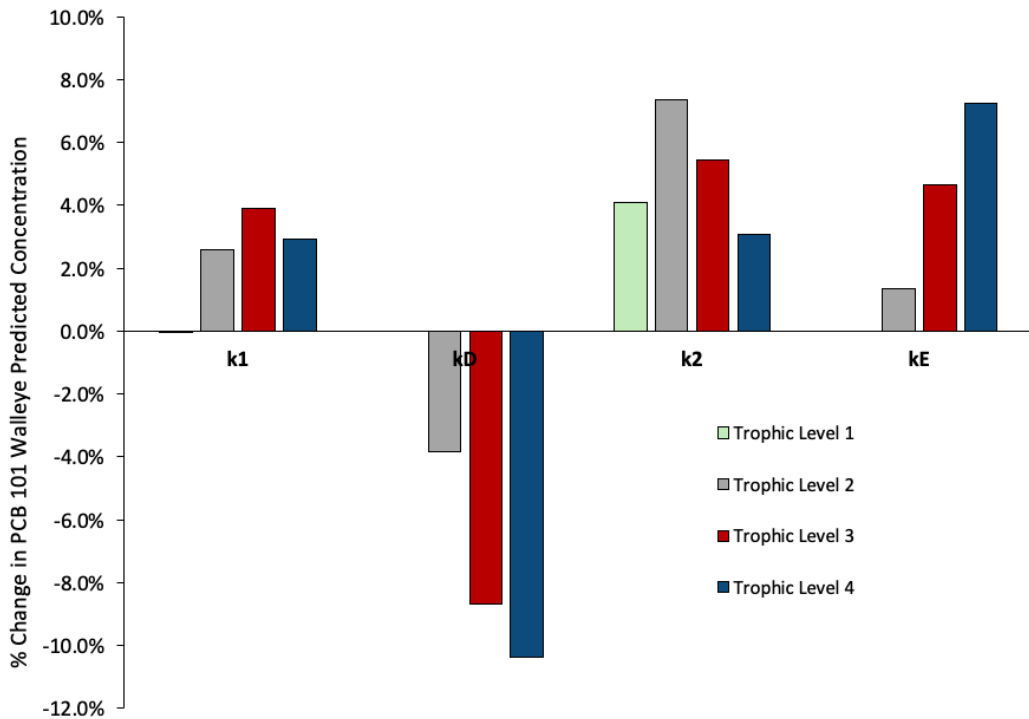


Figure 31. Change in walleye PCB 101 concentration caused by decreasing the model rate constants for trophic levels 1 (green), 2 (grey), 3 (red), and 4 (blue) by 10%.

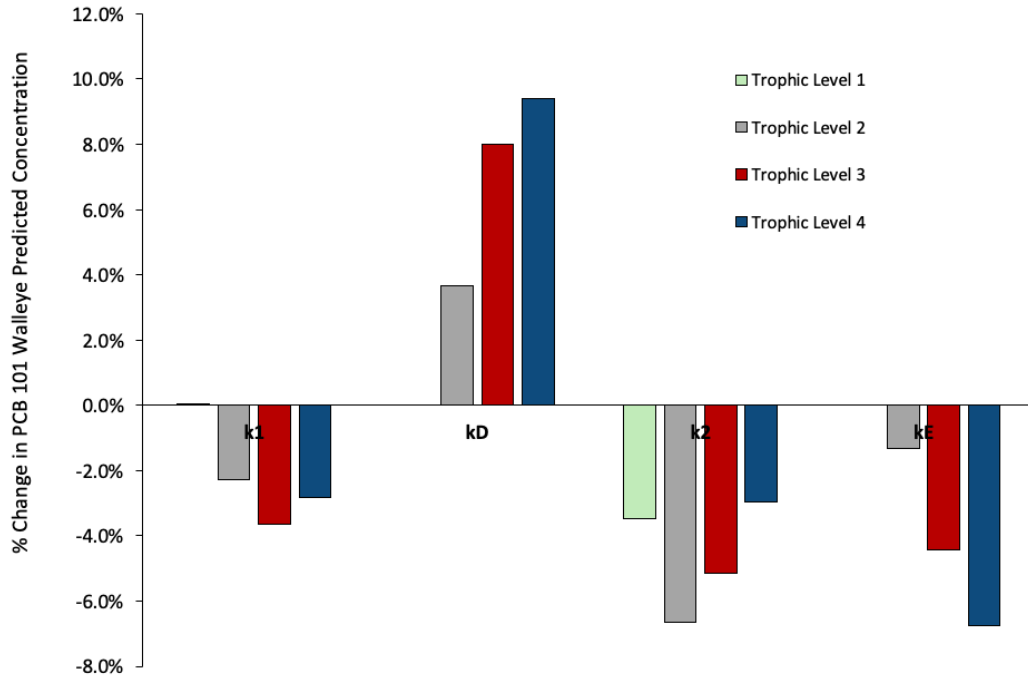


Figure 32. Change in walleye PCB 101 concentration caused by increasing the model rate constants for trophic levels 1 (green), 2(gray), 3 (red), and 4 (blue) by 10%.

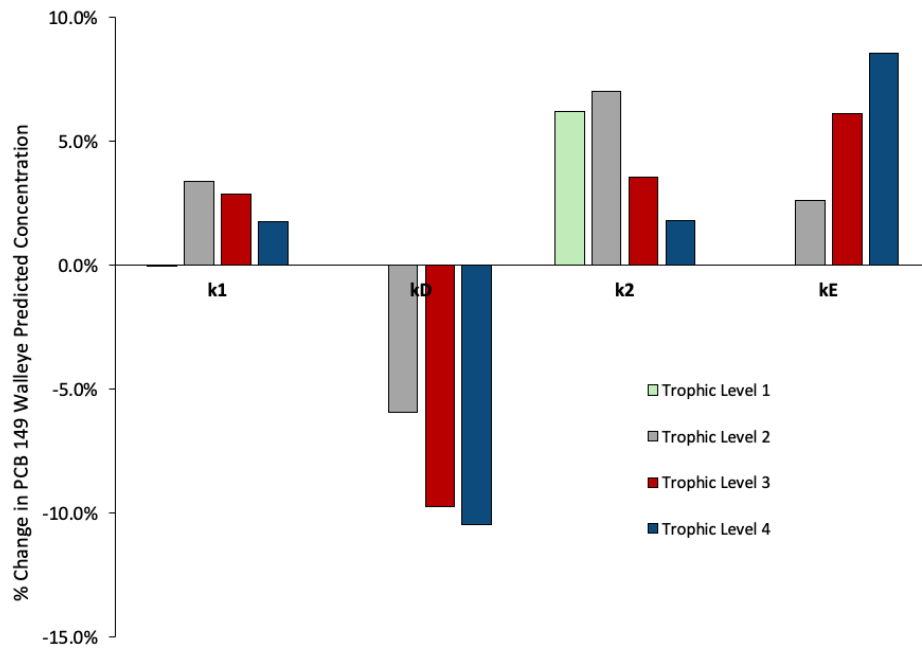


Figure 33. Change in walleye PCB 149 concentration caused by decreasing the model rate constants for trophic levels 1 (green), 2(gray), 3 (red), and 4 (blue) by 10%.

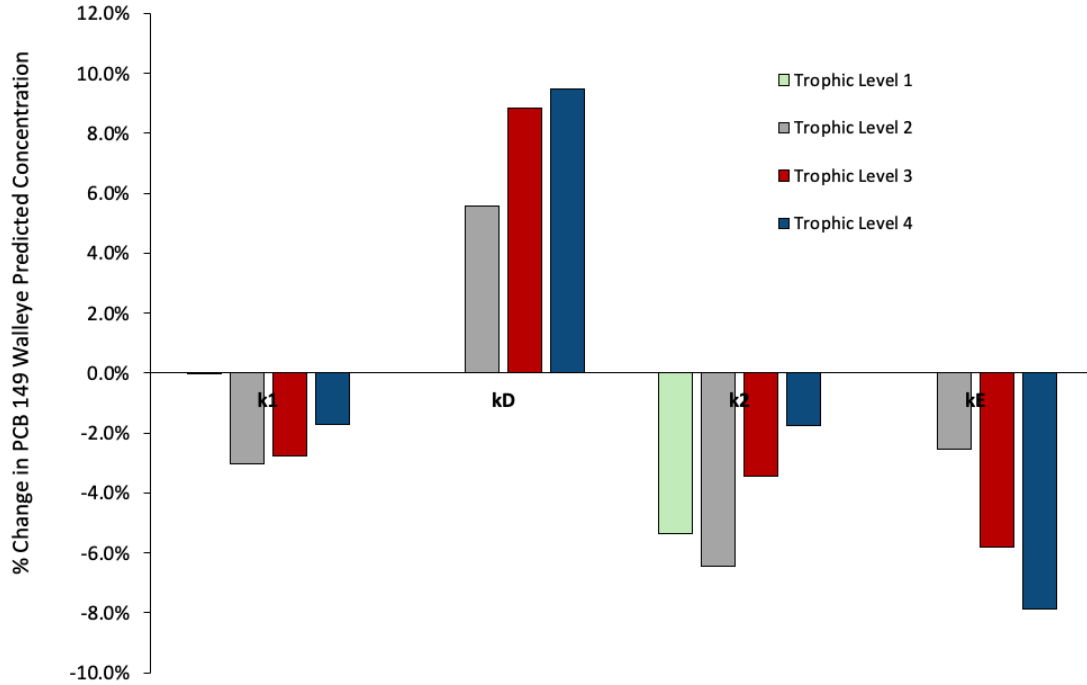


Figure 34. Change in walleye PCB 149 concentration caused by increasing the model rate constants for trophic levels 1 (green), 2(gray), 3 (red), and 4 (blue) by 10%.

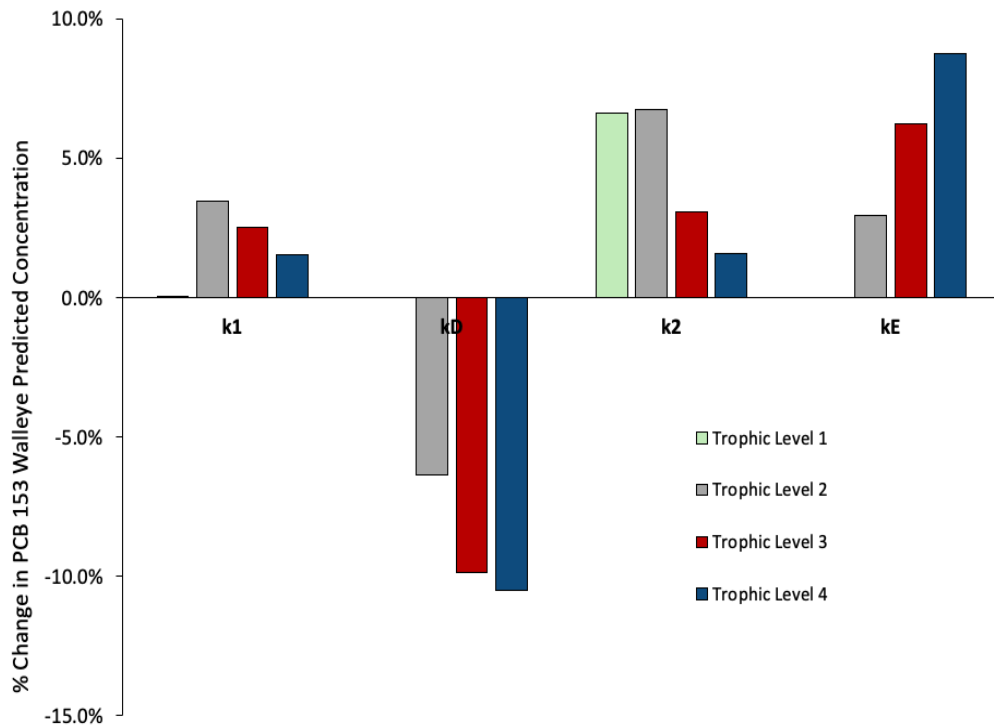


Figure 35. Change in walleye PCB 153 concentration caused by decreasing the model rate constants for trophic levels 1 (green), 2(gray), 3 (red), and 4 (blue) by 10%.

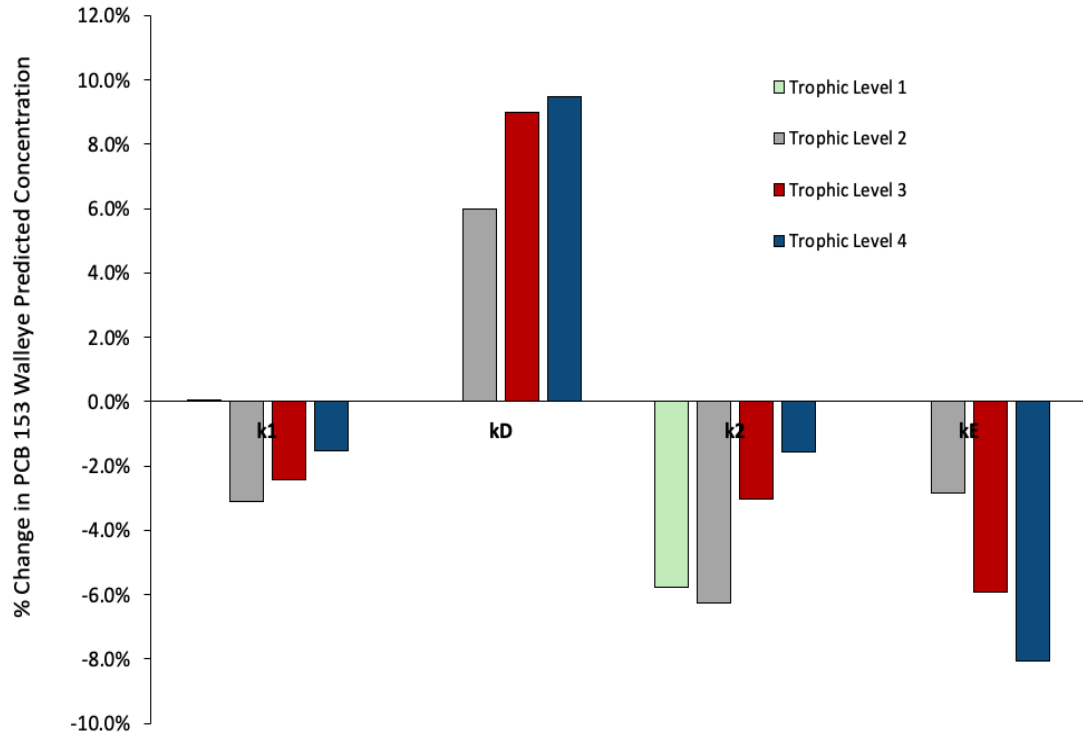


Figure 36. Change in walleye PCB 153 concentration caused by increasing the model rate constants for trophic levels 1 (green), 2 (gray), 3 (red), and 4 (blue) by 10%.

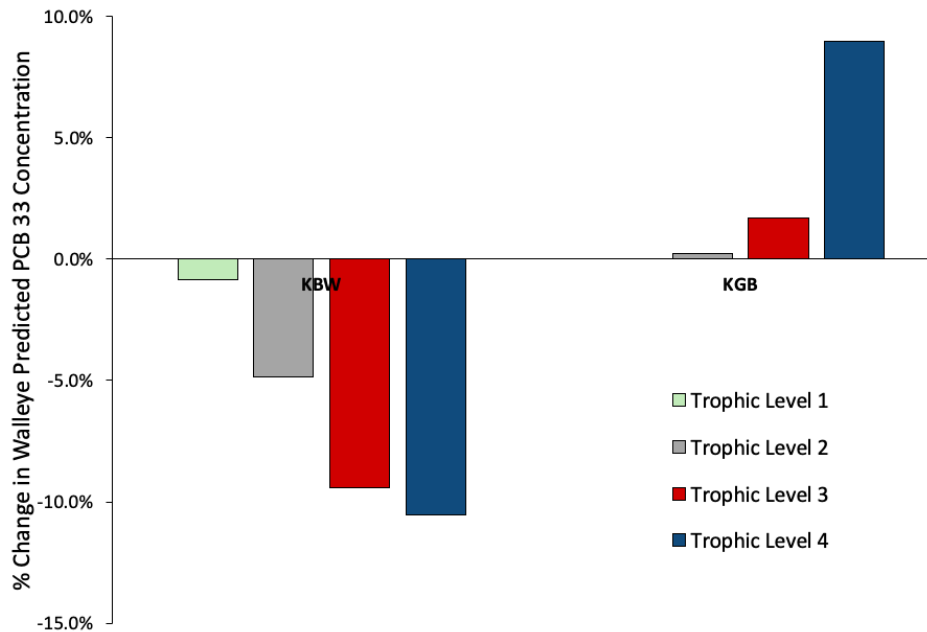


Figure 37. Change in walleye PCB 33 concentration caused by decreasing the model partition coefficients for trophic levels 1 (green), 2 (gray), 3 (red), and 4 (blue) by 10%.

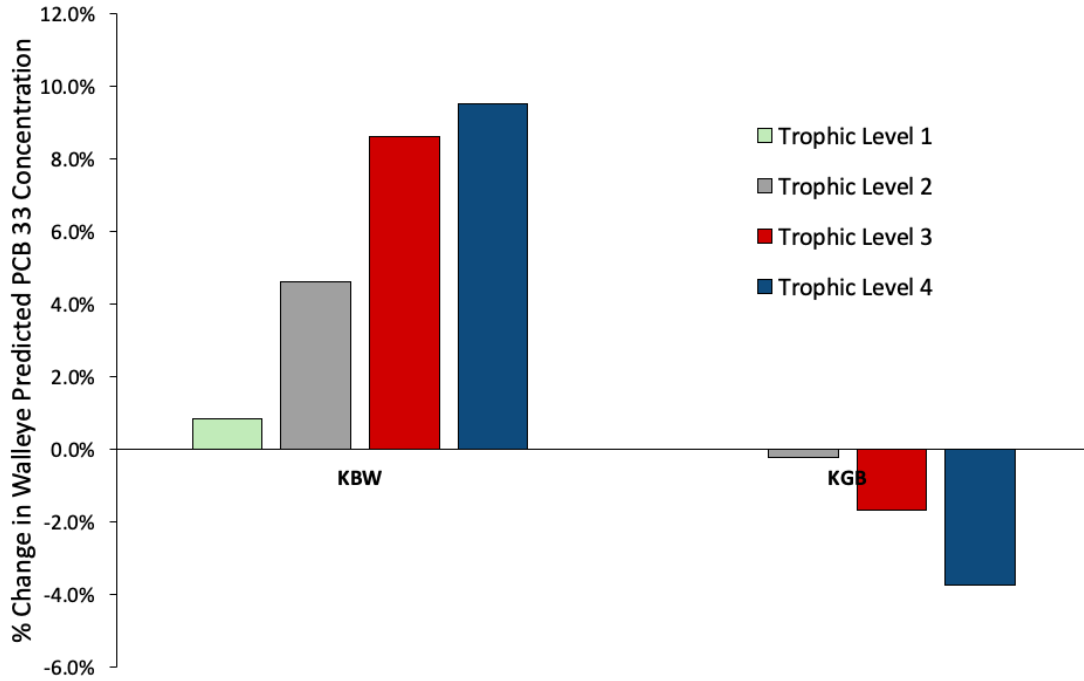


Figure 38. Change in walleye PCB 33 concentration caused by increasing the model partition coefficients for trophic levels 1 (green), 2 (gray), 3 (red), and 4 (blue) by 10%.

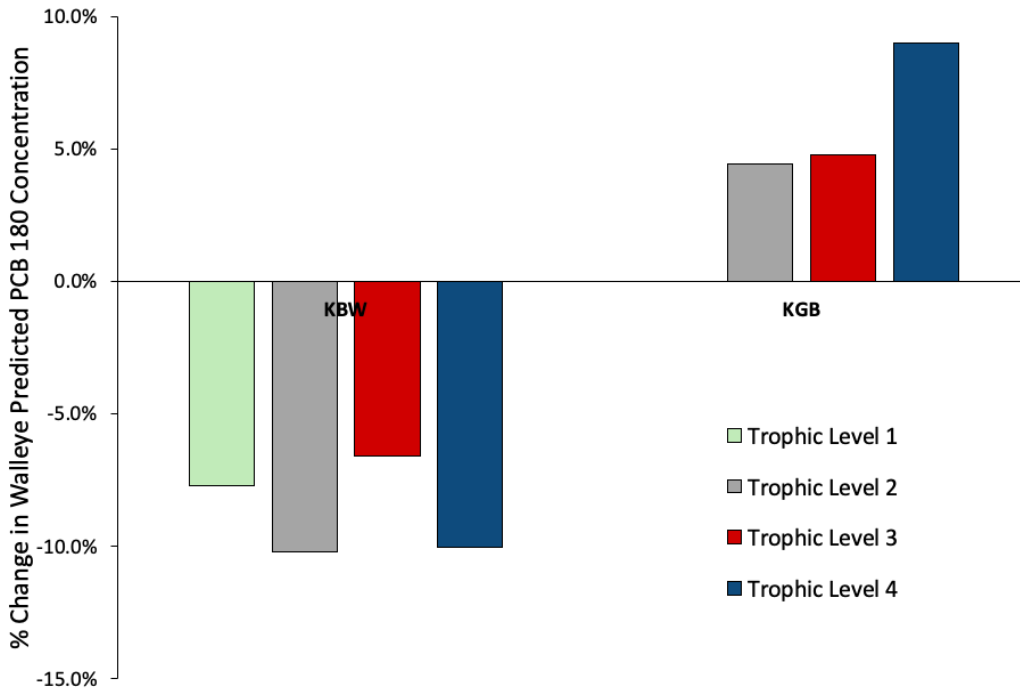


Figure 39. Change in walleye PCB 180 concentration caused by decreasing the model partition coefficients for trophic levels 1 (green), 2 (gray), 3 (red), and 4 (blue) by 10%.

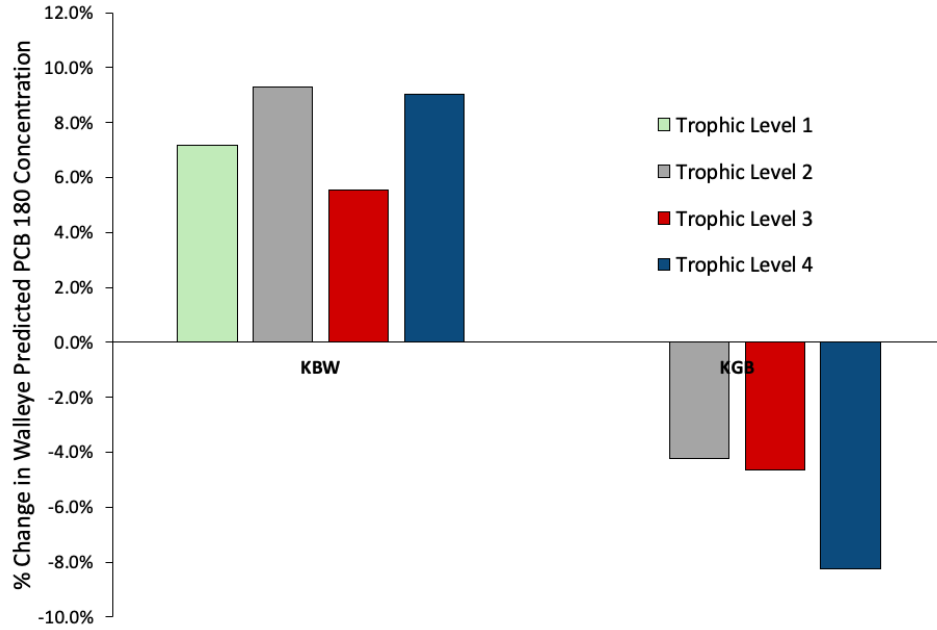


Figure 40. Change in walleye PCB 180 concentration caused by increasing the model partition coefficients for trophic levels 1 (green), 2 (gray), 3 (red), and 4 (blue) by 10%.

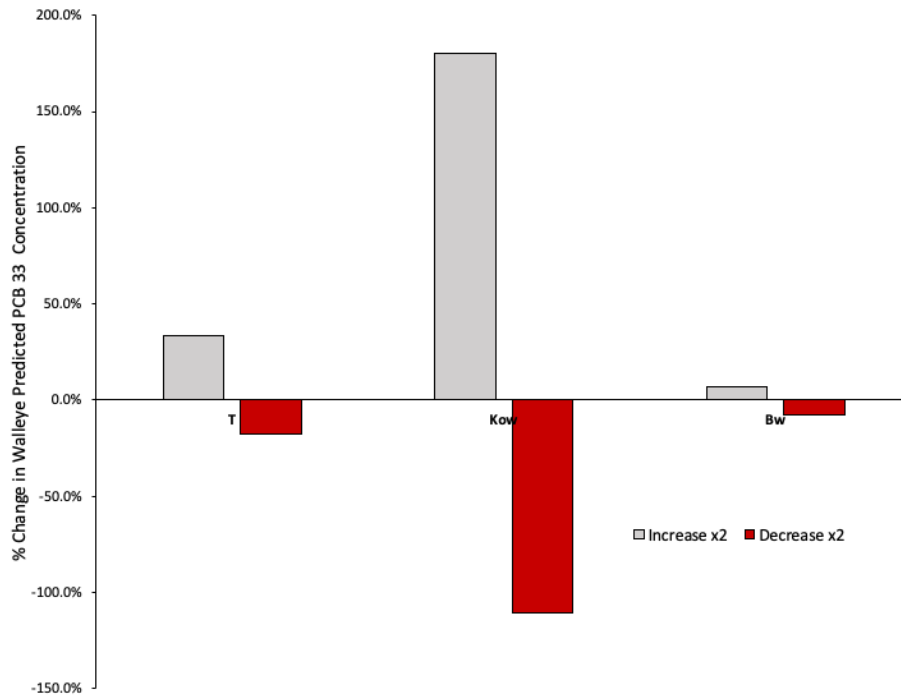


Figure 41. Change in walleye PCB 33 concentration caused by increasing the model temperature, K_{ow} , and body weight by factor of 2 (gray) and decreasing by factor of 2 (red).

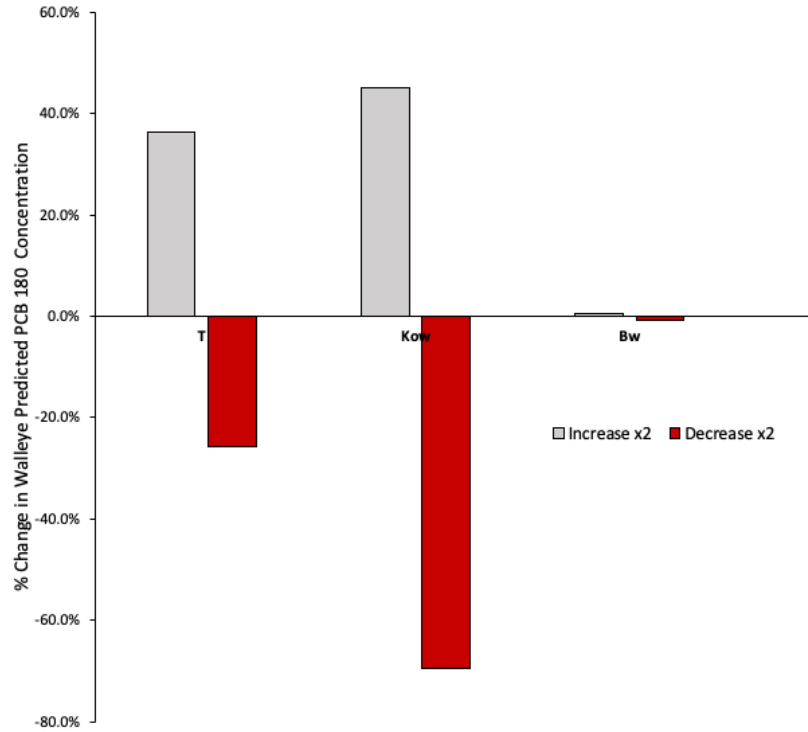


Figure 42. Change in walleye PCB 180 concentration caused by increasing the model temperature, Kow, and body weight by factor of 2 (gray) and decreasing by factor of 2 (red).

A.3.2 MeHg sensitivity analysis

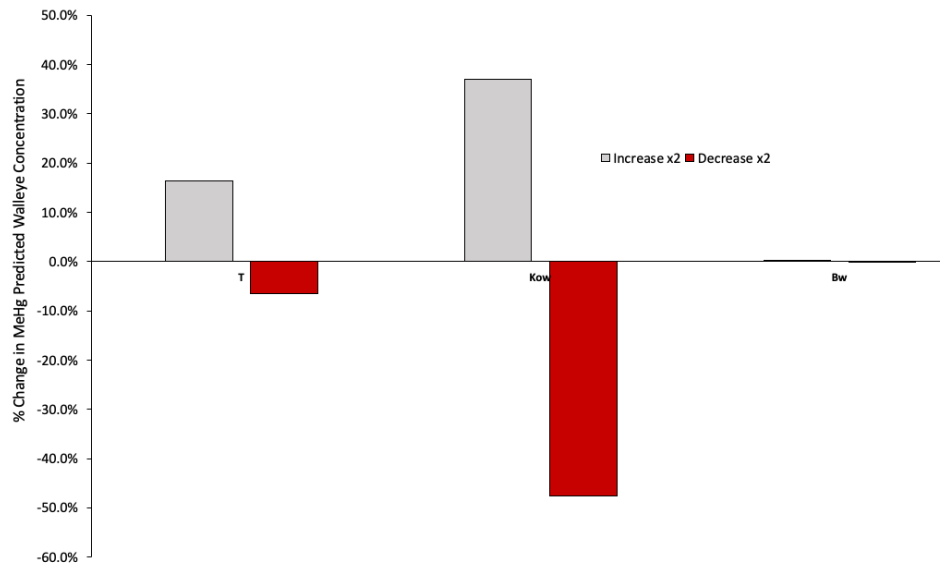


Figure 43. Change in walleye MeHg concentration caused by increasing the model temperature, Kow, and body weight by factor of 2 (gray) and decreasing by factor of 2 (red).

A.4 Mercury temperature profile

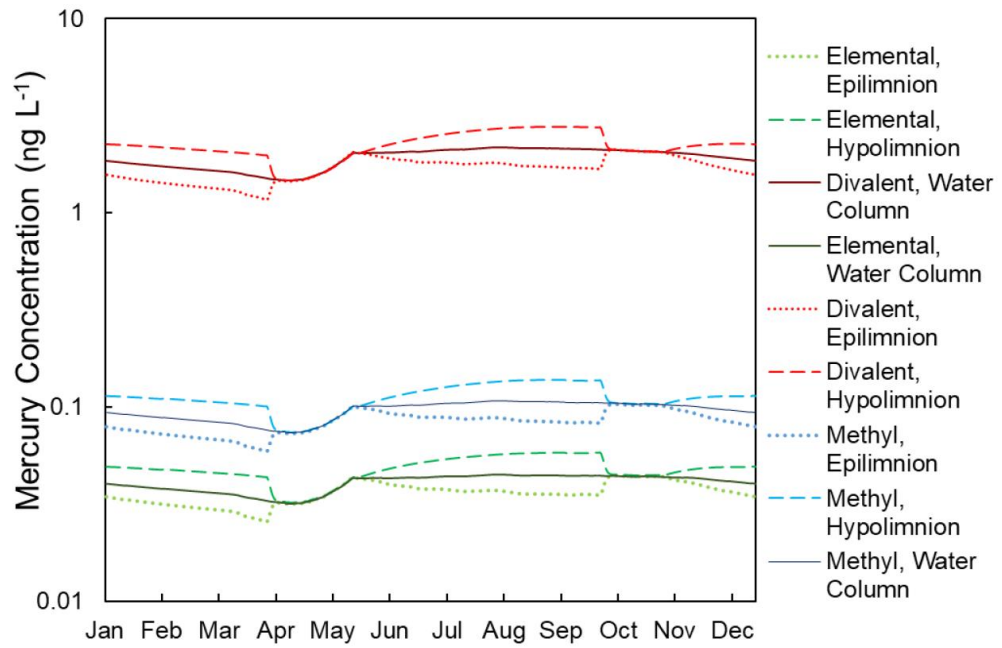


Figure 44. Annual divalent, methyl, and elemental mercury concentrations predicted from Torch Lake mass balance model (Hendricks, 2018)

B Copyright documentation

Figure 44: “*Annual divalent, methyl, and elemental mercury concentrations predicted from Torch Lake mass balance model (Hendricks, 2018)*” by Hendricks, Ashley, "A model to predict concentrations and uncertainty for mercury species in lakes", Open Access Master's Thesis, Michigan Technological University, 2018.
<https://doi.org/10.37099/mtu.edu/dc.etr/585>